University of Alberta

Analysis of Novel Nuclear Pore Complex Functions and of Ribosome Assembly

by

Tatiana Iouk

A thesis submitted to the Faculty of Graduate Studies and Research in partial fulfillment of the requirements for the degree of Doctor of Philosophy

Department of Cell Biology

Edmonton, Alberta
Fall 2002

National Library of Canada
Acquisitions and Bibliographic Services
395 Wellington Street
Ottawa ON K1A 0N4
Canada

Bibliothèque nationale du Canada
Acquisitions et services bibliographiques
395, rue Wellington
Ottawa ON K1A 0N4
Canada

Your file Votre référence

Our file Notre référence

The author has granted a non-exclusive licence allowing the National Library of Canada to reproduce, loan, distribute or sell copies of this thesis in microform, paper or electronic formats.

L'auteur a accordé une licence non exclusive permettant à la Bibliothèque nationale du Canada de reproduire, prêter, distribuer ou vendre des copies de cette thèse sous la forme de microfiche/film, de reproduction sur papier ou sur format électronique.

The author retains ownership of the copyright in this thesis. Neither the thesis nor substantial extracts from it may be printed or otherwise reproduced without the author's permission.

L'auteur conserve la propriété du droit d'auteur qui protège cette thèse. Ni la thèse ni des extraits substantiels de celle-ci ne doivent être imprimés ou autrement reproduits sans son autorisation.

0-612-81204-9

Canada

University of Alberta

Library Release Form

Name of Author: Tatiana Iouk

Title of Thesis: **Analysis of Novel Nuclear Pore Complex Functions and of Ribosome Assembly**

Degree: Doctor of Philosophy

Year this Degree Granted: 2002

Permission is hereby granted to the University of Alberta Library to reproduce single copies of this thesis and to lend or sell such copies for private, scholarly or scientific research purposes only.

The author reserves all other publication and other rights in association with the copyright in the thesis, and except as herein before provided, neither the thesis nor any substantial portion thereof may be printed or otherwise reproduced in any material form whatever without the author's prior written permission.

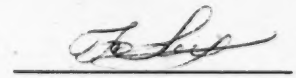

Tatiana Iouk,
425, Rue Beatty
Montreal, QC
H4H 1X7

July 20, 2002

UNIVERSITY OF ALBERTA

FACULTY OF GRADUATE STUDIES AND RESEARCH

The undersigned certify that they have read, and recommend to the Faculty of Graduate Studies and Research for acceptance, a thesis entitled: **Analysis of novel nuclear pore complex functions and of ribosome assembly**, submitted by Tatiana Iouk in partial fulfillment of the requirements for the degree of Doctor of Philosophy.

Richard W. Wozniak, Ph.D.

Richard A. Rachubinski, Ph.D.

Warren J. Gallin, Ph.D.

Michael S. Schultz, Ph.D.

Manfred J. Lohka, Ph.D.

Date

Abstract

Nucleo-cytoplasmic transport is essential for proper temporal and spatial organization of numerous cellular processes, including gene expression, cell division and signal transduction. The transport occurs through the nuclear pore complex (NPC). Using yeast *Saccharomyces cerevisiae* as a model, we have demonstrated a physical and functional link between components of the NPC and the spindle checkpoint machinery. The spindle checkpoint ensures faithful chromosome segregation during cell division. We show that two proteins required for the checkpoint execution, Mad1p and Mad2p, reside predominantly at the NPC throughout the cell cycle. There they are associated with a subcomplex of nucleoporins containing Nup53p, Nup170p, and Nup157p. The interaction of the Mad1p/Mad2p complex with the NPC requires Mad1p and is, in large part, mediated by Nup53p. Similarly, we show that Mad1p plays a role in the stable association of Nup53p with the NPC. Activation of the spindle checkpoint is accompanied by the release of Mad2p from the NPC and the accumulation of Mad2p at kinetochores. This latter event, as well as the checkpoint specific hyperphosphorylation of Mad1p, is dependent on Nup53p. These and previously published results (Marelli et al., 1998 and 2001) demonstrate that Nup53p-containing subcomplex plays a variety of roles in the dynamic organization of nuclear functions.

In our previous work, we have identified and studied yet another multifunctional

nuclear protein, termed Rrb1p. Rrb1p is an essential, WD-repeat containing protein, which is thought to function as a chaperon for a specific ribosomal protein Rpl3p. We have demonstrated that Rrb1p is simultaneously involved in ribosome biogenesis and in the regulation of transcription of ribosomal protein genes.

Acknowledgements

I would like to acknowledge Oliver Kerscher and Shawna Maguire for their experimental contributions to this work. I am grateful to my mentor Dr. Rick Wozniak. He taught me well. I also thank members of my Supervisory Committee Dr. Rick Rachubinski and Dr. Warren Gallin for their aid and understanding. Finally, I am indebted to the Department of Cell Biology and to its wonderful people.

Table of contents

Chapter1. Introduction.....1

1.1. Functional compartmentalization of the nucleus in budding yeast.....2

1.2.1. The assembly of NPCs.....7

1.2.1.1. Regulation of the biogenesis and distribution of NPCs.....7

1.2.1.2. Mitosis-associated changes within NPCs.....9

1.2.1.3. Mechanisms of the post-mitotic NPC assembly in higher eukaryotes.....11

1.2.2. Architecture of the NPC.....12

1.2.3. Components of the yeast nuclear pore..... 15

1.2.3.1. FG-Nups and their role in the passage through the NPC.....16

1.2.3.2. Other NPC-associated proteins.....20

1.2.4. Evolutional conservation and divergence of NPC constituents.....20

1.2.5. Mechanisms of the nucleo-cytoplasmic transport.....22

1.2.5.1. Passive diffusion.....22

1.2.5.2. Active nuclear transport and its receptors.....22

1.2.5.3. Ran and its role in nucleo-cytoplasmic transport.....25

1.2.5.4. Multiple transport pathways: specificity of interactions between the Nups and Kaps.....28

1.2.6. The NPC is a multifunctional complex.....29

1.2.6.1. Alternative functions of nucleoporins.....29

1.2.6.2. Multiple roles of importins and Ran.....32

1.3. The mitotic spindle checkpoint.....33

1.3.1. Chromosome segregation defects.....33

1.3.2. Yeast cell cycle and the mitotic spindle.....34

1.3.3. The spindle checkpoint.....38

1.3.4. The spindle checkpoint proteins.....40

1.3.4.1. Mad1 and its complex with Mad2.....42

1.3.4.2. Mad2 and its role in the mitotic spindle checkpoint.....43

1.3.4.3. Other components of the mitotic checkpoint machinery.....44

1.4. The Focus of this Thesis.....46

Chapter 2. Materials and Methods.....47

2.1. Yeast strains and media.....48

2.2. Construction of yeast strains.....48

2.2.1. Production of *NUP* and Checkpoint Gene Deletions.....48

2.2.2. Generation of nucleoporin and checkpoint gene double deletion mutants.....53

2.2.3. Construction of tagged *MAD1*, *MAD2* and *MTW1* Genes:.....53

2.2.4. Construction of the GFP-tagged *MAD1* and *MAD2* in the nucleoporin deletion strains.....55

2.2.5. *RRB1* gene disruption.....56

2.3. Plasmids.....56

2.4. Cell phenotype analysis.....59

2.4.1. Benomyl- and thermo-sensitivity of *NUP /MAD* gene disruption strains.....59

2.4.2. Cell growth synchronization and activation of mitotic spindle checkpoint.....59

2.4.3. Flow cytometry.....60

2.4.4. Growth curves.....61

2.4.5. Regulation of *GAL1::RRB1* expression.....62

2.4.6. Inhibition of translation.....62

2.5. Yeast subcellular fractionation.....63

2.5.1. Preparation of crude nuclei.....63

2.5.2. Sedimentation analysis of ribosomes.....64

2.6. Immunoprecipitation procedures.....65
2.6.1. Immunoprecipitation of the proteinA-tagged nucleoporins.....65
2.6.2. Immunoprecipitation of GFP-tagged protein fusions and Nup53p.....66
2.6.3. Immunoprecipitation of Rrb1-HA.....67
2.7. Western blotting.....68
2.8. Double-inverted gradient electrophoresis (DG-PAGE).....69
2. 9. Northern blot analysis.....70
2.10. Pulse-chase of RNA.....72
2.11. Fluorescence Microscopy.....72
2.12. Protein Sequence Analysis.....75

Chapter 3. Functional Associations Between the Yeast NPC and the Spindle Checkpoint Machinery.....76
3.1. Overview.....77
3.2. Mad1p and Mad2p are associated with yeast NPCs.....78
3.3. Spindle checkpoint activation induces the release of Mad2p, but not Mad1p, from NPCs and its accumulation at kinetochores.....82
3.4. Mad1p and Mad2p are associated with a specific subset of Nups.....84
3. 5. Changes in molecular interactions between the Mad1p/Mad2p complex and the NPC upon spindle checkpoint activation.....88
3.6. The Mad1p/Mad2p complex associates with the NPC through Mad1p.....91
3.7. Genetic interactions between *MAD1* and *MAD2* and nucleoporin genes.....93
3.8. Nup53p is required for the hyperphosphorylation of Mad1p in nocodazole treated cells.....96
3.9. Mad1p plays a role in the structural integrity of the Nup53p-containing NPC complex.....98

3.10. Discussion.....99

Chapter 4. Rrb1p, a Yeast Nuclear WD-repeat Protein Involved in the Regulation of Ribosome Biosynthesis.....110

4.1. Overview.....111

4.2. Background.....112

4.2. The identification of YMR131c.....115

4.3. *RRB1* encodes an essential nuclear protein.....116

4.4. Construction of a conditional *RRB1* allele.....117

4.5. Depletion of Rrb1p results in decreased levels of 60S ribosomal subunits and ribosomes.....122

4.6. Rrb1p physically interacts with the ribosomal protein L3.....125

4.7. Rrb1p modulates cellular levels of L3.....127

4.8. The nuclear localization of Rrb1p is dependent on protein translation.....131

4.9. *RRB1* regulates the levels of ribosomal protein mRNAs.....134

4.10. Discussion.....138

Chapter 5. Perspectives and future studies.....147

5.1. Synopsis.....148

5.2. Perspectives on the transport of the spindle checkpoint proteins into the nucleus.....149

5.3. On the intranuclear dynamics of the mitotic spindle checkpoint proteins.....150

5.4. On the functions of Mad1p and Mad2p.....150

5.5. On the resistance of nucleoporin gene disruption strains to benzimidazoles.....152

Chapter 6. References.....155

List of Figures and Tables

Figure 1-1. A schematic representation of the yeast nucleus.....4

Figure 1-2. Structure of the nuclear pore complex.....13

Figure 1-3. Positioning of NPC-constituents.....17

Figure 1-4. A simplified schematic of nuclear transport.....27

Figure 1-5. Schematic diagram of the yeast cell cycle.....37

Figure 1-6. A model for the mitotic spindle checkpoint.....41

Figure 3-1. Association of Mad1-Gfp and Mad2-GFP with NPCs.....79-80

Figure 3-2. Spindle checkpoint activation induces the release of Mad2p-GFP, but not Mad1p, from the NPC and its recruitment to kinetochores.....83

Figure 3-3. Mad1p and mad2p associate with a specific subset of nucleoporins.....86-87

Figure 3-4. The effects of mutations in members of the Nup53p-containing complex on the subcellular distribution of the Mad1p/Mad2p complex.....90

Figure 3-5. Mad1p/Mad2p complex associates with the NPC through Mad1p.....92

Figure 3-6. *MAD1*, *MAD2* and Nup-encoding genes of the Nup53p-containing complex interact genetically.....94

Figure 3-7. Requirement of Nup53p for hyperphosphorylation of Mad1p.....97

Figure 3-8. Mad1 is required for integrity of the Nup53-containing complex.....99

Figure 3-9. Model summarizing interactions between the Nup53p-containing complex, Mad1p, and Mad2p.....101

Figure 4-1. Rrb1p is located in the nucleus and concentrated in the nucleolus.....118

Figure 4-2. *GAL1* regulation of *RRB1* expression.....120-121

Figure 4-3. The effect of depletion of Rrb1p on ribosome biosynthesis.....123

Figure 4-4. The ribosomal protein rpL3 is associated with Rrb1p.....126

Figure 4-5. Overproduction of Rrb1p leads to an increase in cellular levels of rpL3.....129

Figure 4-6. RpL3 accumulates in the nuclei of cells overexpressing *RRB1*.....130

Figure 4-7. Inhibition of protein synthesis causes a reversible relocalization of Rrb1p from the nucleus to the cytoplasm.....133

Figure 4-8. Rrb1p modulates RP mRNA levels.....135-136

Table 2-1. Strains used in this study.....49-51

List of Abbreviations and Symbols

AMP.....adenosine monophosphate
APC.....anaphase promoting complex
ATP.....adenosine triphosphate
ben.....benomyl
bp.....base pairs
BSA.....bovine serum albumin
Bub.....budding uninhibited by benzimidazole
CENP-E..... centromeric protein E
Cdc.....cell division cycle
cDNA.....complementary DNA
CM .....complete synthetic medium
CFP.....cyan fluorescent protein
chx.....cycloheximide
c.p.m.....counts per minute
ctf.....chromosome transmission fidelity
cyc.....cycling cells
DFC.....dense fibrillar component
DAPI.....diamidino-2-phenylindole dihydrochloride
dCTP.....deoxycytidine-3'-triphosphate
DMSO.....dimethylsulfoxide
DNA..... desoxyribonucleic acid
EDTA.....ethylene diamine tetra-acetic acid
ECL.....enhanced chemiluminescence
ER.....endoplasmic reticulum
FC.....fibrillar centre
FG-repeat.....phenylalanine-glycine repeat
5-FOA.....5'-fluorootic acid
FRAP.....fluorescence recovery after photobleaching
FRET.....fluorescence resonance energy transfer

g.....gravitational force

Gal.....galactose

GAP.....GTPase activating protein

GC.....granular component

GDP.....guanosine diphosphate

GEF.....guanine nucleotide exchange factor

GFP.....green fluorescent protein

Glc.....glucose

GST.....glutathione-S-transferase

GTP.....guanosine triphosphate

GTPase..... guanosine triphosphatase

h.....hour

HA.....hemagglutinin

His.....histidine

HsMad.....human Mad checkpoint protein

HRP.....horseradish peroxidase

IgG.....immunoglobulin G

Kan.....kanamycin

Kap.....karyopherin

kD.....kilodalton

Leu.....leucine

Lys.....lysine

M.....moles per litre

MAb.....monoclonal antibody

Mad.....mitotic arrest-deficient

Mat.....mating type

Met.....methionine

µCi.....microCurie

mg.....milligram

µg.....microgram

min.....minute

ml.....millilitre

Mps.....monopolar spindle

mRNA.....messenger RNA

MW.....molecular weight

NE.....nuclear envelope

NES.....nuclear export signal

Nic.....nucleoporin-interacting component

NLS..... nuclear localization signal

nm.....nanometer

noc.....nocodazole

Nop.....nucleolar protein

NLS.....nuclear localization signal

NPC.....nuclear pore complex

Ntf2.....nuclear transport factor 2

NuMa.....nuclear mitotic apparatus protein

Nup.....nucleoporin

O.D.....optical density

ORF.....open reading frame

PCR.....polymerase chain reaction

pH.....$-\log[H^+]$

P_i.....inorganic phosphate

Pds1.....premature dissociation of sisters (1)

PMSF.....phenyl methyl sulfonyl fluoride

Poly(A)$^+$.....polyadenylated RNA

Ran.....Ras-related nuclear protein

RanBP.....Ran-binding protein

Rb.....retinoblastoma

RCC1.....regulator of chromosome condensation

Rrb.....regulator of ribosome biogenesis

RNA.....ribonucleic acid

RNP.....ribonucleoprotein

rRNA.....ribosomal RNA

Rpl.....large ribosomal subunit protein

Rps.....small ribosomal subunit protein

S.....Svedberg unit

SDS-PAGE.....sodium dodecyl sulfate polyacrylamide gel electrophoresis

SPB.....spindle pole body

TCA.....trichloroacetic acid

Tcm.....trichodermin

TPX2.....targeting protein for Xenopus (kinesin-like protein) 2

Trp.....tryptophane

ts.....temperature-sensitive

Ura.....uracil

WD-repeat.....tryptophan-aspartate repeat

WT.....wild type

YEP.....yeast extract-peptone medium

YEPD.....YEP-dextrose medium

Chapter 1

Introduction

1.1. Functional compartmentalization of the nucleus in budding yeast

The nucleus is the organelle that contains machinery essential for gene expression and transmission of genetic information. Compared to the cytoplasm, the nucleus has traditionally been viewed as relatively unstructured, mostly due to the absence of intranuclear membrane-bound compartments. However, numerous studies have defined functional domains that exist in this highly dynamic organelle. In addition to the morphological description of the nuclear subcompartments, this chapter explores how the spatial organization contributes to and reflects the various processes that take place in the nucleus.

Many features of the yeast *Saccharomyces cerevisiae*, including the ease of mutant isolation and genetic analysis, make this organism an attractive model system with which to study functional compartmentalization of the nucleus. However, the small size and thick cell wall of budding yeast considerably complicate visual monitoring of processes that occur in the nucleus.

To explore the structure and function of nuclear compartments, several advanced and sensitive techniques have been widely employed in yeast. The power of light microscopic analysis has been substantially enhanced by confocal microscopy and by live-cell imaging employing fluorescently tagged proteins. Electron-microscopic studies have permitted the development of high-resolution immunolocalization protocols and

three-dimensional reconstruction from serial electron micrographs. Recent advances in subcellular fractionation procedures have greatly improved the purification and subsequent biochemical analysis of nuclear structural and functional domains and protein complexes. The use of these advanced technical approaches led to significant progress in our understanding of biological functions associated with various nuclear domains.

The yeast nucleus (Figure 1-1, p.4) is delimited by the nuclear envelope (NE), a double-membrane structure, formerly referred to as the "karyotheca", which acts as a shield harboring and protecting the karyon (Anderson, 1953). The inner nuclear membrane apposes the chromatin and the nucleolus. The outer membrane is contiguous with the rough endoplasmic reticulum and is studded with ribosomes. The inner nuclear membrane faces the nucleoplasm and chromatin. Unlike higher eukaryotes, yeast lack lamina, a fibrous support structure, plunged between the NE and chromatin. Nuclear pores are occupied by eight-fold proteinaceous symmetrical structures termed the nuclear pore complexes (NPCs) (Gall, 1967). NPCs promote molecular trafficking between the nucleus and cytoplasm.

The nucleoplasm is filled with chromatin, which is organized into structurally and functionally distinct compartmentalization territories (reviewed by Bi and Broach, 2001).

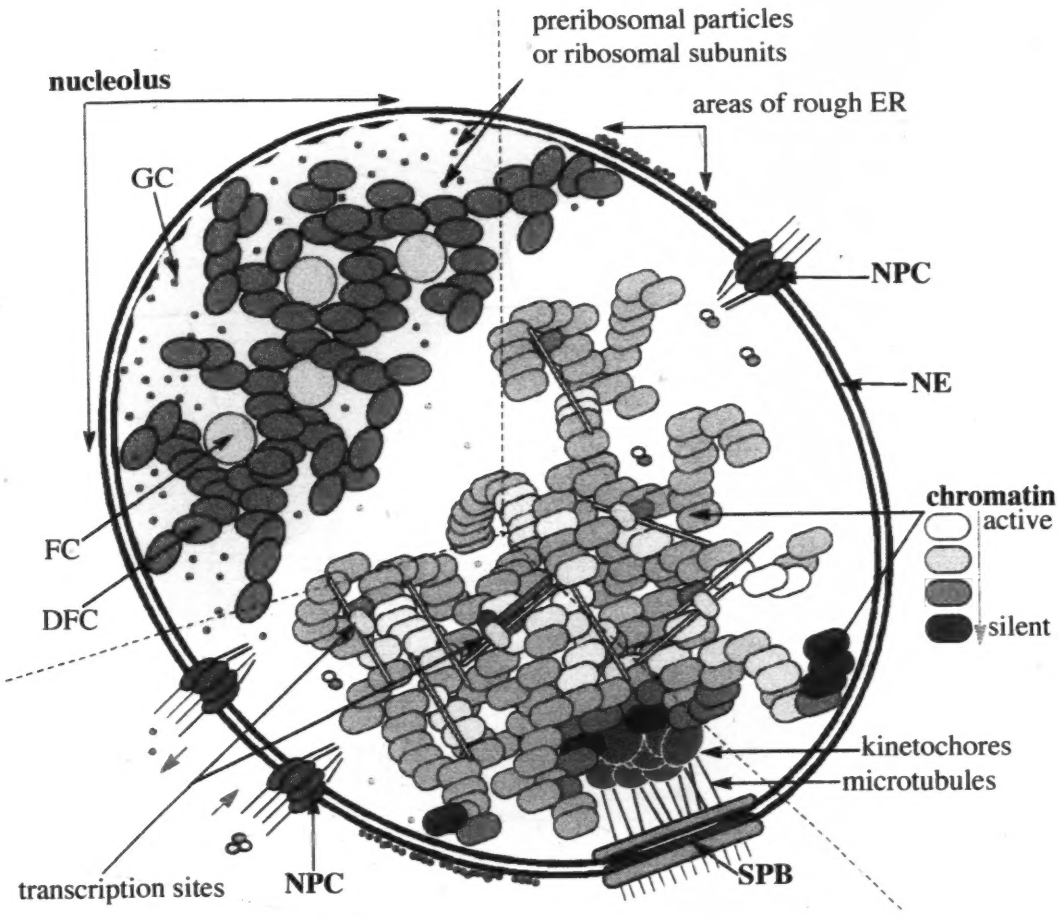

Figure 1-1. A schematic representation of the yeast nucleus. The nucleus is surrounded by a nuclear envelope (NE), which is perforated with nuclear pore complexes (NPCs). The nucleolus is shown as a dense crescent that is attached to the inner membrane of NE. The nucleolus is differentiated into three regions (Leger-Silvestre, 1999). The fibrillar centres (FC) contain ribosomal DNA; the dense fibrillar component (DFC) harbors transcription and processing of rRNA; the granular component (GC) consists of preribosomal particles at different stages of maturation (Trumtel et al., 1999). The nucleoplasm is filled with chromatin. The "silent" chromatin areas are concentrated close to the nuclear periphery (Laroche et al., 2001). Chromosomes are attached to microtubules via kinetochores (Nicklas, 1997). Microtubules are capped at the spindle pole body (SPB) (O'Toole et al., 1999). The microtubule extensions are visible on both nuclear and cytoplasmic sides of the SPB.

Active genes reside throughout the surface of the loosely packed chromatin. The inactive chromatin areas are often observed at the nuclear periphery (Maillet et al., 1996; Laroche et al., 2001). These "silent" domains are characterized by the presence of perinuclear mating-type loci, centromeric regions and telomeric clusters (Maillet et al., 1996; Galy et al., 2000; Jin et al., 2000).

Chromosomes are attached to microtubules, which are organized into a "fibre apparatus" of a mitotic spindle (Robinow, et al., 1966; Peterson and Ris, 1974). This attachment is mediated by kinetochores, distinct protein complexes associated with the centromeric DNA. Kinetochores move chromosomes on the spindle, thus enabling successful progression through mitosis (Nicklas, 1997).

The microtubules are nucleated by the spindle pole body (SPB), the yeast equivalent of the vertebrate centrosome (O'Toole et al., 1999; Doxsey, 2001). The SPB is a multilayered organelle that is embedded in the NE and faces both the nuclear and cytoplasmic surfaces (Bullitt et al., 1997). The microtubule extensions are visible on both nuclear and cytoplasmic sides of the SPB. Cytoplasmic microtubules function in nuclear positioning in the cell, while nucleoplasmic microtubules are responsible for chromosome movement during mitosis (Hildebrandt and Hoyt, 2000).

The nucleolus represents the site of ribosomal RNA (rRNA) synthesis, rRNA processing, and assembly of ribosomal subunits. The organelle is adjacent, and thought

to be attached, to the inner membrane of the NE (Byers, 1981). Indicative of such a physical attachment is the fact that the nucleolus has a specific orientation in the nucleus during cell growth, as it is always seen to be opposite to the spindle pole body (Clark, 1991). Nevertheless, the attachment between the nucleolus and NE does not appear to be essential either for overall nucleolar function or for ribosomal export, since yeast mutants lacking such an attachment do not exhibit ribosomal export defects (De Beus et al., 1994). Moreover, as shown by electron microscopy, ribosomal subunits are able to exit the nucleus through all the pores of the NE, not just those in contact with the nucleolus (Leger-Silvestre et al., 1999; Trumtel et al., 2000).

The yeast nucleolus possesses three morphologically distinct subcompartments similar to those found in higher eukaryotes (Trumtel et al., 2000). The fibrillar centre (FC) compartment serves as a reservoir for ribosomal DNA (rDNA) genes. The maturation of pre-rRNA transcripts occurs in the dense fibrillar component (DFC), whereas the assembly of preribosomal particles takes place in the granular component (GC) compartment (Leger-Silvestre et al., 1999).

Surprisingly, the nucleolus has recently been shown to play a direct role in the regulation of mitosis and meiosis in yeast. It sequesters certain proteins important for regulation of the cell cycle, thereby inhibiting their activity. When necessary, these proteins are released into the nucleoplasm in a regulated manner (reviewed by Visintin

and Amon, 2000; Roeder and Bailis, 2000). Similarly, a rapid and highly coordinated exchange of proteins occurs between various nuclear subcompartments.

The above section provides a brief description of nuclear structure and its relationship to various nuclear functions. Maintenance of this structure and its functional activity requires a distinct ensemble of macromolecules. Any of the numerous processes occurring in the nucleus could be affected if a certain constituent is misplaced or not delivered on time. Nuclear proteins have to be imported from the cytoplasm, while RNPs, including ribosomal subunits, need to be exported from the nucleus. Therefore, nucleo-cytoplasmic transport plays a crucial role in the regulation of nuclear functions and is essential for proper temporal and spatial organization of numerous cellular processes, including gene expression, cell division and signal transduction.

1.2. The nuclear pore complex

1.2.1. The assembly of NPCs

1.2.1.1. Regulation of the biogenesis and distribution of NPCs

The NPC consists of between ~30 (in yeast) and ~50 (in vertebrates) different nucleoporins or Nups that are sequentially assembled into a complex (Reichelt et al., 1990; Rout et al., 2000). In yeast, the NPC assembly begins during interphase and

occurs continuously throughout the cell cycle (Winey et al., 1997). The number of pores correlates with cell cycle stages increasing steadily to a maximum density in S-phase. In both yeast and vertebrates, the number of NPCs per cell is tightly regulated, depending on growth conditions, cell developmental programs, etc. (Winey et al., 1997; Kihlmark et al., 2001). For example, the cell death program includes degradation of NPCs in mammalian cells. The mechanism of NPC disassembly during apoptosis has been partially elucidated (Kihlmark et al., 2001).

Mechanisms of NPC destruction in yeast, if they exist, are not known. In yeast, cell components are known to be recycled via vacuolar autophagy, which is induced by starvation and various metabolic signals (Jones et al., 1997). Although some nuclear constituents are recycled via nucleus-vacuole junction, NPCs do not appear to be subjected to autophagy (Severs et al., 1976; Pan et al., 2000).

The distribution of NPCs within the NE depends on a distinct group of Nups encoded by the *NUP120*, *NUP133* and *NUP145* genes. Mutations in or deletions of any of these genes cause NPC clustering into one or a few regions of the NE (Wente and Blobel, 1994; Aitchison et al., 1995a; Heath et al., 1995; Pemberton et al., 1995; Belgareh and Doye, 1997). Also during mitosis, NPCs are often found concentrated in specific regions of the NE. This is visible in early mitosis in regions near spindle pole bodies (Winey et al., 1997).

Recent studies revealed that changes in expression of certain yeast nucleoporin genes, for example *NUP53*, induce the formation of intranuclear NE-like membranes that are interrupted by pores and contain two integral pore membrane proteins, Pom152p and Ndc1p (Marelli et al., 2001). These membrane structures may represent an intrinsic intermediate of NPC assembly in yeast. In addition to Nup53p, several other nucleoporins, such as Nup170p, Nup82p, Nup192p, Nic96p, and Nup57p, are known to promote formation of NPCs and to ensure proper stoichiometry of NPC constituents (Kenna et al., 1995; Marelli et al., 1998; Bucci and Wente, 1998; Kosova et al., 1999; Gomez-Ospina et al., 2000; Ryan and Wente, 2000).

1.2.1.2. Mitosis-associated changes within NPCs

Once assembled, yeast NPCs last several rounds of cell division, as yeast undergo "closed mitosis", in which the NE and NPCs remain intact (Byers, 1981). Conversely, in higher eukaryotes, NPCs are disassembled during "open mitosis", which involves breakdown of the NE. (Roos, 1973). A "semi-closed" mitosis, when NPCs disassemble while chromosomes remain enclosed within partially destructed NE, has also been observed in early *Drosophila* embryos (Stafstrom and Staehelin, 1984; Kiseleva et al., 2001). The processes of mitotic breakdown of the NE have also been extensively studied using *Xenopus* egg extracts (recently reviewed by Aitchison and Rout, 2002). Initially, it was proposed that the NE disruption and consequent disassembly of the NPC during mitosis in vertebrates is caused by phosphorylation of proteins localized to

the lamina and NPCs (reviewed by Collas and Courvalin, 2000). As shown recently, it is a pulling force created by the mitotic spindle also appears to be a major contributor to the disruption of the NE (Beadouin et al., 2002; Salina et al., 2002).

Nonetheless, a reversible phosphorylation of Nups during mitosis may still be important for the disassembly of NPCs in higher eukaryotes. Several vertebrate Nups are differentially phosphorylated during mitosis. These include Nup153, CAN/Nup214, and Nup358, which are phosphorylated throughout the cell cycle and hyperphosphorylated during M-phase, and the pore membrane glycoprotein gp210, which is dephosphorylated during interphase but specifically phosphorylated during mitosis (Macaulay et al., 1995; Favreau et al., 1996).

In yeast, cell cycle-dependent phosphorylation of Nups does not lead to NPC disassembly. However, it could alter protein-protein interactions within NPCs and therefore affect the dynamics of nucleo-cytoplasmic transport. To date, Nup53p is the only yeast Nup known to be phosphorylated in mitosis (Marelli et al., 1998). In this work, we begin to discover the functional significance of the cell cycle-dependent phosphorylation of Nup53p (see Chapter 3).

1.2.1.3. Mechanisms of the NPC assembly in higher eukaryotes

The NPC assembly is initiated by invagination of the inner and outer membranes until they meet and fuse to create a pore. Scanning electron microscopy has been

employed to study newly assembled NEs. Analysis of structural intermediates of the NPC formation in *Xenopus* egg extracts and early *Drosophila* embryos revealed dimples and holes within the NE, intermediate formations like the star ring, and more complex structures, including nearly assembled or mature NPCs (Goldberg et al., 1997, Kiseleva et al., 2001).

Recruitment of the NPC proteins during post-mitotic reassembly is a sequential process (reviewed by Bodoor et al., 1999b). It has been demonstrated that certain Nups (for example, the putative basket nucleoporin Nup153) become associated with chromatin prior to the formation of NE (Bodoor et al., 1999a, Daigle et al., 2001). The binding of Nup153 to chromatin early in anaphase, followed by its association with the membrane protein Pom121, the later sequential addition of Nup62 and Nup214 and membrane glycoprotein gp210 in telophase, is thought to constitute the first step of NPC assembly (Bodoor et al., 1999a).

1.2.2. Architecture of the NPC

The NPC is a large, octagonally symmetric, cylindrical structure which extends across the NE (Figure 1-2, p.13) (Yang et al., 1998; reviewed by Wente, 2000; Rout and Aitchison, 2001). EM studies have resolved the structural features of the vertebrate and yeast NPCs at an increasingly fine level. In 1993, Akey and Radermacher reported

the three-dimensional reconstruction of Xenopus NPCs resolved by cryo-EM technology (Akey and Radermacher, 1993). The NPC is composed of a series of concentric rings with apparent eight-fold symmetry in top view and double symmetry in side view (Unwin and Milligan, 1982; Akey and Radermacher, 1993; Goldberg and Allen, 1993; Kiseleva et al., 2000). Within the pore is the inner spoke ring, which has a central aperture of ~ 40 nm. This estimate is based on the data suggesting that facilitated translocation through the NPC is almost as effective as free diffusion through an aqueous channel of 40 nm in diameter and length (Ribbeck and Görlich, 2001). Within the channel is the central transporter, whose conformation is thought to be altered during translocation (Akey, 1990; Kiseleva et al., 1998). Eight spokes radiate out from the inner spoke ring, penetrating the pore membrane, and are joined together in the lumen by the radial arms. The cytoplasmic ring consists of a thin ring with eight subunits moulded onto it and short rod-shaped particles extending into the cytoplasm (Panté and Aebi, 1996; Rutherford et al., 1997). Internal filaments join both the cytoplasmic and the nucleoplasmic rings to each end of the central transporter (Goldberg and Allen, 1993; Kiseleva et al., 1998). In addition to these structures, the transport is also dependent on the peripheral elements of the NPC, including distinct sets of cytoplasmic, and nuclear filaments (Meier and Blobel, 1992; Cordes, 1997). The distal ends of nuclear filaments are connected and form a basket-like structure, which is

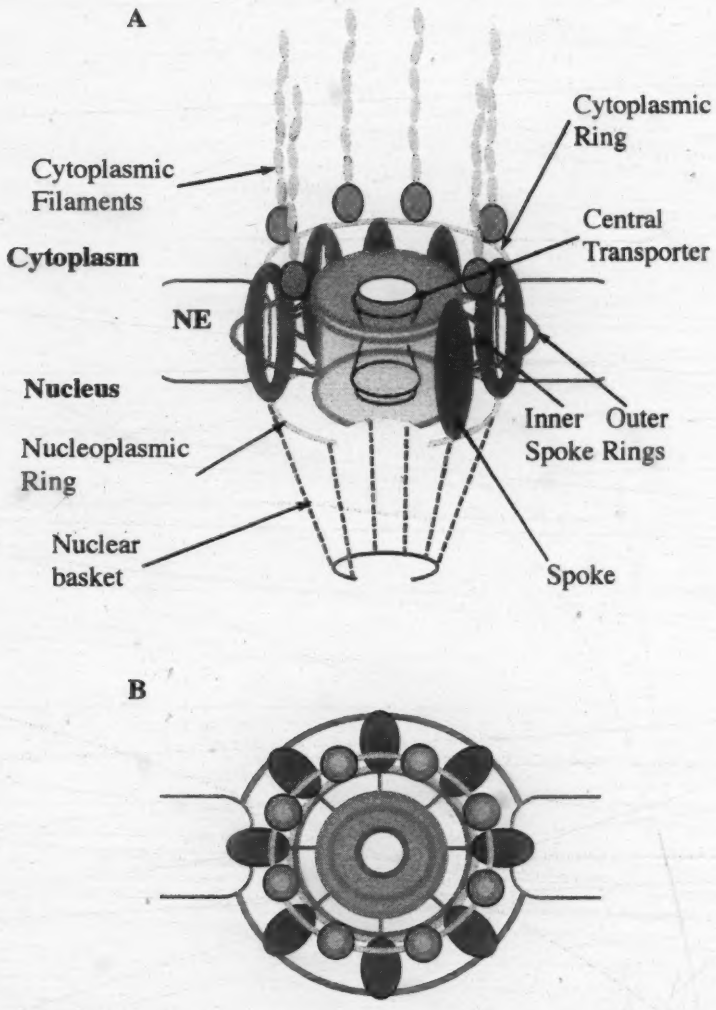

Figure 1-2. Structure of the nuclear pore complex. The model is based on a three dimensional reconstruction of the NPC resolved by scanning electron microscopy (Akey and Radermacher, 1993) and is adapted from Wente, 2000; and Rout and Aitchison, 2001. A) *Cross-section perpendicular to the nuclear envelope.* A central core consists of a central transporter surrounded by eight spokes connected to each other with four coaxial rings. A portion of each spoke is integrated into the NE lumen. Cytoplasmic filaments and nuclear basket constitute peripheral elements of the NPC and contribute to directionality of the nuclear transport. B) *View from the cytoplasm,* showing a symmetrical octagonal structure of the NPC.

thought to bridge the NPC with the nucleoskeleton (Goldberg and Allen, 1992).

NPCs from different organisms share a common fundamental architecture. However, yeast NPCs are smaller than those of vertebrate cells (~30 nm in thickness for yeast vs. the ~70-80 nm for *Xenopus* NPCs) (Rout and Blobel, 1993). The smaller dimensions may reflect the absence of cytoplasmic and/or nuclear ring structures in yeast and suggest actual differences in protein composition between yeast and other eukaryotic NPCs (Rout and Blobel, 1993; Rout et al., 2000).

1.2.3. Components of the yeast nuclear pore

Nucleoporins can be divided into three groups: those that span the nuclear membrane (pore membrane, Poms, non-membrane proteins that contain multiple repeats of phenylalanine-glycine-containing (FG, FXFG or GLFG) motifs, and non-membrane nucleoporins that lack FG-repeats. Some other proteins, including transport cofactors and shared-function proteins, are also associated with NPCs.

Pom152p and Pom34p are two integral membrane proteins found exclusively in the yeast nuclear pore, while Ndc1p an Cdc31p are present in both yeast nuclear pores and spindle pole bodies (Wozniak et al., 1994; Chial et al., 1998; Rout et al, 2000). Integral membrane proteins associated with the NPC are thought to play an important

role in the molecular organization of the NPC and its biogenesis, since they anchor NPCs to the NE.

In yeast, the positioning of the different Nups within the NPC has been roughly determined. Immunoelectron microscopy of the NEs allowed evaluation of surface-accessible locations of proteinA-tagged Nups within the NPC (Marelli et al., 1998; Rout et al., 2000). Since antibodies cannot access the tightly packed interior of the pore structure, the obtained map of the yeast Nups distribution is thought to correspond predominantly to exposed edges of the nuclear pore (Figure 1-3, p.17) (Vasu and Forbes, 2001). To date, the exact subset of Nups that form spokes of the major scaffold of the pore is not known. The immunoelectron microscopy data suggest that Nup57p, Nup170p, Nup188p and Nup192p could be nearest to the central plane of the pore (Marelli et al., 1998; Rout et al., 2000). Furthermore, Nup170p and Nup188p are thought to play a direct role in establishing the resting diameter of the central transporter, because yeast mutants deleted for Nup188p or Nup170p show higher rates of passive diffusion (Shulga et al., 1996).

Alternative electron microscopy techniques have also been considered. For instance, the employment of pre-embedding immunogold electron microscopy established that yeast Nsp1p is a member of three different subcomplexes that map to three separate sections of the yeast pore (Fahrenkrog et al., 1998).

1.2.3.1. FG-Nups and their role in the passage through the NPC

Roughly one-third of Nups carry FG repeat motifs. These FG-containing nucleoporins function as docking sites for cargo-containing complexes (see section *1.2.5.2*, p.22) (Ryan and Wente, 2000; Allen et al, 2001). Although the majority of FG-Nups can be found on both nuclear and cytoplasmic sides of the NPC, some of them exhibit a biased localization, which is thought to contribute to the directionality of nuclear transport (Rout et al., 2000). For instance, the importin-cargo binding Nup1p and Nup2p-Nup60p are found exclusively on the nuclear basket of the yeast pore (Hood et al., 2000; Rout et al., 2000; Dilworth et al., 2001). Such bias has been proposed to define a directionality of transport in the following way: import complexes appear to show a greater affinity to nups in the nuclear basket than to Nups located on the cytoplasmic side of the pore (reviewed by Vasu and Forbes, 2001). Therefore, it has been hypothesized that transport complexes move through NPCs in a stepwise manner, hopping along a path of increasing affinity (also see section *1.2.5.4*, p.27) (Rexach and Blobel, 1995).

Nevertheless, a greater number of FG-Nups is found to be symmetrically located on both sides of the pore. For example, Nup53p, which is engaged in the NPC subcomplex consisting of Nup53p, Nup59p, Nup157p, and Nup170p, functions as a docking site for the import receptor Kap121p (Marelli et al., 1998). It has been shown

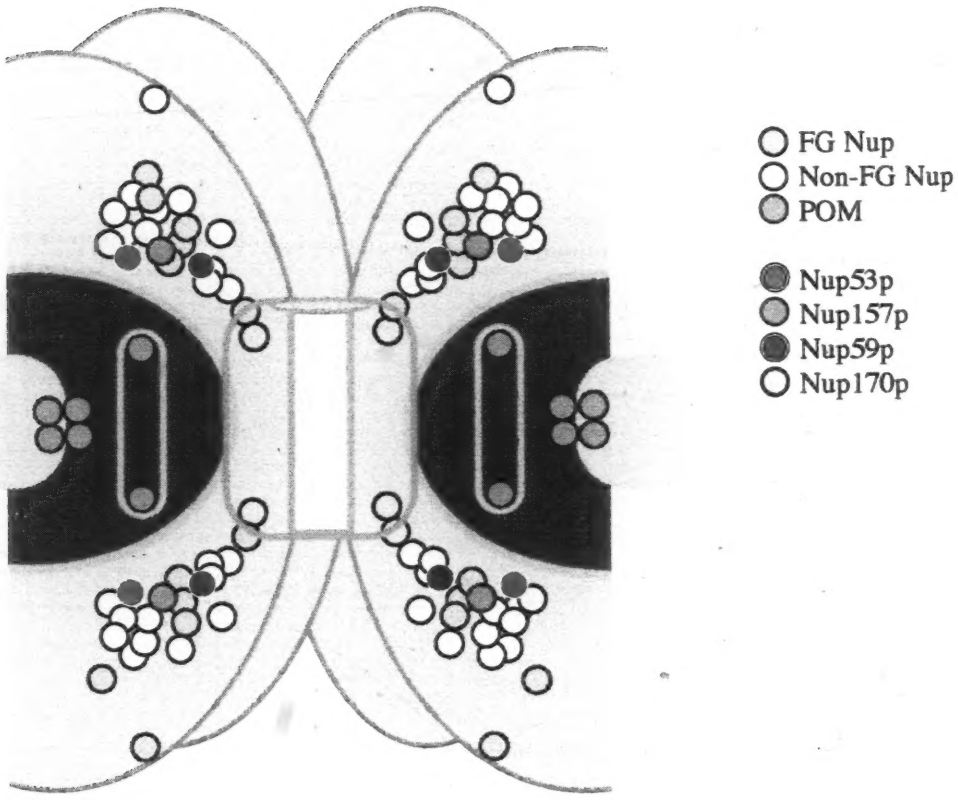

Figure 1-3. Positioning of NPC-constituents. This model shows relative surface-accessible locations of the yeast NPC proteins based on the results of immunoelectron microscopy (Rout et al., 2000). The localization of protein A-tagged NPC-constituents was determined by immunogold labeling. Images were superimposed, and the positions of proteins were determined relative to the NPC cylindrical axis. Figure adopted from Rout et al., 2000. Note the positioning of the nucleoporins of interest, namely Nup53p, Nup157p, Nup59p and Nup170p.

that Nup170p binds to a region of Nup53p that overlaps with the Kap121p binding site and thus competes with Kap121p for binding to Nup53p (Lusk et al., 2002). Consequently, the association of Nup53p with Nup170p is thought to drive the binding and release of Kap121p from Nup53p (Lusk et al., 2002). Thus, not only positioning of FG-Nups at the NPC, but also their interchangeable interactions with other NPC constituents could define the flow of nucleo-cytoplasmic trafficking.

To explain the general role of FG-Nups in movement through the NPC, two principal models have been proposed (Rout et al., 2000; Ribbeck and Görlich, 2001). Both of them state that FG-repeat Nups present a significant barrier to the passive, non-selective diffusion of macromolecules. These models, however, differ in their interpretations of the translocation mechanism.

According to the Brownian affinity gate model (Rout et al., 2000), the NPC channel has a narrow functional diameter and, therefore, large macromolecules are unlikely to enter the channel via random diffusion. On the other hand, the FG-repeat binding substrates increase their occupancy time at the entrance of the channel, because they are docked at the NPC, and therefore are more likely to pass through (Rout et al., 2000).

According to the selective phase translocation model (Ribbeck and Görlich, 2001), interactions between FG-Nups create a meshwork, which acts as a sieve, allowing only

the passage of small molecules. For large molecules, the mesh would become a hydrophobic barrier, excluding them unless they are able to interact with FG-repeats. Only the FG-repeat interacting proteins and their complexes would be soluble in the hydrophobic phase and thus, would be efficiently translocated (Ribbeck and Görlich, 2001). This hypothesis is supported by a recent report demonstrating that a simple hydrophobic interaction column can mimic the selectivity of NPCs (Ribbeck and Görlich, 2002). Furthermore, the interference with hydrophobic interactions between FG-Nups, i.e. by using small amphipathic compound hexanediol, destroys the NPC permeability barrier (Ribbeck and Görlich, 2002).

Though attractive, both models have their weaknesses (reviewed by Rabut and Ellenberg, 2001; Vasu and Forbes, 2001). The Brownian affinity gate model does not account for the translocation of the large particles (up to 36nm diameter) that have been shown to pass through the NPC efficiently. The same argument is valid for the selective phase model, since even a wide hydrophobic channel would exclude fairly large diffusing substrates. In order to suppress the latter argument, Ribbeck and Görlich propose that large cargo may require more than one transport receptor molecule for rapid translocation. However, this idea remains to be tested (Ribbeck and Görlich, 2002).

1.2.3.2. Other NPC-associated proteins

In addition to FG-Nups, non-FG-Nups, and Poms, yeast NPC accommodates a group of proteins that do not appear to be associated with NPC transport functions. These, for example, include myosin-like proteins Mlp1p and Mlp2p that are attached to nuclear filaments of the pore (Strambio-de-Castillia et al., 1999; Rout et al., 2000). In the course of this work, we have identified two additional NPC constituents. These are mitotic spindle checkpoint proteins Mad1p and Mad2p (see Chapter 3).

1.2.4. Evolutional conservation and divergence of NPC constituents

Sequence comparison of *S. cerevisiae* and vertebrate Nups has led to the identification of homologous Nups. Consequently, a few evolutionarily conserved NPC subcomplexes have been characterized (reviewed by Belgareh and Doye, 1997; Vasu and Forbes, 2001).

Among the ~23 vertebrate Nups identified so far, only a few exhibit considerably strong homology to their vertebrate counterparts (reviewed by Fabre and Hurt, 1997; Ryan and Wente, 2000; Vasu and Forbes, 2001). These include Nic96p (vNup93), Nsp1p (vNup62), Gle1p and Gle2p. Yeast GLFG nucleoporins Nup145Np, Nup116p and Nup100p resemble blocks of the single mammalian GLFG nucleoporin, Nup98 (Fontoura et al., 1999). Conserved versions of yeast paralog nucleoporins

Nup157p/Nup170p were found in many species, including *Homo sapiens*, *Mus musculus*, *Rattus norvegicus*, *Fugu rubripes*, *Arabidopsis thaliana*, *Drosophila melanogaster* (Aitchison et al., 1995b; Gigliotti et al., 1998; Zhang et al., 2002). Some yeast Nups, for example Nup53p and Nup59p, have distant homologues in *Schizosaccharomyces pombe*, *H. sapiens*, *M. musculus*, *X. laevis*, *Caenorhabditis elegans*, and *A. thaliana*, though specific structural domains of these ORFs show the higher degree of the cross-species similarity (Marelli et al., 1998). Yeast Pom152p and Pom34p, though without sequence relatives, may have functional orthologs such as Pom121 or gp210 in other species (Vasu and Forbes, 2001). Similarly, Nup153, Nup214 and Nup358 in vertebrates have no sequence homologues in yeast. Nonetheless, yeast FG-Nups, being localized to the nucleoplasmic side of the NPC (Nup1p, Nup2p, Nup60p and Nup159p), could be viewed as functional orthologs of the vertebrate Nups mentioned above (Ryan and Wente, 2000; Vasu and Forbes, 2001).

Although NPCs of yeast and vertebrates are composed of structurally different proteins, certain NPC subcomplexes have been conserved throughout evolution. For example, the yeast subcomplex, containing Nup84p-Nup133p, is thought to be an equivalent of the hNup133-hNup107 complex identified in mammalian cells (Belgareh et al., 2001). Of note, during mitosis, a fraction of hNup133 and h107 localizes to the

kinetochores. This observation was among the first ones to indicate a direct connection between mitotic apparatus and NPC constituents.

1.2.5. Mechanisms of the nucleo-cytoplasmic transport

1.2.5.1. Passive diffusion

Small cargo molecules (< 20-40 kDa) can pass through the NPC by diffusion (Paine et al., 1975). Passive diffusion does not require any specific interaction between the cargo molecule and components of the NPC. In contrast, facilitated translocation, which permits the passage of large molecules or complexes, depends on specific interactions between transport receptors and Nups.

1.2.5.2. Active nuclear transport and its receptors

Active nuclear transport is a highly selective process. Only nuclear transport receptors possess the translocation-promoting properties that allow direct interaction with the NPC. These transport receptors are called karyopherins (from Greek: karyo –nucleus; phere–(to) bear) (Radu et al., 1995). Karyopherins (Kaps) are responsible for substrate recognition, targeting of the transport complex to the NPC and vectorial movement through the NPC (reviewed by Cörlich and Kutay, 1999; Nakielny and Dreyfuss, 1999; Wente, 2000; Macara, 2001).

Kaps recognize specific *cis*-acting signal sequences on surfaces of cargo molecules. These signal sequences are termed the nuclear localization signals (NLSs) if they direct the import of cargo into the nucleus, and the nuclear export signals (NESs) if they direct the export of cargo out of the nucleus (Bonnerot et al., 1987; Dingwall and Laskey, 1991; Gerace, 1995). Accordingly, depending on the direction in which they carry a cargo, Kaps are classified as importins, which bind to the NLS, or exportins, which bind to the NES (Görlich et al., 1994; Stade et al., 1997). Kap α, also known as importin α (Kap60 in yeast) recognizes a variety of classical NLSs (cNLSs), including the basic monopartite SV40 T antigen NLS (PKKKRKV), more hydrophobic monopartite c-myc NLS (PAAKRVKLD) and bipartite nucleoplasmin NLS (VKRPAATKKAGQAKKKKLD) (Conti and Kuriyan, 2000; reviewed by Conti and Izaurralde, 2001; Komeili and O'Shea, 2001). Kap α functions as an adapter protein: it interacts with Kap β1 (Kap95 in yeast), which docks the importin-cargo complex to the NPC (Görlich et al., 1994; reviewed by Mattaj and Englmeier, 1998; Görlich and Kutay, 1999; Nakielny and Dreyfuss, 1999; Conti and Izaurralde, 2001).

Over the past several years, other import pathways, involving transport substrates with NLSs distinct from the cNLSs, have been identified. Unlike the canonical NLS, which interacts with Kap β via Kap α, the non-classical NLSs have diverse sequences and bind directly and specifically to different β–Kaps. The superfamily of β–Kaps

constitutes a major class of nuclear transport receptors (reviewed in Wozniak et al., 1998; Ohno et al., 1998). To date, this family includes 14 members in *S.cerevisiae* and at least 22 members in vertebrates (reviewed by Görlich and Kutay, 2001; Strom and Weis, 2001). β–Kaps contain tandems of helices called HEAT repeats (so named after the proteins in which the motif was first identified, including huntingtin, elongation factor 3, A subunit of protein phosphatase A and lipid kinase Tor1p) (reviewed by Chook and Blobel, 2001; Conti and Izaurralde, 2001). The HEAT repeats are able to rearrange relative to each other, thereby ensuring structural plasticity of β–Kaps. As a result, β–Kaps are able to adopt a variety of conformations and consequently bind to more than one type of NLS within many different substrates. To date, only a few non-classical NLSs have been characterized. Their identification is difficult, because these NLSs are largely defined by three-dimensional epitopes on protein surface, rather than by linear amino acid sequences (Chook and Blobel, 2001).

Members of the β–Kap family also mediate export of proteins containing NESs (reviewed by Nakielny and Dreyfuss, 1997; Chook ad Blobel, 2001). The best-studied exportins are Crm1 (Xpo1p in yeast), which exports a wide variety of cargoes, and Tap-1 (Mex67p in yeast), which is required for the mRNA export (Fornerod et al., 1997; Gruter et al., 1998; Stade et al., 1997). An initial step in protein export from the nucleus involves the binding of the NES-containing cargo protein to the exportin. Unlike

importins, all known export receptors bind their cargoes only in the presence of Ran-GTP (reviewed by Görlich and Kutay, 1999; Macara, 2001).

1.2.5.3. Ran and its role in nucleo-cytoplasmic transport

Ran (Ras-related nuclear protein; Gsp1p in yeast) is a member of the Ras superfamily of proteins that regulates cell growth and proliferation (Bischoff and Postingl, 1991). This protein exists in two states, the GDP-bound and GTP-bound. Under steady state conditions, Ran predominantly localizes to the nucleus (Quimby et al., 2000; Kunzler and Hurt, 2001). Its import into the nucleus depends on the nuclear transport factor 2 (NTF2) (Figure 1-4, p.27) (Ribbeck et al., 1998).

The energy gradient across the NE and the directionality of transport are established by the separation of two pools of Ran, with Ran-GTP present in the nucleus and Ran -GDP distributed in the cytoplasm (reviewed by Görlich and Kutay, 1999). By inverting the normal Ran gradient, it is possible to reverse the usual direction of movement of transport carriers through the pores (Nachury and Weis, 1999). The process of active translocation through the NPC does not require the energy of GTP hydrolysis by Ran (Schwoebel et al., 1998). Instead, Ran acts as a molecular switch that triggers, depending on its nucleotide-bound state, the disassembly of the transport complexes (reviewed by Moore, 1998; Macara, 2001). The Ran-GDP to Ran-GTP interconversion is regulated by a GTPase-activating protein (GAP) in the cytoplasm

and by a guanine-nucleotide exchange factor (GEF) in the nucleus (Bischoff and Postingl, 1991; Bischoff et al., 1995) (Figure 1-4, p.27).

The trimeric complex of exportin/cargo/Ran-GTP translocates to the cytoplasm where it dissociates upon the hydrolysis of Ran-bound GTP. The GTP hydrolysis by Ran is induced by the cytoplasmic Ran-GTPase –activating protein (Ran-GAP) and the Ran-binding protein 1(Ran-BP1) (Bischoff et al., 1995; Kehlenbach et al., 1999).

These transport systems are capable of transporting large number of cargoes through the NPC, with the maximal translocation rates reaching the order of 10^3 transfer events per second (Ribbeck and Görlich, 2001).

1.2.5.4. Multiple transport pathways: specificity of interactions between the Nups and Kaps

Differential interactions between Kaps and Nups define multiple transport pathways through the NPC. Within these pathways, karyopherins bind preferentially to distinct nucleoporins. For example, Kap121p is the only β-Kap that binds to Nup53p suggesting that Nup53p acts as a specific Kap121p docking site (Marelli et al., 1998). Kap121p can be released from Nup53p by the GTP bound form of Ran. Remarkably, *NUP53* mutations alter the subcellular distribution of Kap121p and the Kap121p-mediated import of a ribosomal Rpl25p reporter protein (Marelli et al., 1998).

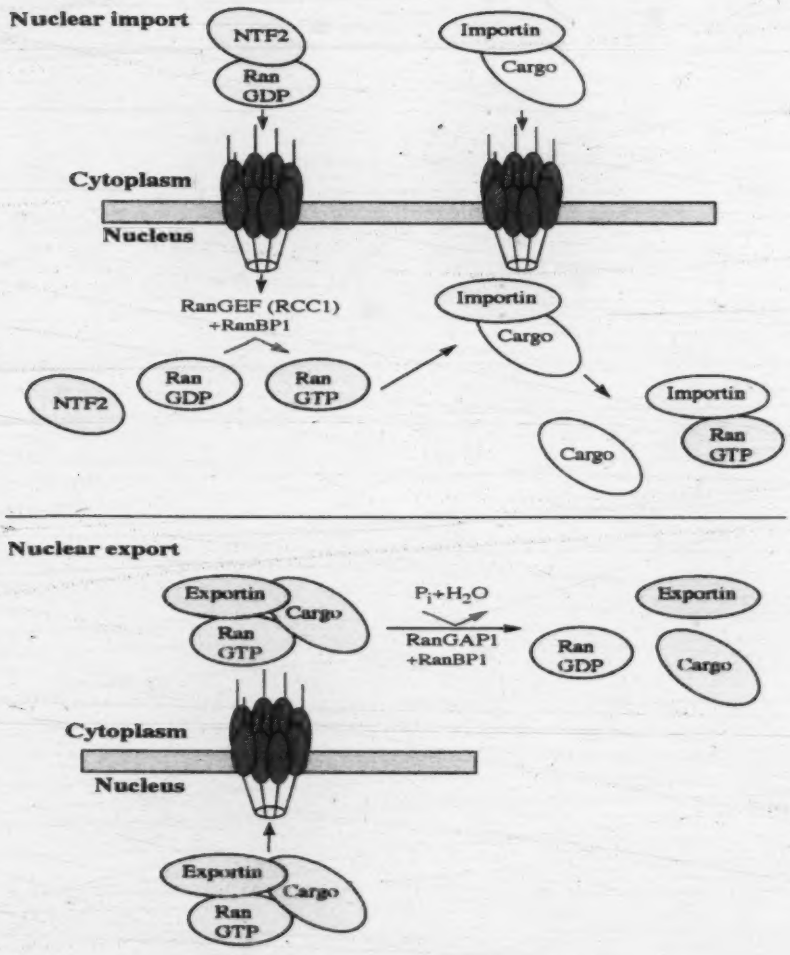

Figure 1-4. A simplified schematic of nuclear transport. The directionality of nuclear transport depends on the RanGTP gradient. *Nuclear import.* The nuclear transport factor NTF2 binds to the GDP-bound form of Ran and mediates its import into the nucleus, where Ran nucleotide exchange factor of Ran (GEF) converts Ran-GDP to Ran-GTP. Importins* bind to their cargoes in the cytoplasm and direct their nuclear import. Once the "importin-cargo" complex is transported into the nucleus, Ran-GTP binds to an import receptor causing the release of the cargo. *Nuclear export.* In the nucleus, an export receptor forms a complex with its cargo in the presence of RanGTP. The triple complex is exported from the nucleus. In the cytoplasm, the RanGTPase activating protein (RanGAP) promotes the hydrolysis of GTP on Ran, stimulating the dissociation of the export complex in the cytoplasm. Elements of this model were adopted from Kaffman and O'Shea, 1999; Künzler and Hurt, 2001.

*-for simplicity, the importin heterodimer is shown as a single module.

In order to elucidate nuclear transport pathways, a variety of experimental approaches have been employed. One of them involves measuring fluorescence resonance energy transfer (FRET) (Stryer, 1978). This technique utilises the ability of excited donor fluorophore to transfer energy to an acceptor under very specific conditions. These include a donor–acceptor separation of ~10–100 Å and a specific relative orientation of the donor and acceptor (Clegg, 1996). In order to assess the specificity of Kap-Nup interactions, FRET levels were determined between Kap fusions to cyan fluorescent protein (CFP) and Nup fusions to yellow fluorescent protein (YFP) in yeast (Damelin and Silver, 2000). Although FRET data supply helpful information, they do not specify whether the observed interactions indicate several distinct transit routes through the pores or suggest specific docking sites.

In an attempt to clarify this uncertainty, Allen and co-workers conducted a series of affinity-capture experiments, aimed to determine relative affinity of different Nups to their binding proteins, including Kaps (Allen et al., 2001). Their results revealed the existence of a hierarchy of binding sites provided by FG Nups. For example, the exportin Crm1p exhibits little or no binding to FG Nups in the nuclear basket and intermediate binding to FG Nups of the central transporter region (i.e. Nup49p, Nup57p, Nup100p, and Nup116p). However, it binds to Nup42p, a component of cytoplasmic fibrils at the opposite end of the NPC. A similar order of interactions,

known as an "affinity trap" is thought to aid the movement of importins across the NPC, but in the opposite direction (described in section *1.2.3.1*, p.18). The latter is true at least for the Kap123p and Kap95p-Kap60p heterodimer, which preferentially bind to FG-Nups on the nucleoplasmic side of the NPC. Nonetheless, the data obtained by Rexach's group suggested that not all importins bind with high affinity to the nuclear basket Nups, as predicted by the model, and raised the question about the existence of alternative mechanism of passing through the NPC (Allen et al., 2001). One of the hypotheses is that Nups interact asymmetrically with each other within the pore to create tracks specific for certain import complexes (Marelli et al., 1998). Such a mechanism would not only guarantee a directionality of transport, but would also account for the pathway specificity. This hypothesis has been supported by the isolation of the Nup53p-Nup59p-Nup170p subcomplex that binds specifically to the Kap121p, but fails to bind to the closely related Kap123p or importin β/Kap95 (Marelli et al., 1998).

1.2.6. The NPC is a multifunctional complex

1.2.6.1. Alternative functions of nucleoporins

Recent studies suggest that the NPC also has a broad range of functions that extend beyond its role in the regulation of nucleoplasmic transport (Chial et al., 1998; Galy et al., 2000; Kosova et al., 2000; Kerscher et al., 2001).

In yeast cells, the NPC extensions are thought to participate in the structural and functional organization of perinuclear chromatin. Defined by the presence of telomere clusters, "silent" perinuclear chromatin domains constitute areas of transcriptional repression and are connected to the NPC via the NE-attached intranuclear filaments (Cordes et al., 1997; Galy et al., 2000; Feuerbach et al., 2002). In yeast, this attachment requires at least two nucleoporins, Nup145p and Nic96p (Galy et al., 2000; Kosova et al., 2000). It remains unclear whether the NPC-constituents play a direct role in transcriptional silencing, as some recent findings suggest that the localization of a telomeric region to the nuclear periphery is not sufficient for its transcriptional repression (Tham and Zakian, 2000; Eissenberg, 2001; Tham et al., 2001). Nonetheless, an inherent link between telomere localization and nuclear pore complexes has been clearly demonstrated.

A direct connection between NPCs and the mitotic apparatus was revealed by studies of the *NDC1* gene. Ndc1p is a NE membrane protein that localizes to both NPCs and SPBs and plays a direct role in the assembly of these macromolecular complexes (Chial et al., 1998). Ndc1p function is required for proper spindle pole body duplication during S-phase (Byers, 1993). Mutations in the *NDC1* gene affect duplication of the spindle pole body. The negative effect of these mutations could be

suppressed by deletion of the *POM152* gene encoding the other integral membrane constituent of the NPC.

NPC constituents may be involved in chromosome segregation. In fact, recent studies demonstrated that both the *nup170-141* mutation and deletion of the nucleoporin-encoding gene *NUP170* cause a defect in chromosome transmission fidelity (*ctf-*) (Kerscher et al., 2001). Due to this defect, chromosome loss in *nup170* mutants was increased ~100-fold, while chromosome nondisjunction was enhanced ~10-fold. Remarkably, a Nup170p paralogue, Nup157p, partially suppresses the *ctf-* phenotype caused by *nup170* mutations (Kerscher et al., 2001). Nup157p and Nup170p are, in part, functionally redundant and evolutionary conserved nucleoporins that are homologous to the mammalian Nup155 and to the Nup154 of *Drosophila melanogaster*. The *Nup154* gene is essential (Gigliotti et al., 1998). In yeast, lack of both Nup157p and Nup170p is lethal (Aitchison et al., 1995b).

It has been demonstrated that hypomorphic mutant alleles of the *Drosophila Nup154* gene impair female and male fertility by affecting spermatocyte proliferation, meiotic progression and oocyte development (Gigliotti et al. 1998; Kiger et al., 1999). Interestingly, unlike its yeast and mammalian counterparts, Nup154p exhibits the intranuclear localization and colocalizes with chromatin at certain stages of ovum development (Gigliotti et al., 1998).

Both yeast paralogues, Nup157p and Nup170p, are localized to the NPC throughout the cell cycle (Aitchison et al., 1995b; Kerscher et al., 2001). Nup170p was shown to be associated with two structurally related FG-repeat nucleoporins, Nup53p and Nup59p (Marelli et al., 1998). One of these FG-repeat nucleoporins, Nup53p, also interacts with Nup157p (Chapter 3).

In this study, we demonstrate that the entire Nup53p-containing complex is involved in the regulation of chromosome transmission fidelity. The mechanism of this involvement will be described in Chapter 3.

1.2.6.2. Multiple roles of importins and Ran

Ras-related GTPases regulate a variety of processes defining cell growth and differentiation. Until recently, the small GTPase Ran has been mainly known for its role in nucleo-cytoplasmic transport. Ran shuttles between the nucleus and cytoplasm, exchanging between the GTP- and GDP-bound forms. Studies in *X.laevis* have shown that Ran-GTP directly regulates microtubule polymerization (reviewed by Kahana and Cleveland, 2001; Moore, 1998; Künzler and Hurt, 2001; Moore, 2001). This effect of Ran may be mediated by β-Kap, which may inhibit spindle formation by sequestering microtubule assembly factors (Nachuri et al., 2001). Activities of at least two microtubule-organizing components, NuMa and TPX2, rely on Ran. During mitosis,

Ran-GTP is found in close proximity to chromosomes where it associates with importins and causes the release of NuMa and TPX2, thereby allowing microtubule polymerization (Nachury et al., 2001; Gruss, et al., 2001).

In addition to its role in nucleo-cytoplasmic transport and microtubule formation, Ran-GTP is also required for the assembly of the NE. The NE formation requires both GTP hydrolysis by Ran and, subsequently, nucleotide exchange, since the absence of either Ran-GAP or GEF is shown to abolish the assembly of NEs (Zhang and Clarke, 2001). The exact mechanism for the involvement of Ran in the NE assembly remains to be elucidated.

The discoveries of novel roles for Ran have established unexpected connection between nucleo-cytoplasmic transport, microtubule assembly and post-mitotic formation of the NE. These links extend much further. For instance, the results of this study suggest that certain NPC-constituents are directly involved in the regulation of mitosis and, more specifically, in the mitotic spindle checkpoint.

1.3. The mitotic spindle checkpoint

1.3.1. Chromosome segregation defects

The accurate transmission of genetic material from the mother to daughter cells is the most demanding process during the cell cycle. The unequal distribution of sister

chromatids during mitosis or meiosis produces aneuploid daughter cells. Aneuploidy in human meiotic cells has been shown to result in severe congenital syndromes. Aneuploidy also plays an important role in tumorogenesis of somatic mitotic cells, since the aneuploidy-associated chromosome instability precedes cell transformation (Cahill et al., 1998). Abnormal chromosome number is a common feature of malignant tumor cells.

Aneuploidy is caused by the appearance of so-called "lagging" chromosomes that are left behind during mitosis, while other sister chromatids move to their spindle poles (Cimini et al., 2001). Historically, the identification of lagging chromosomes raised important questions regarding errors in chromosome segregation and the mechanism responsible for their prevention.

1.3.2. Yeast cell cycle and the mitotic spindle

Spindle morphogenesis in *S.cerevisiae* is initiated by the execution of START at the G1-S transition of the cell cycle (Lew et al.,1997). Progression through START triggers bud emergence, duplication of the SPB and DNA replication (Figure1-5, p.37). Multisubunit complexes termed "cohesins" establish connections between the replicated sister chromatids (reviewed by Nasmyth et al., 2000; Amon, 2001).

Spindle assembly begins when DNA replication and SPB separation are nearly completed (O'Toole et al., 1999). Structurally, the spindle is presented by an array of microtubules with their minus ends anchored at the SPB and their plus ends pointed towards the nucleoplasm (reviewed by Winey et al., 1995, Wittman et al., 2001). Microtubules are formed by the polymerization of αβ-tubulin dimers.

In prometaphase, sister chromatids of each duplicated chromosome form bipolar attachments with the microtubules. Recent studies suggest that centromere-bound cohesin is important for this attachment (Tanaka et al., 2000). During the metaphase to anaphase transition, cohesin prevents sister chromatids from separation and thereby creates a dynamic tension between microtubules and centromeres (reviewed by Nasmyth et al., 2000).

Chromatid separation is promoted by the proteolytic cleavage of the cohesin subunit Scc1p, executed by the Esp1p (separin) protease (recently reviewed by Amon, 2001). Esp1p is also required for the elongation of mitotic spindle (Jensen et al., 2001).

The dual activity of the Esp1p is regulated via its association with Pds1p (Premature dissociation of sisters) factor (Ciosk et al., 1998). Recent studies demonstrate that Pds1p is required for the nuclear targeting of Esp1p and for its localization to the spindle apparatus (Jensen et al., 2001). On the other hand, Pds1p

inhibits proteolytic activity of Esp1p, thereby preventing premature sister chromatid separation (Ciosk et al., 1998). Ultimately, Pds1p destruction during the metaphase to anaphase transition (see sections *1.3.3-4*) releases Esp1p and thus initiates chromosome segregation (Zacharie and Nasmyth, 1999; Nasmyth et al., 2000).

Chromosome segregation is completed at the end of anaphase, when the spindle stretches for up to 10 μm in length thereby greatly increasing the pole-to-pole distance (reviewed by Winey and O'Toole, 2001). This extended spindle is formed by fewer (2-6) microtubules, none of which are attached to chromatids. In contrast, the chromatid-bearing microtubules shorten to allow chromatin concentration near the poles (Winey et al., 1995). The mechanism regulating these selective changes in microtubule length is presently unknown.

In order for cells to exit mitosis, the mitotic spindle must be disassembled. The newly formed cells will contain a single SPB with short microtubules which are thought to remain from the previous round of cell division (Winey and O'Toole, 2001). The disassembly of the spindle is preceded by proteolysis of mitotic cyclins (Li, 2000). The degradation of cyclins is also necessary for the SPB to enter a new round of duplication in the next cell cycle (Hoyt, 2000).

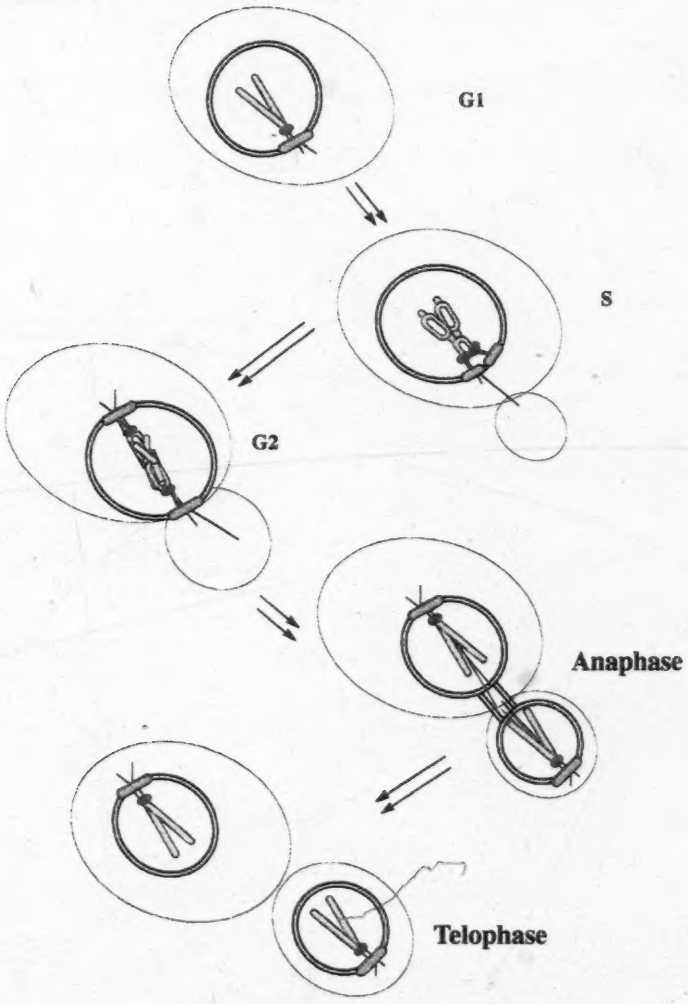

Figure 1-5. Schematic diagram of the yeast cell cycle. G1 or early **S** phase: the cycle begins with bud emergence, DNA replication and duplication of the SPB. **G2:** spindles align along the cell polarity axis, and sister chromatids are pulled to opposite poles. The nucleus migrates to the bud neck. **Anaphase:** the spindle increases in length and sister chromatids separate. **Telophase** and **exit from mitosis:** chromosome segregation is complete, the spindle disassembles, and cells complete cytokinesis.
Note: 1) yeast cells undergo a closed mitosis (i.e., the NE remains intact);
2) in yeast, chromosomes are attached to microtubules throughout most of the cell cycle.

1.3.3. The spindle checkpoint

The spindle checkpoint restrains cells from entering anaphase until all replicated chromatids have been properly attached to the mitotic spindle. Each chromatid is connected to spindle microtubules via the kinetochore (reviewed by Skibbens and Hieter, 1998; Kitagawa and Hieter, 2001). Chromatid separation and subsequent cytokinesis are delayed until all chromosomes achieve bipolar attachment. Anaphase progression is also impaired by defects in spindle assembly caused by microtubule-disrupting drugs such as benomyl and nocodazole (Straight and Murray, 1997).

The process of chromatid-microtubule attachment is well understood in vertebrate cells. Early in mitosis, a chromosome moves along the spindle in order to establish bivalent contacts with microtubules. Once attached to microtubules, a chromosome is pulled to the metaphase plate (for review see Brunet and Vernos, 2001). Microtubule dynamics cause aligned chromosomes to vibrate (reviewed by Wittmann et al., 2001). These oscillatory movements place sister chromatids under strong tension. This tension is essential for proper chromosome disjunction. It also signals to block the spindle assembly checkpoint. The exact mechanism of this inhibition remains to be established.

The attachment of microtubules to the kinetochore is mediated by a distinct set of motor-like proteins, including CENP-E, a kinesin that establishes a contact between spindle microtubules and the checkpoint proteins (Wood et al., 1997; for review see

Brunet and Vernos, 2001) (Figure 1-6, p.41). Defects in CENP-E function weaken the microtubule-kinetochore binding and impair chromosome segregation, thereby resulting in mitotic arrest (McEwen et al., 2001).

The checkpoint pathway transmits a signal generated by kinetochores that lack proper attachment to microtubules (reviewed by Kitagawa and Hieter, 2001). A specific subset of checkpoint proteins (described below) bind to improperly attached kinetochores and block entry into anaphase (reviewed by Page and Hieter, 1999). Anaphase progression requires the proteolytic destruction of Pds1p, an anaphase inhibitor that regulates sister chromatid cohesion (described in section **1.3.2**, p.35; Zacharie and Nasmyth, 1999). The degradation of Pds1p is dependent on the ubiquitin protein ligase known as the anaphase promoting complex (APC) (reviewed in detail by Page and Hieter, 1999). The APC is involved in regulating progression through mitosis at two different stages: at the metaphase to anaphase transition (for Pds1p degradation) and when exiting from mitosis (for mitotic cyclin degradation). In the context of this study, we are focused on the metaphase to anaphase transition. The specificity of the APC towards Pds1p is conferred by Cdc20p, a WD-repeat protein that activates the APC at the end of metaphase (reviewed by Page and Hieter, 1999). Binding of a distinct subset of checkpoint proteins (described in section **1.3.4,** p.42) to Cdc20p

blocks activation of the APC and therefore prevents the segregation of sister chromatids (Shah and Cleveland, 2000; Sudakin et al., 2001, Tang et al. 2001) (Figure 1-6, p.41).

1.3.4. The spindle checkpoint proteins

Mitotic arrest caused by microtubule depolymerizing agents impairs the transition from metaphase to anaphase (reviewed by Amon, 1999). In yeast, the *bub* (budding uninhibited by benzimidazole, Hoyt et al., 1991) and *mad* (mitotic arrest deficient, Li and Murray, 1991) mutants fail to arrest in mitosis when treated with benzimidazoles, and consequently enter anaphase without a functional spindle. This in turn leads to chromosome loss and cell death. Moreover, mutations in the *MAD* and *BUB* genes increase the chromosome loss rate even in the absence of spindle defects, suggesting that their encoded protein products may regulate the anaphase progression during physiologically normal cell cycles (Hoyt et al., 1991; Li and Murray, 1991). The mitotic checkpoint proteins are involved in alternating pair-wise interactions throughout the cell cycle, suggesting the existence of an interdependent regulatory complex (Chen et al., 1999; Brady and Hardwick, 2000; Hardwick et al., 2000; reviewed by Gardner and Burke, 2000)

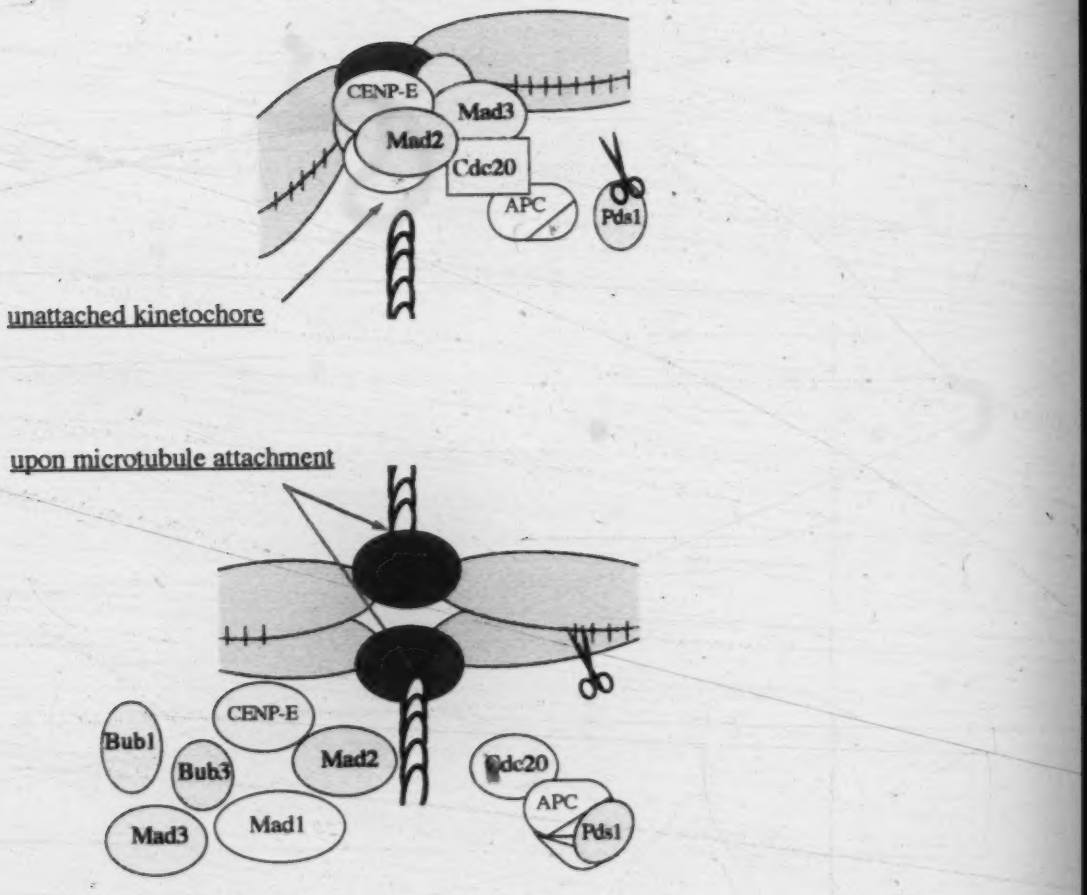

Figure 1-6. A model for the mitotic spindle checkpoint. *Unattached kinetochore:* A subset of the checkpoint proteins is recruited to kinetochores in the absence of kinetochore-microtubule attachment. Cdc20 is the downstream target of the checkpoint and is regulated by Mad2. By binding to Cdc20, Mad2 prevents it from activating the APC and thereby protects the anaphase inhibitor Pds1 from degradation. The onset of anaphase is thereby blocked. *Upon microtubule attachment*, the checkpoint proteins, including Mad2, disassociate from kinetochores, thereby releasing Cdc20. Cdc20 activates the APC, which in turn, targets Pds1 for ubiquitin-mediated proteolysis. Once Pds1 has been degraded, sister chromatid separation occurs and chromosome segregation takes place.

1.3.4.1. Mad1 and its complex with Mad2

The *MAD1* gene encodes a 90kD coiled-coil protein (Hardwick and Murray, 1995). Mad1p is phosphorylated during mitosis, and it becomes hyperphosphorylated upon the activation of the spindle checkpoint (Hardwick and Murray, 1995). Mps1p kinase is thought to be responsible for the phosphorylation of Mad1p (Lauze et al., 1995). *MPS1* was originally identified as an essential gene for spindle pole duplication, a mutation in which yielded monopolar spindles (e.g., Winey et al., 1991). *MPS1* overexpression causes mitotic arrest in the absence of spindle disruption, which correlates with the hyperphosphorylation of Mad1p (Hardwick et al., 1996). Although Mad1p phosphorylation is associated with the activation of the spindle assembly checkpoint (Hardwick and Murray, 1995), it is not necessarily required for checkpoint signaling. In fact, the overexpression of another spindle checkpoint protein Bub1p leads to the activation of spindle checkpoint without Mad1p being phosphorylated (Farr and Hoyt, 1998). It should also be noted that neither mammalian (HsMad1) nor *Xenopus* (Xmad1) homologues of Mad1p appear to be phosphorylated during mitosis (Campbell et al., 2001; Chen et al., 1998).

Mad1p forms a tight complex with another spindle checkpoint protein, Mad2p (see section *1.3.4.2*, p.44) (Chen et al., 1999). This interaction is thought to be a prerequisite for Mad2p binding to Cdc20p (Chung and Chen, 2002). Moreover, Mad1p-Mad2p

complex is hypothesized to act as a regulatory gate, which controls the release of Mad2p towards Cdc20p (Chung and Chen, 2002; Sironi et al., 2002).

During mitosis, Mad1p and Mad2p homologues in *Xenopus* eggs (Xmad1 and Xmad2) and mammalian cells (HsMad1 and HsMad2) immunolocalize to kinetochores that lack microtubule attachments and accumulate on the chromosomes that fail to align at the metaphase plate (Chen et al., 1996; Chen et al., 1998; Campbell et al., 2000; Howell et al., 2000).

Throughout interphase, however, Mad1 and Mad2 are seen at the nuclear periphery of cells (Gorbsky et al., 1998; Campbell et al., 2000; Ikui et al., 2002). These observations, confirmed in a variety of species, have been refined in mammalian systems, by Campbell and co-workers, who demonstrated that mammalian homologues of Mad1 and Mad2 are localized to the nucleoplasmic face of the NPC (Campbell et al., 2000). Interestingly, the localization studies in fission yeast indicated that Mad1 may anchor Mad2 to the nuclear membrane and may thereby regulate its entry into the nucleus (Ikui et al., 2002).

1.3.4.2. Mad2 and its role in the mitotic spindle checkpoint

The *MAD2* gene encodes a 22 kDa protein, whose association with unattached kinetochores is thought to generate the inhibitory signal that blocks anaphase

progression (reviewed by Taylor, 1999; Shah and Cleveland, 2000; Hoyt, 2001). The microinjection of antibodies to Mad2 into cultured mammalian cells leads to premature anaphase onset and results in chromosome missegregation, presumably due to sequestration of Mad2 away from the kinetochore (Gorbsky et al., 1998). Knock-out mice, deficient in the checkpoint gene *MAD2*, die during early embryogenesis (Dobles et al., 2000). Therefore, vertebrate cells may require the spindle checkpoint for proper timing of anaphase, even when the spindle assembly is intact (Taylor, et al., 1998; Dobles, et al., 2000).

In yeast, Mad2p is shown to directly interact with Cdc20p (Hwang, et al., 1998; Li, et al., 1997). When the spindle checkpoint is activated, Mad2p associates with the Cdc20-APC complex and thus participates in the inhibition the APC ubiquitin ligase activity (reviewed by Shah and Cleveland, 2000). This inhibition prevents the Pds1p proteolysis and subsequent separation of the sister chromatids.

1.3.4.3. Other components of the mitotic checkpoint machinery

The proper functioning of Mad2p relies on its interaction with other components of the mitotic checkpoint machinery (Hardwick et al., 2000; Sudakin et al., 2001). Subcellular localization studies in *D. melanogaster*, *X. laevis*, and humans have shown that Mad3 (BubR1), Bub1, and Bub3 also localize to kinetochores prior to chromosome

alignment at the metaphase plate (Chen et al., 1996 & 1998 (XMad2 and XMad1), Jablonski et al., 1998 (hsBUB1, hsBUBR1), Basu et al., 1998 (Dm BUB3), Li and Benezra, 1996 (hsMAD2)). In yeast, Mad2p transiently associates with Mad3p and Bub3p, which are also complexed with Cdc20p (Hardwick et al., 2000). In HeLa cells, BubR1 (an orthologue of yeast Mad3p) forms a mitotic checkpoint complex along with Mad2, Bub3 and Cdc20 (Sudakin et al., 2001; Fang, 2002). Interestingly, in the *in vitro* assay system, recombinanat BubR1 was found to be a more potent inhibitor of the APC activity than Mad2 (Tang et al., 2001).

Studies in *Xenopus* also demonstrated that a spindle checkpoint protein, Bub1, is required for the localization of Mad2 and other checkpoint proteins to unattached kinetochores (Sharp-Baker and Chen, 2001). Nonetheless, the molecular mechanisms of this recruitment remain largely unknown.

Here, we demonstrate that a distinct subset of nucleoporins defines the localization and regulates the activity of the Mad1p and Mad2p proteins and has a role in the regulation of the mitotic spindle checkpoint.

1.4. The Focus of this Thesis

We have used a variety of genetic, biochemical and cell-imaging approaches to define novel functions for the NPC. This thesis focuses on the involvement of the

NPC-constituents in regulation of the mitotic spindle checkpoint and, more specifically, on the significance of functional associations between the Mad1p and Mad2p checkpoint proteins and a distinct subset of Nups.

In addition, we aimed to define a role for the essential nuclear protein Rrb1p. To accomplish this, we have analyzed the involvement of Rrb1p in the regulation of transcription of ribosomal protein genes and in ribosome assembly.

Chapter 2

Materials and Methods

2.1. Yeast strains and media

The yeast strains used in this study are described in **Table 2-1**.

Procedures for yeast manipulation were conducted as described (Sherman et al., 1986). Cells were grown at 30°C (unless otherwise noted) in YP or CM medium supplemented with 2% galactose, glucose, or a mixture of galactose and glucose added in the indicated ratios for a 2% final concentration of sugar. 5-fluoroorotic acid (5-FOA) (Toronto Research Chemicals, Toronto, Ontario, Canada) plates were prepared as described (Ausubel et al., 1992). Yeast transformations were performed by electroporation (Delorme et al., 1989).

2.2. Construction of yeast strains*

*The following strains were constructed and studied in collaboration with Dr. Oliver Kerscher from the laboratory of Dr. Munira Basrai, Department of Genetics, National Cancer Institute, National Institutes of Health, Bethesda, Maryland

2.2.1. Production of *NUP* and Checkpoint Gene Deletions

Deletions of Nup and checkpoint genes were produced by two similar PCR mediated gene deletion techniques (Baudin et al., 1993). In the first technique (referred to as deletion technique 1), we used a PCR product derived from 40 bp of sequences immediately upstream of the start and downstream of the stop codon of the

TABLE 2-1

Strains used in this study

Strain	Genotype	Source, Derivation or Reference
W303	*Mat a/α ade2-1/ ade2-1 ura3-1/ ura3-1 his3-11,15/ his3-11,15 trp1-1/ trp1-1 leu2-3, 112/ leu2-3, 112 can 1-100/112 can1-100*	
DF5a	*Matâ ura3-52 lys2-801 his3-200 leu2-3,112 trp1-1*	
DF5α	*Matα ura3-52 lys2-801 his3-200 leu2-3,112 trp1-1*	
DF5	*Matâ/α ura3-52/ura3-52 lys2-801/52/lys2-801 his3-200/his3-200 leu2-3,112/leu2-3,112 trp1-1/trp1-1*	
NP53/NP59	*Matα ade2 ura3 his3 trp1 leu2 nup53Δ::HIS3 nup59Δ::HIS3*	Marelli et al., 1998
NP53-B1	*Matâ ura3-52 lys2-801 his3-200 leu2-3,112 trp1-1 nup53Δ::HIS3*	Marelli et al., 1998
NP53/NP157	*Matâ/α ura3 his3 trp1 leu2 nup53::HIS3 nup157::URA3*	Marelli et al., 1998
NP59-23	*Matâ ade2-1 ura3-1 his3-11,15 trp1-1 leu2-3,112 can1-100 nup59Δ::HIS3*	Marelli et al., 1998
NP120-25-4	*Matâ ura3-52 lys2-801 his3-200 leu2-3,112 trp1-1 Nup120Δ::URA*	Aitchison et al.,1995a
NP120M1G	*ura3 his3 trp1 leu2 nup120Δ::URA3 MAD1-GFP/HIS5*	segregant of sporulated NP120-25-4/YMB1299
NP120M2G	*ura3 his3 trp1 leu2 nup120Δ::URA3 MAD2-GFP/HIS5*	segregant of sporulated NP120-25-4/ YMB1296
NP157-2.1	*Matâ ura3-52 lys2-801 his3-200 leu2-3,112 trp1-1 nup157Δ::URA3*	Aitchison et al.,1995b
NP170pA	*Matâ ura3-52 lys2-801 his3-200 leu2-3,112 trp1-1 Nup170-protA (URA3-HIS3)/+*	Rout et al., 2000
NP157pA	*Matâ ura3-52 lys2-801 his3-200 leu2-3,112 trp1-1 Nup157-protA (URA3-HIS3)/+*	Rout et al., 2000
NP60pA	*Matâ ura3-52 lys2-801 his3-200 leu2-3,112 trp1-1 Nup607-protA (HIS3)/+*	Rout et al., 2000
YMB1296	*Matα ura3-52 lys2-801 ade2-101 his3Δ200 leu2Δ1*	this work

Strain	Genotype	Source, Derivation or Reference
	MAD2-GFP/HIS5 CFIII (CEN3L.YPH278)URA3 SUP11	
YMB1299	*Matα ura3-52 lys2-801 ade2-101 his3Δ200 leu2Δ1 MAD1-GFP/HIS5 CFIII (CEN3L.YPH278)URA3 SUP11*	this work
YMB1451	*Mata ura3-52 lys2-801 ade2-101 his3Δ200 trp1Δ1 nup170Δ::KAN*	this work
YMB1482	*Matα ura3-52 lys2-801 his3Δ200 leu2-3,112 trp1-1 nup170Δ::KAN*	this work
YMB1900	*Mata ura3-52 lys2-801 his3-200 leu2-3,112 trp1-1 mad2Δ::HIS3 [pMAD2/URA3]*	this work
YMB1906	*Matα ura3-52 lys2-801 his3-200 leu2-3,112 trp1-1 mad2Δ::HIS3*	this work
YMB1908	*Matα ura3-52 lys2-801 his3-200 leu2-3,112 trp1-1 mad1Δ::KAN*	this work
YMB1911	*Mata ura3-52 lys2-801 his3-200 leu2-3,112 trp1-1 mad1Δ::KAN [pMAD1/URA3]*	this work
YMB1979	*Matα ura3-52 lys2-801 his3-200 leu2-3,112 trp1-1 nup170Δ::HIS3 mad1Δ::KAN*	segregant of sporulated YMB1482/1911
YMB2008	*ura3-52 lys2-801 his3-200 leu2-3,112 trp1-1 nup170Δ::HIS3 mad2Δ::HIS3*	segregant of sporulated YMB1482/1900
YMB2018	*Matα ura3-52 lys2-801 his3-200 leu2-3,112 trp1-1 MAD1-GFP/HIS5*	this work
YMB2020	*Mata ura3-52 lys2-801 his3-200 leu2-3,112 trp1-1 MAD1-GFP/HIS5*	this work
YMB2022	*Mata ura3 his3 nup53Δ::HIS3 mad2Δ::HIS*	segregant of sporulated NP53/NP15782/YMB1906
YMB2029	*Matα ura3 his3 nup157Δ::URA3 mad2Δ::HIS3*	segregant of sporulated NP53/NP1578-2/YMB1906
YMB2032	*Matα ura3 his3 nup157Δ::URA3 mad1Δ::KAN*	segregant of sporulated NP53/NP1578-3/YMB1908
YMB2035	*Mata ura3 his3 nup53Δ::HIS3 mad1Δ::KAN*	segregant of sporulated NP53/NP1578-3/YMB1908
YMB2064	*ura3-52 lys2-801 his3-200 leu2-3,112 trp1-1*	segregant of sporulated

Strain	Genotype	Source, Derivation or Reference
	nup170Δ::HIS3 MAD1-GFP/HIS5	YMB1482/YMB2020
YMB2067	*ura3-52 lys2-801 his3-200 leu2-3,112 trp1-1*	segregant of sporulated
	nup53Δ::HIS3 MAD1-GFP/HIS5	NP53-B1/YMB2018
YMB2081	*ura3-52 lys2-801 his3-200 leu2-3,112 trp1-1*	segregant of sporulated
	nup157Δ::URA3 MAD1-GFP/HIS5	DF2:1:2 /YMB2018
YMB2086	*Matα ura3-52 lys2-801 ade2-101 his3-200 leu2Δ1*	this work
	nup170Δ::KAN MAD2-GFP/HIS5 CFIII (CEN3L.YPH278)URA3 SUP11	
YMB2087	*Matα ura3-52 lys2-801 ade2-101 his3-200 leu2Δ1*	this work
	nup53Δ::KAN MAD2-GFP/HIS5 CFIII (CEN3L.YPH278)URA3 SUP11	
YMB2088	*Matα ura3-52 lys2-801 ade2-101 his3-200 leu2Δ1*	this work
	mad1Δ::KAN MAD2-GFP/HIS5 CFIII (CEN3L.YPH278)URA3 SUP11	
YMB3048	*ura his3 trp1-1 leu2-3,112*	segregant of sporulated
	nup59Δ::HIS3 mad2Δ::HIS3	NP59-23/YMB1906
YMB3051	*ura his3 trp1-1 leu2-3,112*	segregant of sporulated
	nup59Δ::HIS3 mad1Δ::KAN	NP59-23/YMB1908
YPH278	*Matα ura3-52 lys2-801 ade2-101 his3-200 leu2Δ1*	Spencer et al., 1990
	CFIII (CEN3L.YPH278)URA3 SUP11	
R1HA	*Mat a ade2-1 ura3-1 his3-11,15 trp1-1 leu2-3,112*	
	can 1-100/112 rrb1::HIS3 pRS316-RRB1-HA (URA3)	Iouk et al., 2001
GR1HA	*Mat a ade2-1 ura3-1 his3-11,15 trp1-1 leu2-3,112*	
	can 1-100/112 rrb1::HIS3 pYEUra3-RRB1-HA (URA3)	Iouk et al., 2001
GR1GFP	*Mat a ade2-1 ura3-1 his3-11,15 trp1-1 leu2-3,112*	
	can 1-100/112 rrb1::HIS3 pYEUra3-RRB1-GFP (URA3)	Iouk et al., 2001
prt1-1	*Mata prt1-1 leu2-3,112 ura 3-52*	D. Goldfarb
(TB11B-4-1)		(University of Rochester, Rochester, NY)

gene to be deleted and 20bp of sequence homologous to pRS303 (*HIS3*) or pRS400 (*KAN*) (Sikorski and Hieter, 1989, Brachmann et al., 1997) immediately adjacent to the vector selectable marker. The oligonucleotides were used to amplify a *HIS3* marker from pRS303 or a *KAN* marker from pRS400. The second technique (referred to as deletion technique 2) utilizes genomic DNA of an existing deletion strain to PCR amplify a deletion cassette module containing ~200bp upstream of the start and downstream of the stop codon of the deleted gene of interest plus the deletion marker. In both techniques the products of PCR reactions were transformed into the indicated strains to produce the deletions of interest.

Deletion and replacement of the *NUP170* ORF with the *HIS3* marker in the DF5α strain (YMB1482) was performed using deletion technique 1 and with the *KAN* marker in the strain YMB1451 using deletion technique 2. Heterozygous *mad1Δ::KAN/MAD1* (YMB1488) and *mad2Δ::HIS3/MAD2* (YMB1496) deletions were made in diploid wild-type strain DF5 using deletion technique 2. For these deletions, a *mad1Δ::KAN* module was derived from a *mad1Δ::KAN* strain (YFS1120, kindly provided by F. Spencer, Johns Hopkins University, Baltimore, MD) or a *mad2Δ::HIS3* module from a *mad2Δ::HIS3* strain (YKH447, kindly provided by K. Hyland and P.Hieter, University of British Columbia,BC). The resulting strain *mad1Δ::KAN/MAD1* (YMB1488) was transformed with a *MAD1/URA3* plasmid (pKH130, Hardwick and Murray, 1995) and

mad2Δ::HIS3/MAD2 (YMB1496) was transformed with a *MAD2/URA3* containing plasmid (pCD2, Warren and Spencer, submitted for publication). pKH130 and pCD2 are generous gifts from F.Spencer. The diploid strains were sporulated and haploid *mad1Δ::KAN* (YMB1908 and YMB1911) and *mad2Δ::HIS3* strains (YMB1900 and YMB1906) were used for subsequent crosses.

2.2.2. Generation of nucleoporin and checkpoint gene double deletion mutants

To produce double deletion mutants, *mad1Δ::KAN* (YMB1908 or YMB1911) or *mad2Δ::HIS3* (YMB1900 and YMB1906) were mated to *nup170Δ::HIS3* (YMB1482), *nup157Δ::URA3* (NP157-2.1), *nup53Δ::HIS3* (from NP53/NP157 and *nup59Δ::HIS3* (NP59-23) (Table 2-1, p.49). Diploid strains were dissected and haploid meiotic progeny were analyzed. The genotype of each double mutant was confirmed by PCR analysis and marker analysis.

2.2.3. Construction of tagged *MAD1*, *MAD2* and *MTW1* Genes:

MAD1 and *MAD2* were tagged with *GFP* following their last amino acid codon using an integrative PCR based transformation procedure. Primers and the *GFP/HIS5* template plasmid pGFP (Wigge et al., 1998) were generously supplied by Dan Burke (University of Virginia, Charlottsville, VA). *GFP* and the *HIS5* marker were PCR

amplified from plasmid pGFP using a sense primer containing a region of *MAD1* extending from nucleotide position 2209 to 2248 just prior to the termination codon and an antisense primer containing a region of *MAD1* extending from nucleotide position 2251 to 2290 just past the termination codon. For *MAD2*, the sense primer extended from nucleotide position 550 to 591 just prior to the termination codon and the anitisense primer from nucleotide position 595 to 631 just past the termination codon. PCR products were transformed into a wild-type strain (YPH278) and His^+ transformants were screened for in-frame fusions of *MAD1-GFP* and *MAD2-GFP* by PCR and Western blot analysis. Strains *MAD1-GFP/HIS5* (YMB1299) and *MAD2-GFP/HIS5* (YMB1296) were used for subsequent studies.

The gene encoding the centromere associated protein Mtw1p (Goshima et al., 2000) was tagged with the gene encoding GFP or the cyan fluorescent protein (CFP) as follows. First, *MTW1* and the adjoining promotor sequences were amplified from genomic DNA with the following primers: OMB338 (5'-CCGCTCGAGTGCGCTGTGAAAACCGACCC-3') and OMB339 (5'-ATAGTTTAGCGGCCGCGTAACACATCATCAAGTAAATCC-3'). The resulting PCR product was digested with *XhoI* and *NotI* and cloned into *LEU2/CEN* plasmid pAA3 (Sesaki and Jensen, 1999). In pAA3, *MTW1* was placed in frame with *GFP* to form pOKMTW1-GFP. pOKMTW1-CFP was constructed by replacing a *NotI SacII* GFP

containing fragment of pOKMTW1-GFP with a corresponding segment from *CFP* derived from the plasmid pDH3 (pFA6a-*CFP-KAN*) by PCR.

2.2.4. Construction of the GFP-tagged *MAD1* and *MAD2* in the nucleoporin deletion strains

For the examination of Mad1-GFP protein in nup deletion mutants, a *MAD1-GFP/HIS5* module (from strain YMB1299) was PCR amplified using an approach similar to deletion technique 2 described above and transformed into the wild type strain DF5 to produce *MAD1-GFP/HIS5* strains (YMB2018 or YMB2020). Subsequently, these *MAD1-GFP/HIS5* strains were crossed to the nucleoporin deletion strains *nup53Δ::HIS3* (NP53-B1), *nup170Δ::HIS3* (YMB1482), *nup157Δ::URA3* (NP157-2.1), and *nup59Δ::HIS3* (NP59-23). Meiotic progeny from these crosses were analyzed and appropriate haploid strain was chosen for further analysis (see Table 2-1, p.49).

For the examination of Mad2-GFP in Nup deletion mutants, several Nup deletions were made directly in the *MAD2-GFP* strain (YMB1296) using deletion technique 2 (see section **2.2.1**, p.48) described above and these are listed in Table 2-1. The *nup170Δ::KAN* deletion module was derived from a *nup170Δ::KAN* strain (YMB1451), the *nup53Δ::KAN* deletion module was derived from a

nup53Δ::kanMX4 deletion strain (strain no. 10734; Research Genetics, Huntsville, AL), the *nup59Δ::KAN* deletion module was derived from a *nup59Δ::kanMX4* deletion strain (strain no. 3785; Research Genetics, Huntsville, AL) and the *mad1Δ::KAN* deletion module was derived from a *mad1Δ::KAN* strain (YMB1979).

2.2.5. *RRB1* gene disruption

The *RRB1* gene was disrupted in diploid W303 cells by deletion of an Msc1/BstB1 fragment extending from +83 nucleotides (were +1 is the A of the ATG intitation codon) to +1454, 169 nucleotides downstream of the termination codon. This fragment was replaced with the *HIS3* selectable marker. The integration of the *HIS3* marker within the *RRB1* gene was confirmed by Southern blotting. Heterozygous diploids were sporulated and tetrads were dissected on YPD plates. Spores showed a 2:2 segregation of viable to nonviable haploids and no His^+ haploids were recovered. Heterozygous diploids carrying *RRB1::HIS3* alleles were also transformed with either pRS316-RRB1-HA *(URA3)* or pYEUra3-RRB1-HA *(URA3)* and the resulting strains were sporulated. Each of the His^+ haploids recovered was also URA^+. These haploids failed to grow on 5-FOA plates.

2.3. Plasmids

The following plasmids were used in this study: pRS315, *CEN/LEU2*; pRS316,

CEN/URA3; pRS303, *CEN/HIS3* (Sikorski and Hieter, 1989); pRS400, *CEN/KAN* (Brachman et al., 1998); pYEUra3, *CEN/URA3/GAL1-GAL10* (CLONTECH Laboratories, Inc.); pBluescriptII SK (pBs) and pBSSKII11^{+} (Stratagene, La Jolla, CA); pRS315-RRB1-HA and pRS316-RRB1-HA, a DNA fragment encoding the hemagglutinin (HA) epitope GYPYDVPDYASG and a stop codon were inserted using PCR following the C-terminal amino acid codon of the *RRB1* ORF and the tagged gene was inserted into SalI sites in pRS315 and pRS316; pYEUra3-RRB1, the complete ORF of *RRB1* with a flanking 5' XbaI site and a 3' ClaI-termination codon-XhoI fragment was synthesized by PCR and inserted following the *GAL1* promoter in the plasmid pYEUra3; pYEUra3-RRB1-GFP, the *GFP* ORF containing flanking 5' ClaI and 3' XhoI sites was synthesized by PCR and inserted at the 3' end of the *RRB1* ORF in pYEUra3-*RRB1*; pYEUra3-*RRB1-HA*, an MscI-BstBI fragment from pRS315-RRB1-HA containing the HA-tag was cloned into the MscI-XhoI sites in pYEUra3-RRB1; pMB259 and pMB261 containing the *NUP157* and *NUP170* ORFs, respectively were identified by functional complementation of *Ctf-* phenotype of the *sl41*(*nup170-141*) strain (Kerscher et al., 2001); pNUP157-GFP, C-terminal *GFP* was subcloned into NruI site of pRS315-NUP157; pBSN170, the complete ORF of *NUP170* and adjoining promoter sequences with a flanking 5' XhoI and a 3' NotI sites was inserted into pBSSKII+ (Stratgene, La Jolla, CA); pNUP-170: the *XhoI/NotI NUP170*

fragment from pBSN170 was placed into pAA3 in frame with *GFP* (Kerscher et al., 2001); pOKMTW1-GFP and pOKMTW1-CFP were constructed as follows: *MTW1* and the adjoining promoter sequences were amplified from genomic DNA with the following primers: OMB338 (5'-CGCTCGAGTGCGCTGTGAAAACCGACCC-3') and OMB339 (5'-ATAGTTTAGCGGCCGCGTAACACATCATCAGTAAATCC-3'). The resulting PCR product was digested with XhoI and NotI and cloned into *LEU2/CEN* plasmid pAA3 (Sesaki and Jensen, 1999). In pAA3, *MTW1* (containing its own promoter) was placed in frame with *GFP* to form pOKMTW1-GFP. A second plasmid, pOKMTW1-CFP, was constructed by replacing a *NotI/SacII* GFP-containing fragment with the gene encoding the cyan fluorescent protein (*CFP*). *CFP* was amplified from plasmid pDH3 ((pFA6a-CFP-KAN), The Yeast Resource Center at the University of Washington) with the following primers:

OMB410 (5'-ATAAGAATGCGGCCGCAGTAAAGGAGAAGAACT -3') and OMB411 (5'-TCCCCGCGGCTATTTGTATAGTTCATCCATGCC -3'). The resulting *CFP* PCR product was digested with *NotI* and *Sac II* and inserted into the *NotI/SacII* digested pOKMTW1-GFP backbone to replace *GFP*.

RPL3-GFP, RPL4A-GFP, RPL25-GFP fusions under the control of the triose phosphate isomerase promoter in the plasmid pYX242 (*LEU2*) were a generous gift from Michael Rout (The Rockefeller University, NY); *NUP53-GFP*, *NUP49-GFP*,

NUP188-GFP fusions under the control of the *MET25* promoter in pGFPc-fus plasmid (*CEN/URA3*) were received from David Goldfarb (University of Rochester, Rochester,NC); the *MAD1* covering plasmid pKH 130 (*CEN/URA3*) and *MAD2*-covering plasmid pCD2 (*CEN/URA3*) were kindly provided by Munira Basrai (NCI NIH, Bethesda, MD).

2.4. Cell phenotype analysis

2.4.1. Benomyl- and thermo-sensitivity of *NUP /MAD* gene disruption strains

Strains were grown at 30°C in YPD medium to mid-logarithmic phase. Two OD_{600} units of cells were pelleted, washed and resuspended in 1ml of water. 6.5µl of a 10-fold dilution series were spotted on YEPD plates containing 20 or 25µg/ml benomyl and on YEPD plates containing drug vehicle alone (0.2µl DMSO/1ml medium). Cell growth was examined after 3 days of growth at 27°C, 30°C or 37°C.

2.4.2. Cell growth synchronization and activation of mitotic spindle checkpoint.

α-factor synchronization was performed as described (Breeden, 1997). Cultures were grown overnight to a maximum OD_{600} of 0.8 and diluted down to about 0.20 in YEPD medium. To arrest cells permanently in G1, 1µg/ml of α-factor (Sigma-Aldrich,

Inc.) was added to a culture and cells were incubated for 90min or longer if necessary. The G1 arrest was monitored with phase-contrast microscopy. For synchronization (arrest/release) experiments α-factor arrested cells were harvested by filtration, washed and released into fresh medium lacking α-factor. Cells were arrested in mitosis by addition of nocodazole (Sigma-Aldrich, Inc.) to the final concentration of 15μg/ml, or benomyl to 30μg/ml (Sigma-Aldrich, Inc.) (the latter was prepared by addition of 30mg/ml stock solution of benomyl in DMSO to hot medium), and subsequent incubation for 90-120 min (Hardwick and Murray, 1995). The DNA content of cells stained with propidium iodide was measured on a FACScan (Becton Dickinson, San Jose, CA) as described in the section **2.4.3,** p.60. To confirm that the microtubules were depolymerized, cells were subjected to immunofluorescence analysis using anti-tubulin staining (section **2.11,** p.72).

2.4.3. Flow cytometry

5ml of yeast culture grown to mid-logarithmic phase were washed with 10ml of 50mM Tris-HCl, pH 8.0, pelleted, resuspended in 5ml of 70% ethanol and allowed to fix for 1h at room temperature. Fixed cells were harvested and resuspended in 1ml of 50mM Tris-HCl, pH 8.0 containing 10mg/ml RNAase A. Cells were transferred to a 1.5ml microfuge tubes and incubated for 2h at 37°C with occasional mixing, then

pelleted and resuspended in 0.2ml of Pepsin solution (5ml MilliQ, 25µl concentrated HCl, 25mg Pepsin (Sigma-Aldrich, Inc.)). Samples were incubated for 1h at 37°C, then neutralized by diluting with 1ml of 50mM Tris-HCl, pH 8.0 and pelleted. The cell pellet was resuspended in 500ml of propidium iodide solution (180mM Tris-190mM NaCl, pH 7.5, 1.42% $MgCl_2x6H_2O$, 0.05% propidium iodide (Sigma-Aldrich, Inc.)) and incubated for 1h in the dark. Cells were diluted with 2.5ml of 50mM Tris-HCl, pH 8.0, and 50µl aliquots were sonicated for 2-3 seconds and subjected to the FACS analysis.

Flow cytometry of GR1GFP and R1GFP cells was performed as follows. Cultures were grown overnight to mid-logarithmic phase in YP media containing a mixture of galactose and glucose added in the indicated ratios to a final concentration of 2% total sugar; 5ml of each culture were washed with 10ml of 50mM Tris-HCl, pH 8.0, resuspended in 1ml of this buffer and analyzed by flow cytometry. Levels of GFP autofluorescence were measured using a detector with a 515- to 535-nm band-pass filter. Data was analyzed using CellQuest software, version 3.1.

2.4.4. Growth curves

In order to compare cell growth rates on different carbon sources, GR1HA and R1HA strains were grown overnight in media containing a galactose:glucose mixture (70:30), washed and then used to inoculate 100 ml cultures containing either 2%

galactose, 2% glucose or 70:30 mixture of both in YP medium at an OD_{600} of 0.05. Cell growth was monitored for 36 hours.

2.4.5. Regulation of *GAL1::RRB1* expression

The general procedure for altering the levels of *GAL1*-controlled *RRB1* expression were as follows. The GR1HA, GR1GFP, and R1HA strains were grown overnight to mid-logarithmic phase in medium containing a mixture of galactose and glucose added in ratios of 70:30 or 60:40 for a 2% final concentration of sugar as indicated. Cells were harvested, washed, and used to inoculate fresh medium containing either 2% galactose, 2% glucose or the indicated mixture of both at an OD_{600} of 0.2 and then incubated for the indicated times. When necessary, cultures were diluted with fresh medium so the OD_{600} would not exceed 0.7. The effects of altering *RRB1* expression on various cellular functions were examined as follows with the indicated modifications.

2.4.6. Inhibition of translation

Cultures of R1HA and GR1HA with or without the pYX242 plasmid containing *RPL3-GFP*, and prt1-1 strain, containing pRS316-RRB1-HA plasmid, were grown overnight in selection media containing 2% glucose (R1HA and prt1-1) or 2%

galactose (GR1HA) at 23ºC to mid-logarithmic phase. Cells were then shifted to the non-permissive temperature of 37ºC for 20 min and then allowed to recover at 23ºC. Aliquots of the culture were withdrawn periodically, and cells were either immediately fixed for immunofluorescence analysis or examined directly by fluorescence microscopy to determine the distribution of Rrb1-GFP or rpL3-GFP. In order to study the effects of chemical protein synthesis inhibitors, either cycloheximide (100 µg/ml) or sodium fluoride (1 mM) was added to the cultures and incubated at 30ºC for 1.5 h prior to examination. To remove the drugs, cells were repeatedly washed with water and resuspended in fresh medium. Cells were allowed to recover for 30 min at 30ºC and then examined.

2.5. Yeast subcellular fractionation

2.5.1. Preparation of crude nuclei

For the isolation of crude nuclei, the mini-scale procedure described by Tcheperegine et al., 1999 was used, except that the scale was increased for up to 250ml of culture. Cells were grown in the appropriate conditions (section **2.4.2,** p.62). Cells were harvested and washed two times with water and two times with 1.1 M sorbitol. The cells were then resuspended in 1 ml of 1.1M sorbitol. To digest the cell wall, 2µg of zymolyase 100 T (ICN Biomedicals Inc.) per 1g of wet cells was added, and the cells

were incubated for 30min at 30°C with occasional shaking. After digestion, spheroplasts were collected by centrifugation (5,000 × *g* for 20 min), washed one time with ice-cold 1.1 M sorbitol, and resuspended in 2ml of 1.1 M sorbitol. All subsequent steps were performed at 4°C. The cell suspension was then layered over a cushion of 7.5% Ficoll 400 in 1.1 M sorbitol and then sedimented at 5,000 x *g* for 20 min. Spheroplasts were then resuspended in 2.5 ml of 8% polyvinylpyrrolidone in 0.5 mM $MgCl_2$ and 20 mM KH_2PO_4, pH 6.5, (PVP medium) containing 1% of solution P (0.1 M phenylmethylsulfonyl fluoride and 0.4 mg/ml pepstatin A (Boehringer Mannheim)) and lysed with a Polytron (4 x 30 s). 2.5 ml of 0.6 M sucrose in PVP medium containing solution P was then added, and nuclei were sedimented at 10,000 x *g* for 10 min. The pellet containing crude nuclei was resuspended in 1ml of 1.5 M sucrose, 0.1 mM $MgCl_2$, and 10 mM bis-Tris, pH 6.5. This procedure typically yielded ~2-2.5 mg of crude nuclei.

2.5.2. Sedimentation analysis of ribosomes.

Sedimentation analysis of ribosomes was performed essentially as described by Baim et al., 1985, with some modifications. Cultures were grown to an OD_{600} of ~0.5-0.6, treated with cycloheximide (50 µg per 1ml of culture), and harvested on ice. Glass bead lysis was performed in buffer containing 10mM Tris-HCl, pH7.4, 10mM NaCl,

30mM $MgCl_2$, 1mM DTT, 50 µg/ml cycloheximide, 200µg/ml heparin and 0.1µg/ml DEPC, by vortexing 8x15sec with 30s periods of cooling on ice. Lysates were cleared by centrifugation, loaded onto the 7 to 47% (w/v) sucrose density gradients and centrifuged at 22,000 rpm for 7 h at 13°C in an SW40 rotor (Beckman Instruments, Inc.) and analyzed using an Econo EM-1 UV monitor (Bio Rad) at 254nm.

2.6. Immunoprecipitation procedures

2.6.1. Immunoprecipitation of the proteinA-tagged nucleoporins.

Crude nuclei were prepared from the DF5, *NUP60*-pA, *NUP157*-pA and *NUP170*-pA strains were prepared as described in section **2.5.1**, p.63. Crude nuclei were digested with DNAase (10µg/ml) in 10 mM Bis-Tris pH 6.5, 0.1 mM $MgCl_2$, 0.5 mM PMSF, and 3 µg/ml of pepstatin at room temperature for 15 min. Digests were extracted with an equal volume of 2 times extraction buffer to final concentration of 50 mM Tris-HCl, pH 7.5, 150 mM NaCl, 0.1 mM $MgCl_2$, 1 mM DTT, 50 mM NaF, 0.2 mM PMSF, 2 µg/ml leupeptin, 2 µg/ml aprotinin, and 0.4 µg/ml pepstatin A, containing 20% dimethyl sulfoxide and 1% Triton X-100. The extracts were cleared by centrifugation (75,000rpm for 15min at4°C in a Beckman Coulter TLA.120 rotor) and incubated in batch with IgG-Sepharose beads (Pharmacia Biotech) using10µl of bead slurry per 1ml of extract, for 3 h at 4°C. The bound complex was washed extensively in wash buffer

(50 mM Tris-HCl, pH 7.5, 150 mM NaCl, 0.1 mM $MgCl_2$ 1mM DTT, 50 mM NaF, 0.2 mM PMSF, 2 μg/ml leupeptin, 2 μg/ml aprotinin, and 0.4 μg/ml pepstatin A, 0.1% Tween20) followed by three additional washes in wash buffer containing 50 mM $MgCl_2$. Bound proteins were eluted in wash buffer containing increasing concentrations of magnesium chloride 0.1M, 0.5M and 2.0 M, followed by elution with 0.5M acetic acid, pH 3.4. Samples were concentrated by TCA precipitation, washed with acetone, resuspended in SDS-PAGE sample buffer and resolved by SDS-PAGE.

2.6.2. Immunoprecipitation of GFP-tagged protein fusions and Nup53p

Crude nuclear extracts were prepared as described in the previous section. Mad1-GFP and Mad2-GFP were immunoprecipitated with rabbit polyclonal anti-GFP antibodies (kindly provided by L.Berthiaume, University of Alberta, Edmonton, AB) or polyclonal antibodies directed against Nup53p (Marelli et al., 1998) followed by the addition of 20 μl of protein G-Sepharose beads (Amersham Pharmacia Biotech). Subsequent washing and elution steps were performed as described in section **2.6.1,** p.65. Nup53p-containing complexes were immunoprecipitated similarly, except polyclonal antibodies directed against Nup53p (Marelli et al., 1998) were used.

2.6.3. Immunoprecipitation of Rrb1-HA

For immunoprecipitation experiments, nuclei isolated from R1HA strains were digested with DNAase (10µg/ml) in 10 mM Bis-Tris pH 6.5, 0.1 mM $MgCl_2$, 0.5 mM PMSF, and 3µg/ml of pepstatin at room temperature for 15 min. Digested nuclei were then extracted for 15 min on ice by the addition of an equal volume of 2 times extraction buffer to a final concentration of 100 mM Tris-HCl, pH 8.0, 240 mM NaCl, 2 mM EDTA, 1mM DTT, and 1% Triton-X100. Extracts were then centrifuged at 50,000 x g for 15 min at 4°C and the supernatant fractions were used for immunoprecipitation experiments. To reduce nonspecific binding, the supernatant was preincubated with 100µl of Protein G-Sepharose and 1µl of mouse serum for 1h at 4°C, and then spun to remove the beads.

The 12CA5 mAb conjugated Protein G-Sepharose 4 Fast Flow beads (Pharmacia Biotech.) were produced as previously described (Voos et al., 1994). The pre-adsorbed supernatant fraction was incubated with mAb 12CA5 conjugated beads for 3h at 4°C. Beads were washed three times with extraction buffer and then with extraction buffer lacking detergent. Immunoprecipitates were eluted with 100µl of 0.5M acetic acid, pH 3.4. The eluate was then lyophilized and resuspended in SDS-sample buffer. Proteins were separated by SDS-PAGE and the gels were analyzed by Coomassie blue staining, silver staining, and Western Blotting. In order to identify the 40 kD polypeptide (rpL3)

that copurified with Rrb1-HA, the 40 kD species was digested in-gel with endopeptidase Lys-C and peptides were purified and sequenced by the Protein/DNA Technology Center at the Rockefeller University (New York, NY).

2.7. Western blotting.

In preparation for Western analysis, total cell extracts from the appropriate cultures were prepared as follows. Cells were collected by centrifugation, washed with water, and then lysed with 7.4% β-mercaptoethanol in 1.85N NaOH. Proteins were precipitated with 10% trichloroacetic acid and then solubilized in SDS-sample buffer. Proteins were separated by conventional SDS-PAGE (except for phoshorylated proteins that were resolved using the double-inverted gradient resolution gel, described in section **2.8**, p.69 (Zardoya et al., 1994)) and transferred to nitrocellulose membranes (Trans-Blot, Bio-Rad). Membranes were stained with amido black to visualize separated proteins, and then blocked in TBS (20 mM Tris pH 7.5 and 150 mM NaCl) containing 0.1% Tween-20 and 5% dried skim milk. Proteins of interest were detected using the following antibodies.

Protein A fusions were detected with rabbit anti-mouse IgG (at a 1:2500 dilution). GFP fusions were detected using rabbit polyclonal anti-GFP antibodies (1:2500) a generous gift from Michael Rout, The Rockefeller University, NY). The α-Mad1 sheep

polyclonal antibody, kindly provided by Kevin Hardwick (Wellcome Trust Centre for Cell Biology, University of Edinburgh, UK) was used to detect Mad1p (1:1000) and required a subsequent incubation with the rabbit anti-sheep serum (1:5000). Anti-Mad2 polyclonal antibodies used to detect Mad2p (1:1000) were a kind gift from Rei-Huei Chen, Cornell University, Itaca, NY (Chen et al., 1999). Nup2p was detected using anti-Nup2 rabbit polyclonal antibodies kindly provided by Dwayne Weber, from John Aitchison's laboratory, University of Alberta, Edmonton. Rrb1-HA was detected using the mAb 12CA5 (Boehringer Mannheim, Laval, QC, Canada) and rpL3 was detected using the α-rpL3 monoclonal antibody TCM1. A polyclonal rabbit serum directed against rpL30 (which also cross reacts with the ribosomal protein rpS2 (Vilardell and Warner, 1997) was generously provided by Jonathan Warner. Polyclonal antibodies directed against Nup53p have been previously described (Marelli et al.,1998). Antibody binding was detected with HRP-conjugated secondary antibodies (Amersham Pharmicia Biotech) and the ECL system.

2.8. Double-inverted gradient electrophoresis (DG-PAGE)

DG-PAGE was performed as described by Zardoya et al., 1994. The double-inverted gradient gel consisted of two successive separating polyacrylamide gradient gels that were set under the stacking gel (125mM Tris-HCl, pH 6.8, 0.1% SDS, 3%

Acrylamide:Bis (30:0.8), 0.1%APS, 0.5% TEMED). In the upper separating gel, occupying 40% of the resolving gel volume, the gradient was in the standard direction, i.e. progressive by increasing concentration of polyacrylamide (32% to 19% glycerol, 375mM Tris-HCl, pH 8.8, 0.1%SDS, 9% to 12.5% Acrylamide:Bis (30:0.8), 0.01APS, 0.025% TEMED). In the bottom gel, occupying 60% of the resolving gel volume, the gradient was inverted, i.e. progressive by decreasing concentration of polyacrilamide (16% to 3% glycerol, 375mM Tris-HCl, pH 8.8, 0.1%SDS, 7.5% to 5% Acrylamide:Bis (30:0.8), 0.01APS, 0.025% TEMED). Electrophoresis was run at 150V until samples reached the separating gel, and then it was run at 250V. Standard sample and running buffers were used.

2. 9. Northern blot analysis

Cells were harvested from 40 ml of cultures at an OD_{600} of 0.5-0.6 and total RNA was extracted by hot-phenol essentially as described (Köhrer and Domdey, 1991), with some modifications. Cells were washed with 50mM sodium acetate, pH5.2, supplemented with 10mM EDTA, and resuspended in 600µl of this solution. Cells were beaten for 4min with ~0.6g of glass beads, in the presence of 80µl of 10%SDS and 400µl of water-saturated phenol. The samples were heated for 15min at 65°C, allowed to cool and then subjected to phenol-chloroform extraction. The RNA was precipitated

with 95% ethanol at -80°C overnight and then was thoroughly washed with 70% ethanol, pellets were dried and resuspended in 50µl of RNAase-free water.

Equal amounts of total RNA were loaded for each sample and separated on a 1.2% agarose gel. RNA was then transferred to Hybond-N+ nylon membrane (Amersham Pharmicia Biotech), and UV cross-linked. Membranes were then incubated for 2h in prehybridization buffer (5x Denhardts solution, 5xSSC, 50% formamide, 1%SDS) and hybridized in sample buffer with the appropriate probe at 37°C for 12-16 h. Following a final wash in 0.2 x SSC and 0.1% SDS at 56°C, the blots were exposed to BioMax MR film (Kodak). For Northern analysis using the Y159 stain, cultures were grown as described above in a medium containing a 70:30 galactose:glucose mixture and then shifted to glucose or galactose containing medium for 12 h.

Probes for *RRB1, RPL3, RPL30, RPS28A* were generated by PCR using genomic DNA as a template. The following cDNA fragments were used to detect corresponding mRNAs: a BamHI-HindIII fragment from the plasmid p*ACT1* for actin (kindly provided by D.Stuart, University of Alberta); an EcoRI-EcoRV fragment from the plasmid pRS314-L25-GFP (kindly provided by Ed Hurt, University of Heidelberg, Germany) for *RPL25*; a FokI-FokI fragment from pYX242-RPS10A-GFP for *RPS10A*; a BalI-BalI fragment from pYX242-RPL4A-GFP for *RPL4A*. Each of the DNA

fragments was labeled with α-^{32}P-dCTP using DNA Labeling Beads (Amersham Pharmicia Biotech).

2.10. Pulse-chase of RNA

Pulse-chase analysis was performed as previously described (Warner, 1991) with the following modifications. 5 ml culture aliquots were labeled with 125 µCi of [5,6-^{3}H] uridine (Sigma, St. Louis, Mo, USA) in YPD medium for 3 min and chased by the addition of uracil to 2 mM. At each time point, 1.25 ml of culture was mixed with ice and the cells were pelleted. Pellets were immediately frozen and stored at -80°C until RNA was extracted. RNA samples (~10^5 cpm/lane) were separated on 1.2% agarose gel and transferred to Hybond-N+ nylon membrane. Membranes were sprayed with En3Hance (Du Pont NEN) and exposed to X-ray film.

2.11. Fluorescence Microscopy

Immunofluorescence microscopy was performed essentially as described (Kilmartin and Adams, 1984; Wente 1992). Logarithmically growing cells were washed in phosphate buffer (100mM KH_2PO_4, pH 6.8, 37.4mM KOH) and fixed in 3.7% (v/v) formaldehyde in phosphate buffer, at room temperature for 5 min. Fixed cells were washed in phosphate buffer and spheroplasted in an equal pellet volume of sorbitol citrate buffer (100mM K_2HPO_4, 36.4 mM citric acid, 833 mM sorbitol)

containing 10μg of Zymolyase 100T/ml for 30min at 30°C. The fixed spheroplasts were washed and resuspended in sorbitol citrate buffer at 1:20 dilution. Cells were spotted onto microscope slides precoated with a solution of 0.1% poly-L-lysine and allowed to settle. Excess cells were removed by aspiration and the remaining cells were permeabilized by submerging them in 100% ice-cold methanol for 4 min, followed by transfer to acetone for 30 sec. Slides were allowed to dry and then blocked in 2% milk in the PBS-T solution for 30min. Cells were probed with a primary antibody, followed by the incubation with an appropriate secondary antibody. The incubations were 1h each. Cells were washed with PBS-T containing2% skim milk, and then with PBS-T containing 2% BSA. Samples were immersed in mounting media, containing 90% glycerol, 0.2% phenylenediamine, and 0.025% DAPI in PBS.

Tubulin was detected using anti-α-tubulin monoclonal antibody (Santa Cruz, La Jolla, CA), Rrb1-HA was detected with the monoclonal antibody 12CA5 (Boehringer Mannheim, Laval, QC, Canada), rpL3 was detected using the monoclonal anti-rpL3 antibodies (kindly provided by Jonathan Warner, Albert Einstein College of Medicine, Bronx, NY), and Nop1 was detected with a α-Nop1 monoclonal antibody ((Aris and Blobel, 1988); kindly provided by M. Rout). The monoclonal antibodies were visualized with rhodamine-conjugated, goat anti-mouse antibodies (Jackson ImmunoResearch). Nuclear DNA was visualized by DAPI staining.

MAD1-GFP, MAD2-GFP and *MTW1-CFP* expressing strains were manipulated as described in section **2.4.2**, p.60. Cells were examined for GFP-and CFP-tagged proteins on a Zeiss Axioscope 2 microscope (Carl Zeiss Inc.) fitted with a Cooke Sensicam (Cooke, Auburn, MI), a Chroma GFP filter set (CZ909, Chroma Technology Corp., Brattleboro, VT), an Omega Optical CFP filter set (XF114-2, Omega Optical Inc. Brattleboro, VT) and a Uniblitz Shutter assembly (Uniblitz, Rochester, NY). Images were collected using IP-lab software (Scanalytics Inc., Fairfax, VA) and assembled using Adobe Photoshop software (Adobe Systems Inc., San Jose, CA).

nup170, mad1, mad2 and *nup170mad1* gene disruption strains, expressing *NUP53-GFP, NUP49-GFP* and *NUP188-GFP* were grown at 27° to early logarithmic phase, split into two cultures and then maintained at 23°C or shifted to 37°C for 3h. GR1HA and R1HA strains expressing *RPL3-GFP, RPL4A-GFP* and *RPL25-GFP* chimeras were grown in selection medium lacking leucine and subjected to carbon source shift as described above. The distribution of GFP-fusion proteins was directly visualized in the fluorescein channel. Slides were viewed in 100 X objective lenses of Olympus BX-50 microscope with a Spot HRD060-NIC digital camera (Diagnostic Instruments Inc. MI, USA) or a Zeiss LSM501 confocal microscope.

2.12. Protein Sequence Analysis

The location of WD-repeats in Rrb1p was determined using programs available at http://bmerc-www.bu.edu/wdrepeat/. Protein sequence alignments were done using BLAST and CLUSTALW programs at NCBI.

Chapter 3

Functional Associations Between the Yeast NPC and the Spindle Checkpoint Machinery

3.1. Overview

In response to defects in the assembly of the mitotic spindle or errors in chromosome attachment to the spindle, the spindle checkpoint restrains cells from entering anaphase and arrests them in mitosis. Chromosome attachment to the spindle is mediated by kinetochores, distinct protein complexes associated with the centromeric DNA.

Kinetochores move chromosomes on the spindle, thus enabling successful progression through mitosis. Mad1p and Mad2p are two evolutionary conserved proteins that play critical roles in the execution of the mitotic checkpoint (Li and Murray, 1991).

We have examined the subcellular localization of GFP-tagged Mad1p and Mad2p in *Saccharomyces cerevisiae*. Our data show that both proteins dynamically associate with NPCs (Iouk et al., 2002). Surprisingly, we observed that, unlike their mammalian homologues, both Mad1-GFP and Mad2-GFP remained associated with NPCs throughout the cell cycle and were not extensively recruited to kinetochores during mitosis. Only the activation of the mitotic spindle checkpoint induced by the microtubule depolymerizing drugs resulted in the recruitment of Mad2-GFP from the NPC to kinetochores. Even under these conditions, the majority of Mad1-GFP was found to associate with the NPC.

We have identified a subset of nucleoporins that are associated with the Mad1p-Mad2 complex. This subset includes Nup170p, Nup157p and Nup53p. The activation of mitotic spindle checkpoint releases Mad2p from its association with nucleoporins, whereas phosphorylated Mad1p remains bound to Nup53p. Furthermore, we demonstrate that Nup53p anchors Mad1p to the NPC and that the deletion of the *NUP53* gene abolishes checkpoint-induced phoshorylation of Mad1p. We also show that the localization of Mad2p to the NPC and its subsequent recruitment to kinetochore depends on the Mad1p.

3.2. Mad1p and Mad2p are associated with yeast NPCs

Mad1p and Mad2p are members of a group of at least seven conserved yeast proteins that are critical for executing a mitotic checkpoint in response to kinetochore and spindle integrity defects. We have investigated the subcellular localization of these two proteins by attaching a green fluorescence protein (GFP) tag to the C-terminus of each protein. This was accomplished by integrating the coding region of GFP into chromosomal copies of *MAD1* and *MAD2* following the last codon of their ORFs. Both the Mad1-GFP and Mad2-GFP proteins were functional in checkpoint control. This conclusion is based on three observations. First, haploid cells expressing these fusion proteins grew at rates not detectably different from isogenic wild-type (WT)

Figure 3-1. Association of Mad1-GFP and Mad2-GFP with NPCs. A) Cells expressing Mad1-GFP and Mad2-GFP are not sensitive to the microtubule destabilizing drug benomyl. Growth of the parental strain (WT) was compared to *MAD1-GFP*, *MAD2-GFP*, *mad1Δ* and *mad2Δ* strains. All strains were grown to logarithmic phase in YEPD at 30°C, diluted, and spotted in 10-fold increments on YEPD and YEPD containing benomyl (BEN 20μg/ml) and incubated for 4 days at 27°C. B) Western blot analysis of Mad1-GFP and Mad2-GFP producing cells. Nuclear extracts were isolated from *MAD1-GFP* and *MAD2-GFP* stains arrested in G1 with α-factor (α) or G2/M with nocodazole (noc) and proteins were separated by double-inverted gradient PAGE. Western blots were performed using anti-GFP antibodies. Mad1p-GFP prepared from nocodazole treated cells runs as a doublet indicative of Mad1p hyperphosphorylation. The positions of molecular mass markers are indicated on the left in kDs. C) Mad1-GFP and Mad2-GFP are associated with nuclear pore complexes. WT cells (WT) or an NPC clustering mutant, *nup120Δ*, synthesizing Mad1-GFP or Mad2-GFP were grown to logarithmic phase in YEPD at 30°C and examined by confocal fluorescence microscopy. Bar, 5 μm. **D)*** Mad1p and Mad2p are associated with isolated nuclear fractions. Western bolt analysis was preformed on subcellular fractions derived from the *MAD1-GFP* using anti-GFP, anti-Mad2p, and anti-Nup53p antibodies. Fractions are defined as follows: C, cytosol; CN, crude nuclei; PN, purified nuclei; NE, nuclear envelope pellet; NP, nucleoplasmic fraction. The material loaded in the C an CN lanes were derived from equal cell equivalents and PN, NE, and NP from 10-fold higher cell equivalents.

*This experiment was performed by Carl Thulin, from Dr. R.W. Wozniak laboratory, University of Alberta, Edmonton.

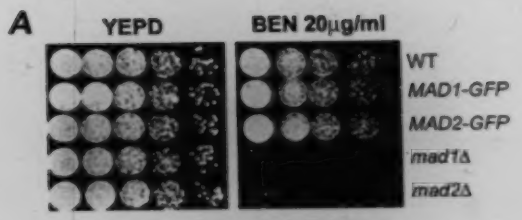
A
YEPD
BEN 20µg/ml
WT
MAD1-GFP
MAD2-GFP
mad1Δ
mad2Δ

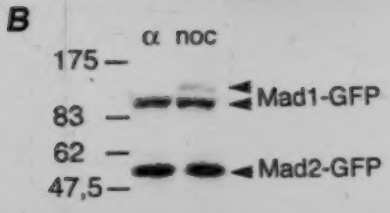
B
α noc
175
83
62
47,5
Mad1-GFP
Mad2-GFP

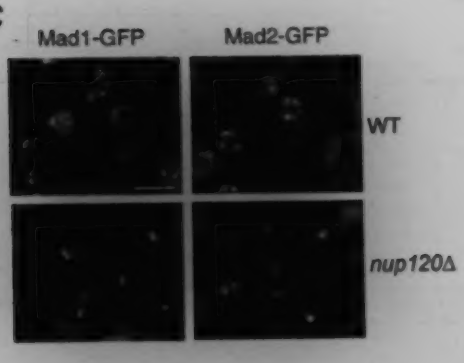
C
Mad1-GFP
Mad2-GFP
WT
nup120Δ

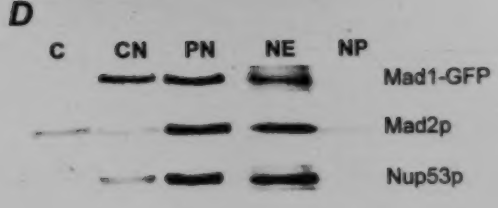
D
C
CN
PN
NE
NP
Mad1-GFP
Mad2p
Nup53p

cells in the presence of the microtubule depolymerizing drug benomyl (Figure 3-1A, p.79-80). This was in contrast to strains containing null mutations in *MAD1* or *MAD2* (*mad1Δ* and *mad2Δ*; Figure 3-1A, p.79-80), which exhibited a severe growth deficiency in the presence of benomyl due to a defect in mitotic checkpoint arrest. Secondly, Mad1-GFP, but not Mad2-GFP, was hyperphosphorylated in a manner similar to the WT protein when the spindle checkpoint was activated by the microtubule destabilizing drug nocodazole (Figure 3-1B, p.79-80; see Hardwick and Murray, 1995). Finally, chromosome segregation defects observed in *mad1Δ* and *mad2Δ* mutants were not detected in the *MAD1-GFP* and *MAD2-GFP* containing strains.

The subcellular localization of the Mad1-GFP and Mad2-GFP proteins was examined by fluorescence microscopy in asynchronously growing cells (Figure 3-1C, p.79-80). Mad1-GFP and Mad2-GFP were predominately visible along the NE in a distinct punctate pattern reminiscent of proteins associated with NPCs. One difference between their localization patterns was that Mad2-GFP also exhibited low levels of a diffuse signal throughout both the cytoplasm and the nucleoplasm. To confirm that the NE localization of Mad1-GFP and Mad2-GFP reflects their association with NPCs, we examined their distribution in a mutant strain (*nup120Δ*) where NPCs exhibit a distinct change in their distribution. In the *nup120Δ* strain, NPCs cluster within a single region of the NE and, as a consequence, signals derived from NPC associated proteins can be

discriminated from other NE proteins. As shown in Figure 3-1C, in *nup120Δ* strains both Mad1-GFP and Mad2-GFP were concentrated within a single patch of the NE, indicative of their clustering with other components of the NPC. Consistent with these data, subcellular fractionation experiments showed that Mad1-GFP was enriched in nuclear and NE fractions (Figure 3-1D, p.79-80). Both of these fractions also contained Mad2p; however, significant levels of Mad2p were also present in a cytosolic fraction (Figure 3-1D, p.79-80).

3.3. Spindle checkpoint activation induces the release of Mad2p, but not Mad1p, from NPCs and its accumulation at kinetochores

Numerous studies have shown that the mammalian orthologs of Mad1p and Mad2p are recruited to kinetochores during mitosis (Chen et al., 1996; Gorbsky et al., 1998). To explore whether Mad1p and Mad2p exhibit similar dynamics in yeast cells, we monitored the localization of Mad1-GFP and Mad2-GFP within an asynchronously growing cell population. We observed that the bulk of both Mad1-GFP and Mad2-GFP remained associated with the NPCs throughout the cell cycle, including mitosis (see Figure 3-2A, p. 83), and no extensive redistribution of either protein from NPCs to kinetochore clusters was visible (Figure 3-2B, p.83, rows I and III) as judged by comparison to the cyan fluorescent protein (CFP)-tagged kinetochore protein Mtw1p

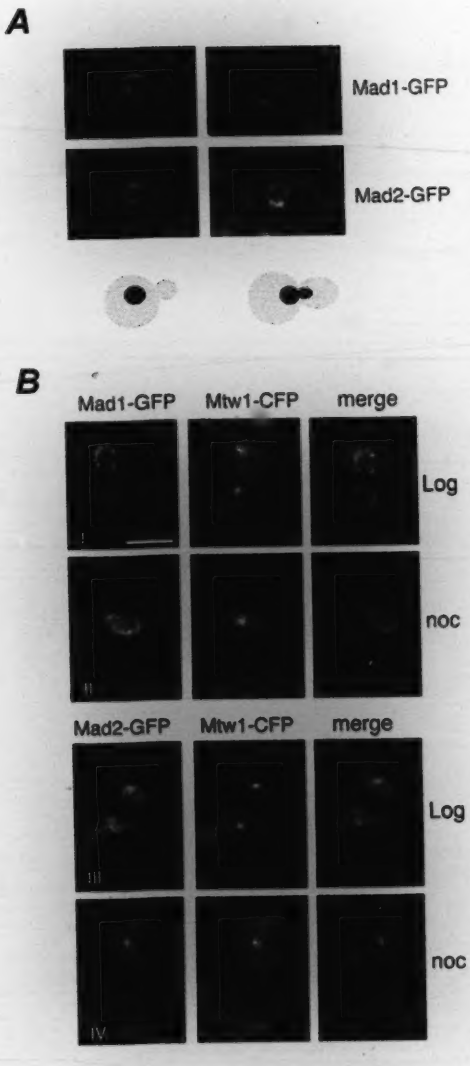

Figure 3-2*. Spindle checkpoint activation induces the release of Mad2p-GFP, but not Mad1p, from the NPC and its recruitment to kinetochores. A) Localization of Mad1-GFP and Mad2-GFP to NPCs throughout the cell cycle. Strains producing Mad1-GFP or Mad2-GFP were grown to logarithmic phase in YEPD at 30°C and examined by fluorescence microscopy. Representative images of cells in late S-phase (*left*) and M-phase (*right*) are shown. Corresponding shapes of cells (gray) and nuclei (black) are indicated on the *bottom panel*. B) Co-localization of Mad2-GFP and Mtw1-CFP to kinetochores upon spindle checkpoint activation. Strains synthesizing the kinetochore marker Mtw1-CFP and either Mad1-GFP or Mad2-GFP were grown to early logarithmic phase of growth (control -- *Rows I* and *III*, respectively) or G2/M arrested with nocodazole (noc -- *Rows II* and *IV*) and visualized by fluorescence microscopy. Subsequently, images were merged. Bar, 5 μm.

*This figure was contributed by Dr. Oliver Kerscher, from the laboratory of Dr. Munira Basrai, Department of Genetics, National Cancer Institute, National Institutes of Health, Bethesda, Maryland

(Goshima et al., 2000). We could not, however, exclude the possibility that low levels of Mad1-GFP and Mad2-GFP were associated with the kinetochores since these structures are closely juxtaposed to the NE.

Vertebrate homologues of Mad1p and Mad2p are recruited to kinetochores during mitosis. We reasoned that in yeast, the release of these proteins from the NPC and their localization to kinetochores might depend on activation of the spindle checkpoint. To test this, we examined the distribution of Mad1-GFP and Mad2-GFP and compared it to that of Mtw1-CFP after nocodazole treatment. As shown in Figure 3-2B row II, checkpoint arrest had no effect on the NPC localization of Mad1-GFP and little or no overlap was observed with the Mtw1-CFP signal. In contrast, checkpoint activation had a striking affect on Mad2-GFP. In nocodazole arrested cells, Mad2-GFP was no longer visible at the NPC and instead co-localized with Mtw1-CFP at the kinetochores (Figure 3-2B, p.83, row IV).

3.4. Mad1p and Mad2p are associated with a specific subset of Nups

To further understand the functional significance of the associations of Mad1p and Mad2p with the NPC and the dynamics of Mad2p's localization to kinetochores, we focused on identifying components of the NPC that anchor Mad1p and Mad2p to this structure. Clues as to the identity of these Nups came from two previous observations.

First, it was recently demonstrated that mutations that affect the function of Nup170p lead to defects in chromosome segregation and kinetochore integrity (Kerscher et al., 2001). Second, a paralog of Nup170p, Nup157p, was shown to interact with Mad2p in a genome-wide two-hybrid screen (Uetz et al., 2000).

These observations led us to investigate whether Mad1p and Mad2p could be detected in association with Nup170p and Nup157p following the purification of these Nups from disassembled NPCs. For these experiments, protein A (pA)-tagged versions of either Nup (Nup157-pA or Nup170-pA) were purified from nuclear extracts derived from logarithmically growing or α-factor arrested cultures expressing the tagged genes. Associated proteins were eluted with a step gradient of increasing $MgCl_2$. Similar results were obtained using either growth condition with the results from the α-factor arrested cultures shown in Figure 3-3, p.86-87. Consistent with our previous results, Nup170p was associated with Nup53p (Figure 3-3A, p.86-87; Nup170-pA, α-factor) (Marelli et al.,1998). Nup53p was also present in eluates from Nup157-pA (Figure 3-3A, p.86-87; Nup157-pA, α-factor). Moreover, in addition to Nup53p, we detected Mad1p and Mad2p in association with both Nup170-pA and Nup157-pA. By comparison, neither protein was detected in experiments using strains lacking a protein A tag or containing another tagged Nup such as Nup60-pA (Figure 3-3B, p.86-87; Nup60-pA, α-factor), which interacts with Nup2p (Dilworth et al., 2001).

Figure 3-3. Mad1p and Mad2p associate with a specific subset of nucleoporins. A) Protein A tagged Nup170-pA or Nup157-pA was affinity purified using IgG-Sepharose from nuclear extracts isolated from of α-factor (α-factor) and nocodazole (noc) treated cells. Proteins were eluted with a $MgCl_2$ step gradient, separated by SDS-PAGE, and immunoblotted with specific antibodies to detect Mad1p, Mad2p, Nup53p, and Nup2p, and the protein A fusion. An aliquot of the load fraction (L) is also shown. B) Similar experiments were performed with a WT strain (DF5) lacking a protein A tagged construct and a strain synthesizing Nup60-pA. Note, Nup60-pA interacts with previously identified binding partner, Nup2p, but not Mad1p or Mad2p. C) Mad1p, but not Mad2p, is associated with Nup53p in nocodazole treated cells. Nup53p was immunoprecipitated using Nup53p-specific antibodies out of nuclear extracts derived from α–factor (α–factor) and nocodazole (noc) treated cells synthesizing Mad1-GFP or Mad2-GFP. D) Nup53p and Mad2p are associated with immunoprecipitated Mad1p. Mad1-GFP was immunoprecipitated from nuclear extracts of α–factor (α–factor) treated cells synthesizing Mad1-GFP. In both panels C and D, bound complexes were eluted and analyzed as described in panel A using antibodies direct against GFP (for all GFP fusions), Nup53p, and Mad2p.

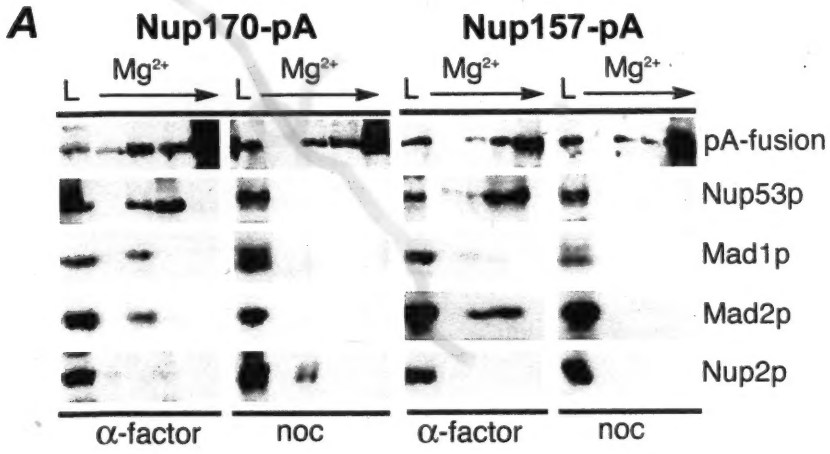
A
Nup170-pA
Nup157-pA
L
Mg2+
pA-fusion
Nup53p
Mad1p
Mad2p
Nup2p
α-factor
noc

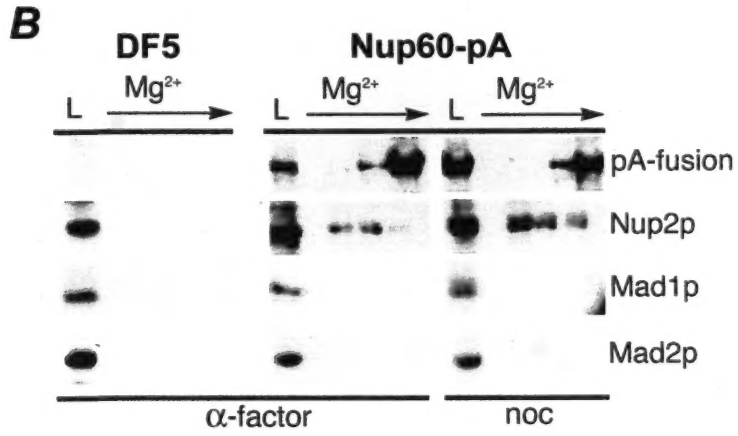
B
DF5
Nup60-pA
L
Mg2+
pA-fusion
Nup2p
Mad1p
Mad2p
α-factor
noc

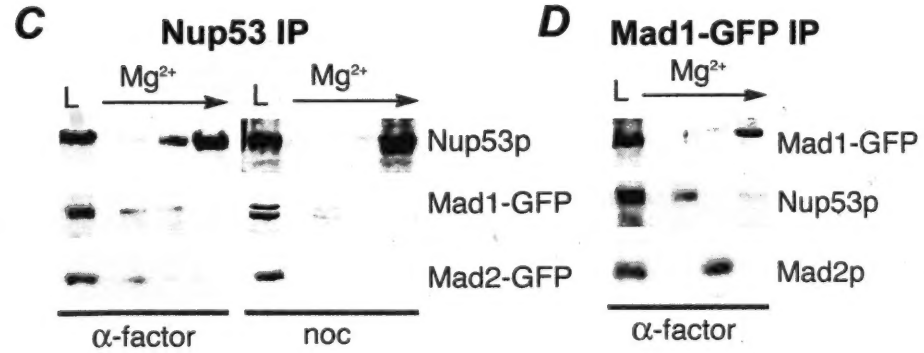
C
Nup53 IP
D
Mad1-GFP IP
L
Mg2+
Nup53p
Mad1-GFP
Mad2-GFP
Mad2p
α-factor
noc

Since Nup53p is associated with both Nup157p and Nup170p, we also tested whether Mad1p and Mad2p could be detected in association with this complex of Nups by immunoprecipitating Nup53p. For these experiments, nuclear extracts were isolated from cells expressing *MAD1-GFP* or *MAD2-GFP* and Nup53p was affinity purified using specific antibodies. As shown in Figure 3-3C (Nup53 IP, α-factor), both the Mad1-GFP and Mad2-GFP proteins were detected in association with Nup53p. Moreover, reciprocal immunoprecipitations performed with anti-GFP antibodies also detect Nup53p, as well as Mad2p, bound to Mad1-GFP (Figure 3-3D, p.86-87).

3. 5. Changes in molecular interactions between the Mad1p/Mad2p complex and the NPC upon spindle checkpoint activation

The activation of the spindle checkpoint leads to the release of Mad2-GFP from NPCs and its recruitment to kinetochores (Figure 3-2B, p.83) but does not effect the NPC association of Mad1p or Nup53p, Nup157p, and Nup170p (data not shown). To investigate the biochemical basis for these events, we analyzed the effects of spindle checkpoint activation on interactions between these proteins. As predicted, following checkpoint activation induced by either nocodazole or benomyl, Mad2p no longer associated with affinity-purified Nup157pA, Nup170pA, or Nup53p (Figure 3-3A and C, p.86-87). In contrast, Mad1p remained associated with Nup53p; however neither

Mad1p nor Nup53p were detected in association with Nup170-pA or Nup157-pA (Figure 3-3A and C, p.86-87). These results suggest that a complex containing Nup53p and Mad1p is disassociated from Nup170p and Nup157p. We excluded the possibility that these were non-specific effects caused by nocodazole or benomyl, since benomyl treatment of cells arrested with α-factor did not induce these changes (data not shown). Moreover, checkpoint activation did not affect the association of Nup60p or Nup170p with Nup2p even though Nup2p appears to be modified in these cells (Figure 3-3A and B), possibly by phosphorylation (Ficarro et al., 2002).

We further investigated the association of the Mad1p/Mad2p complex with the NPC by examining the localization of the checkpoint proteins in the absence of specific Nups. Since strains lacking genes encoding individual members of the Nup53p/Nup170p/Nup157p complex are viable, we tested the effects of their deletions on the localization of Mad1-GFP and Mad2-GFP. As shown in Figure 3-4A, p.90, the localization of Mad1-GFP to the NPC in strains lacking *NUP170*, *NUP157*, or *NUP59*, a gene encoding a Nup structurally similar to Nup53p, was not altered in asynchronous or nocodazole treated cells. However, in strains lacking Nup53p, the levels of Mad1-GFP associated with the NPCs were reduced in asynchronous cultures and undetectable in nocodazole treated cells. These results are consistent with a model in which Nup53p play a role in the association of Mad1p with the NPC .

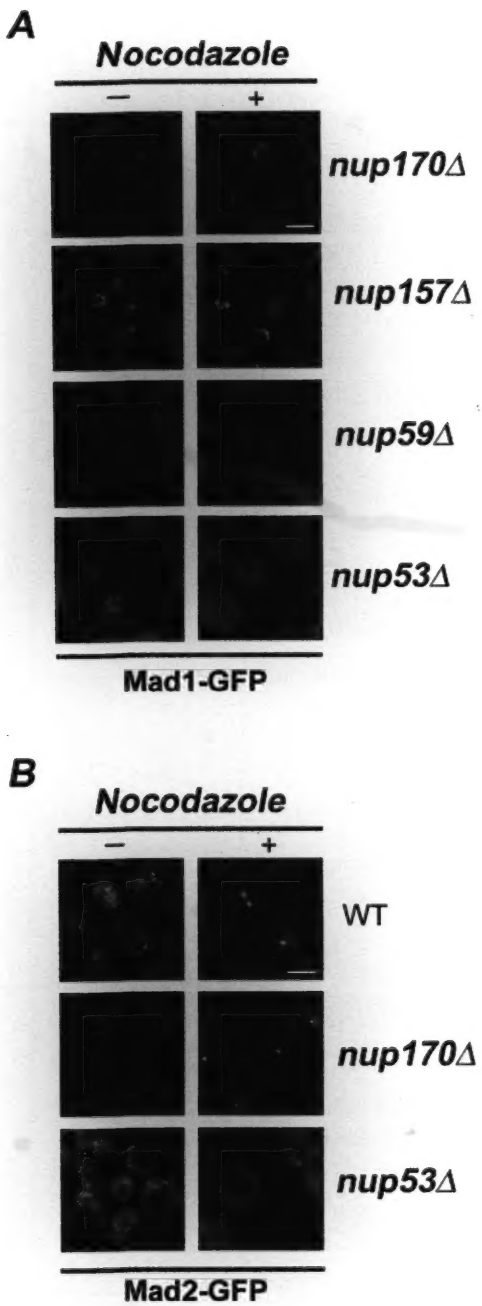

Figure 3-4. The effects of mutations in members of the Nup53p-containing complex on the subcellular distribution of the Mad1p/Mad2p complex.

A) Mislocalization of Mad1-GFP in a nocodazole treated *nup53Δ* strain. The subcellular localization of Mad1-GFP in logarithmically growing (-) or nocodazole treated (+) *nup170Δ*, *nup157Δ*, *nup59Δ* and *nup53Δ* strains was examined using confocal fluorescence microscopy.

B) Mislocalization of Mad2-GFP in a nocodazole treated *nup53Δ* strain. The localization of Mad2-GFP in logarithmically growing (-) or nocodazole treated (+) WT, *nup170Δ*, and *nup53Δ* strains was examined using confocal fluorescence microscopy. Bar, 5 μM.

The results obtained for Mad1p led us to examine the effects of Nup deletions on the subcellular distribution of Mad2p. As previously noted, in WT strains, Mad2-GFP is localized to the NPC in asynchronous cultures (Figures 3-1A, p.79-80; and 3-2A, p. 83) and recruited to kinetochores upon checkpoint activation. A similar localization pattern for Mad2-GFP was observed in a *nup170Δ* strain (Figure 3-4B, p.90). However, in a *nup53Δ* strain, the levels of Mad2-GFP at the NPC were visibly reduced in asynchronous cultures (Figure 3-4B, p.90). In addition, checkpoint activation in this strain failed to induce the accumulation of Mad2-GFP at kinetochores and instead the protein was diffusely distributed throughout the cell.

3.6. The Mad1p/Mad2p complex associates with the NPC through Mad1p

It was unclear whether Mad1p or Mad2p or both proteins interacted with the Nup53p-containing complex. We investigated these possibilities by removing Mad1p and examining the effect on the association of Mad2p with NPC or vice versa. To do this, Nup53p was immunoprecipitated from WT, *mad1Δ*, and *mad2Δ* strains and the eluates were probed with antibodies directed against Mad1p and Mad2p. As shown in Figure 3-5A, p.92, Mad1p was bound to Nup53p in the absence of Mad2p, but Mad2p was not detected in association with Nup53p in the absence of Mad1p. Consistent with these data, Mad1-GFP was localized to NPCs *in vivo* in the absence of Mad2p (Figure

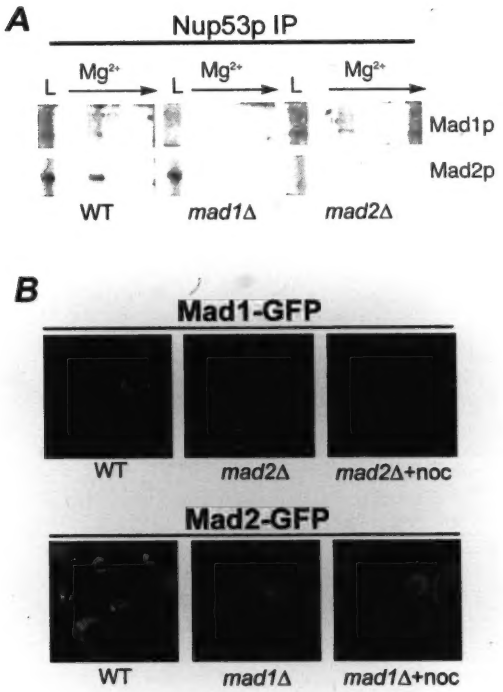

Figure 3-5. Mad1p/Mad2p complex associates with the NPC through Mad1p. A) The association of Nup53p with the Mad1p/Mad2p complex requires Mad1p. Nup53p was immunoprecipitated from nuclear extracts of WT, *mad1Δ* and *mad2Δ* strains. Proteins were eluted with a $MgCl_2$ gradient, separated by SDS-PAGE, and immunoblotted with specific antibodies directed against Mad1p or Mad2p. An aliquot of the load fraction (L) is also shown. B) Mislocalization of Mad2-GFP in a *mad1Δ* strain. The localization of Mad1-GFP and Mad2-GFP was examined in WT, *mad2Δ*, and nocodazole treated *mad2Δ* (+noc) strains using confocal fluorescence microscopy. Bar, 5 μm.

3-4B, p.90). However, Mad2-GFP failed to concentrate at the nuclear periphery and was visible throughout the cell in a strain lacking Mad1p. Furthermore, Mad2-GFP was not recruited to kinetochores in nocodazole-treated *mad1Δ* cells (Figure 3-4B, p.90). Together these data are consistent with a model in which the Mad1p/Mad2p complex binds the NPC through Mad1p (Figure 3-9, p.101).

3.7. Genetic interactions between *MAD1* and *MAD2* and nucleoporin genes

We investigated genetic interactions between *MAD1* and *MAD2* and four Nup genes, *NUP170*, *NUP157*, *NUP53* and *NUP59* to further assess the functional significance of the association of Mad1p and Mad2p with the NPC. Initially, we assayed the growth characteristics of each single deletion strain on rich media at 27°C and 37°C. Our analysis of serial dilutions revealed that all the strains formed colonies of approximately equal size with the exception of the *nup170Δ* strain, which grows slower then WT cells at both temperatures (Figure 3-6A, p.94).

Each of the nup null haploids was crossed with the *mad1Δ* and *mad2Δ* deletion strains. When we analyzed the haploid meiotic progeny, the expected numbers of double mutants were retrieved, suggesting that the double null mutations are not synthetically lethal. We tested the growth characteristics of each double deletion strain and, as shown in Figure 3-6A, p.94, all of these strains formed colonies of

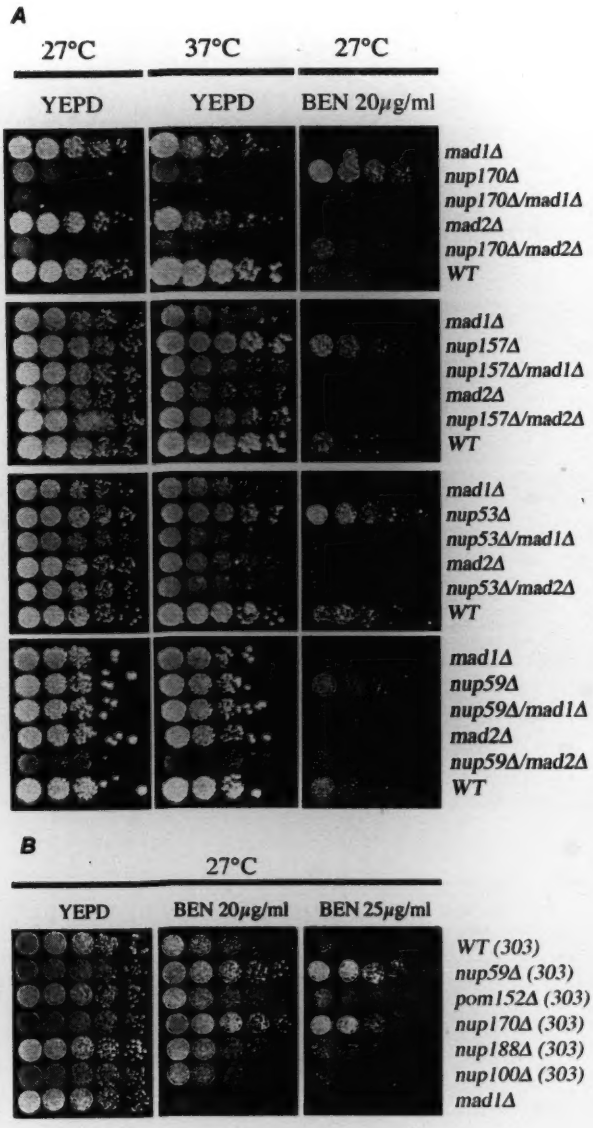

Figure 3-6*. *MAD1*, *MAD2* and Nup-encoding genes of the Nup53p-containing complex interact genetically. A) Growth chracteristics of strains containing deletions of *MAD1*, *MAD2* and *NUPs* reveal genetic interactions between nucleoporin and checkpoint genes. The growth of a WT, *mad1Δ*, *mad2Δ*, *nup170Δ*, *nup157Δ*, *nup53Δ*, and *nup59Δ* strains and combinations of double nulls were assessed at 27°C, 37°C, and 30°C (data not shown). Strains were grown to early logarithmic phase in YEPD at 30°C, diluted and spotted in 10-fold increments on YEPD and YEPD containing benomyl (BEN 20μg/ml) and incubated for 4-5 days at the indicated temperatures (27°C or 37°C).

B) Benomyl resistance of nup mutants. Serial dilutions of *nup59Δ*, *pom152Δ*, *nup170Δ*, *nup188Δ*, *nup100Δ* and *mad1Δ* strains, using W303 as the parental WT strain (WT 303), were spotted on YEPD plates containing either 20 μg/ml or 25 μg/ml of benomyl and incubated for 3 days at 27°C.

*This figure was contributed by Dr. Oliver Kerscher, from the laboratory of Dr. Munira Basrai, Department of Genetics, National Cancer Institute, National Institutes of Health, Bethesda, Maryland

approximately equal size. Two exceptions were the *nup170Δ mad1Δ* and *nup170Δ mad2Δ* deletion strains, both of which grew slower than *nup170Δ* and exhibited impaired growth at 27°C and either slow (*nup170Δ mad2Δ*) or barely detectable (*nup170Δ mad1Δ*) growth at 37°C.

We have tested the benomyl sensitivity of various null mutants to further assess the functional interactions between Mad1p and Mad2p and specific components of the NPC. As expected, growth of the *mad1Δ* and *mad2Δ* deletion strains was inhibited by benomyl (Figure 3-6A and B, p.94). However, null mutants of *NUP170*, *NUP157*, *NUP53*, and *NUP59* grew better than WT cells on benomyl containing plates (Figure 3-6A and B, p.94). This resistance to benomyl appears to be specific for these Nups as several other Nup null mutants, including two, *nup188Δ* and *pom152Δ* of the Nup53p-containing complex (Aitchison et al, 1995; Marelli et al.,1998), were not resistant to benomyl (Figure 3-6B, p.94).

We also tested each of the mad/nup double mutants for growth on benomyl containing plates. As shown in Figure 3-6A, p.94, the *mad1Δ* and *mad2Δ* deletions render the *nup53Δ*, *nup59Δ* and *nup157Δ* cells benomyl sensitive. However, we found that the *nup170Δ mad2Δ* strain was more resistant to benomyl than a *mad2Δ* deletion and was similar to WT cells. From these analyses, we conclude that the increased benomyl resistance of the tested nup deletions is dependent on Mad1p

and Mad2p. These genetic analyses thus suggest an important functional interplay between Mad1p, Mad2p and Nup53p, Nup59p, Nup170p and Nup157p in spindle dynamics.

3.8. Nup53p is required for the hyperphosphorylation of Mad1p in nocodazole treated cells

Our data are consistent with a model in which Nup53p plays a key role in anchoring Mad1p to the NPC (Figure 3-9, p.101). This is particularly evident following checkpoint activation when the association of Mad1p with the NPC is dependent on Nup53p (Figure 3-4, p.90). In response to checkpoint activation, Mad1p is hyperphosphorylated. We therefore examined what effects removing Nup53p and releasing Mad1p from the NPC would have on the nocodozole induced hyperphosphorylation of Mad1p. For these experiments, WT, *nup53Δ*, and *nup170Δ* strains containing Mad1-GFP or Mad2-GFP were treated with or without nocodazole. In the presence of nocodazole, each of these strains arrested with a 2C DNA content suggesting that the spindle checkpoint was functional (Figure 3-7A, p.97). As shown in Figure 3-7B, p.97, a reduction in the mobility of Mad1-GFP, diagnostic of its phosphorylation, was visible in arrested samples from WT and *nup170Δ* strains.

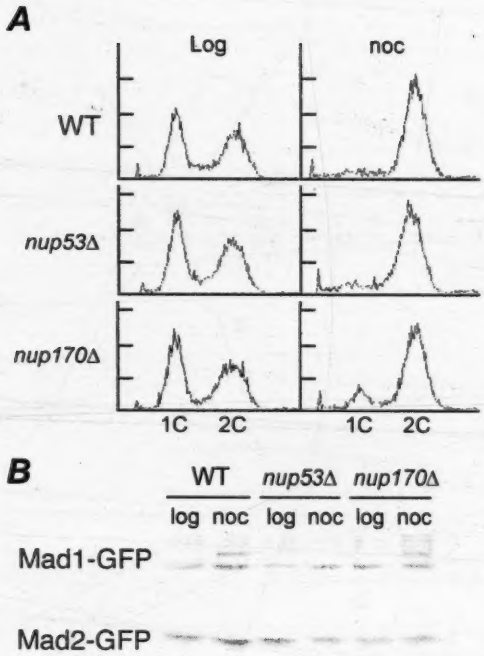

Figure 3-7. Requirement of Nup53p for hyperphosphorylation of Mad1p. A)* *nup170Δ* and *nup53Δ* deletion strains arrest in G2/M after treatment with nocodozole. FACS analysis was performed on logarithmically growing (log) and nocodazole (noc) treated (1.5 h) WT, *nup53Δ*, and *nup170Δ* strains. The positions of 1C and 2C DNA peaks are indicated. B) Western blot analysis indicating absence of Mad1p hyperphosphorylation in a *nup53Δ* strain. Logarithmically growing wild type (WT), *nup53Δ*, and *nup170Δ* strains expressing either Mad1-GFP or Mad2-GFP were treated with (noc) or without (log) nocodazole for 1.5 h. Protein samples were prepared from total cell lysates and separated by double-inverted gradient PAGE and then analyzed by immunoblotting using anti-GFP antibody. The position of hyperphosphorylation Mad1-GFP is indicated by an arrow.

* This experiment was performed by Dr. Oliver Kerscher, from the laboratory of Dr. Munira Basrai, Department of Genetics, National Cancer Institute, National Institutes of Health, Bethesda, Maryland

However, under the same conditions, no change in the mobility of Mad1-GFP was seen in the *nup53Δ* strain suggesting that it was not hyperphosphorylated in nocodazole arrested cells. These results suggest that the Nup53p-dependent association of Mad1p with the NPC is critical for its hyperphosphorylation.

3.9. Mad1p plays a role in the structural integrity of the Nup53p-containing NPC complex

We have shown that Mad1p resides primarily at the NPC throughout the cell cycle and after activation of the spindle checkpoint. This raises obvious questions of what role Mad1p, as well as Mad2p, might play in NPC functions including nuclear transport. To begin to address these questions, we examined the functional basis for the temperature-sensitive slow growth phenotype of the *nup170Δ mad1Δ* deletion strain and the effects of these mutations on nuclear transport and the structural integrity of the NPC. By introducing various reporter proteins into the *nup170Δ*, the *mad1Δ*, and the *nup170Δ mad1Δ* strains, we assessed nuclear transport mediated by the karyopherins Kap95p, Kap121p, and Xpo1p. In each case, transport of a cognate reporter was not affected at either 23°C or within a 3 hr shift to the non permissive temperature of 37°C.

We also examined the effects of *nup170Δ* and *mad1Δ* deletions on the structure integrity of the Nup53p-containing subcomplex by monitoring the localization of

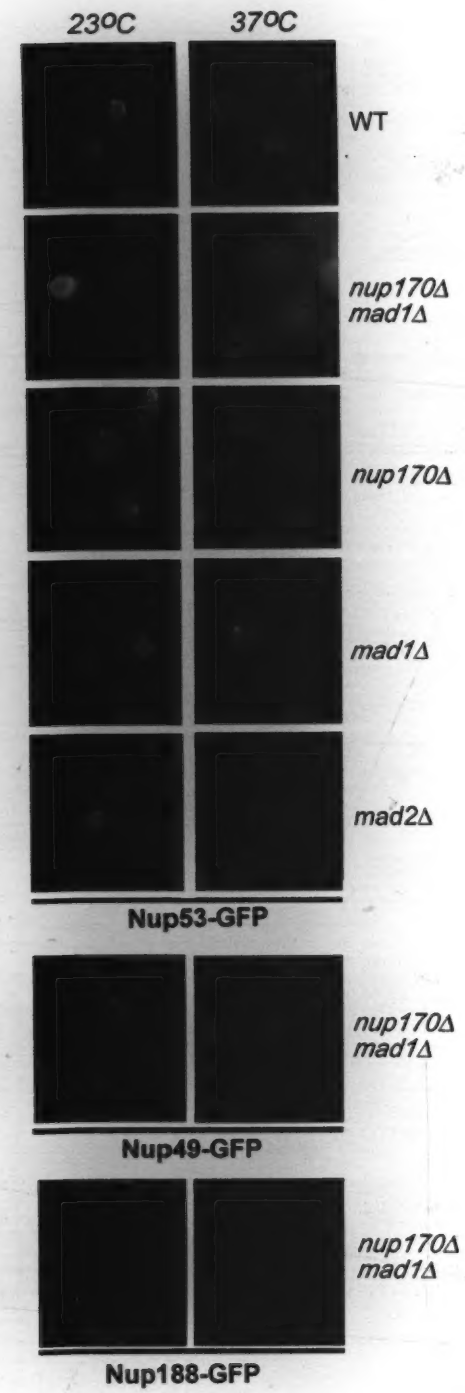

Figure 3-8*. Mad1 is required for integrity of the Nup53-containing complex. WT, *nup170Δmad1Δ*, *nup170Δ*, *mad1Δ* and *mad2Δ* strains expressing a plasmid born copy of *NUP53-GFP* (pNP53) were growth to logarithmic phase and either maintained at 23°C or shifted to 37°C for 3h. The localization of Nup53p-GFP was then examined by fluorescence microscopy. The results of similar experiments examining the localization of two other nucleoporins, Nup49-GFP and Nup188-GFP, in *nup170Δ mad1Δ* strain at 23°C or 37°C are shown in the bottom two rows.

*These experiments were performed by Dr. Rick Wozniak, Department of Cell Biology, University of Alberta, Edmonton

Nup53-GFP in the *nup170Δ mad1Δ* strain at 27°C and 37°C (Figure 3-8, p.99). At 27°C, Nup53-GFP was clearly associated with the NPCs. However, after shifting to 37°C for 3 hr, Nup53-GFP was no longer concentrated at the NE but appeared distributed throughout the cell. This effect was specific, as temperature shift had no effect on the localization of two other Nups, Nup49-GFP and Nup188-GFP. Moreover, shifting WT cells to 37°C has no effect on the localization of Nup53p-GFP. We also examined the effects of temperature shift on Nup53-GFP in strains containing single deletions of *mad1Δ*, *nup170Δ*, and *mad2Δ*. Strikingly, in both the *mad1Δ* and *nup170Δ* strains, but not in a *mad2Δ* strain, the amount of Nup53-GFP bound to the NPCs was also decreased at 37°C. These results are consistent with a role for Mad1p in the stability of the Nup53p-containing complex.

3.10. Discussion

Here we have identified a functional link between components of the *S. cerevisiae* NPC and the mitotic checkpoint machinery. We have shown by a variety of criteria that a complex of the checkpoint proteins Mad1p and Mad2p resides largely at the NPC throughout the cell cycle. At the NPC, these proteins are associated with the Nup53p-containing subcomplex (Marelli et al.,1998). These interactions can be detected by reciprocal affinity purification of this Nup complex,

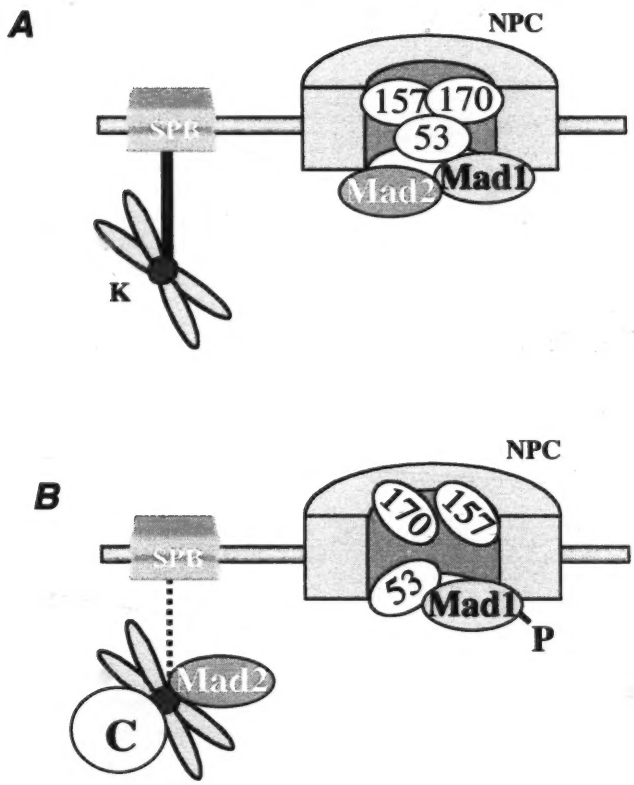

Figure 3-9*. Model summarizing interactions between the Nup53p-containing complex Mad1p, and Mad2p. A) Shown is an NPC with Nup53p, Nup157p, and Nup53p (53, 157 and 170). The Mad1p /Mad2p complex is associated with the NPC through Mad1p via Nup53. Additional interactions between Mad proteins and/or the NPC may also exist. Also depicted are one of the spindle pole bodies (SPB) connected to a chromosome's kinetochore (K) via a microtubule (black line). B) Defects in microtubule interaction (interrupted line) of the SPB with the kinetochore lead to spindle checkpoint activation, hyperphosphorylation of Mad1p (P), dissociation of Mad2p from the NPC and the recruitment of Mad2p to the kinetochores along with other checkpoint proteins (C). At the same time, Nup157p and Nup170p are not longer associated with phosphorylated Nup53p (P). In the scenario depicted, Nup53p is required for optimal localization of Mad1p and Mad2p.

*This model was created by Dr. Rick Wozniak, Department of Cell Biology, University of Alberta, Edmonton.

Mad1p or Mad2p (Figure 3-3, p.86-87). Our data are consistent with a model in which the association of Mad2p with these Nups is dependent on Mad1p (Figure 3-9, p.101). In the absence of Mad1p, Mad2p fails to associate with NPCs and is dispersed throughout the cell. The association of the Mad1p/Mad2p complex with the NPC is, in large part, mediated by the association of Mad1p with Nup53p. Removal of Nup53p (*nup53Δ*) causes a reduction in levels of Mad1p and Mad2p associated with NPCs and increased levels in the cytoplasm (Figure 3-4, p.90), but no significant changes in the cellular levels of either protein. It remains to be determined what Nups, in the absence of Nup53p, would support the reduced levels of Mad1p/Mad2p complex binding to the NPC. One explanation is that their association is partially maintained by lower affinity interactions with other members of the Nup53p-containing complex including Nup157p and Nup170p.

Our observation that *S. cerevisiae* Mad1p and Mad2p remain associated with NPCs throughout the cell cycle differs from the events described in vertebrate cells. Recent data have shown that vertebrate homologs of these proteins are also associated with NPCs during interphase (Campbell et al., 2001). However, in these cells, upon entering mitosis, the NE and the NPCs are disassembled and Mad1p and Mad2p accumulate at unattached kinetochores in prometaphase where they remain until the

spindle fully engages all the kinetochores. This situation does not occur in *S. cerevisiae* where the NE and NPCs do not disassemble during mitosis. Moreover, following replication of centromeric DNA, kinetochores are assembled and rapidly engaged by microtubules (reviewed by Winey and O'Toole, 2001). Thus, kinetochores unattached to spindle microtubules are not detected during mitosis. This may partially explain why Mad1p and Mad2p remain at the NPC during mitosis. Consistent with these predictions, only upon activation of the spindle assembly checkpoint is Mad2p released from the NPCs (Figure 3-2, p.83). In contrast, the bulk of Mad1p remains at the NPC and we fail to detect a discernible accumulation of Mad1p at the kinetochores. It is possible that a portion of Mad1p is also recruited to kinetochores but that it is either below the level of detection, obscured by the NPC signal, or its association with the kinetochores is transient with Mad1p being quickly recycled back to the NPCs.

In addition to the release of Mad2p, checkpoint arrest induced by nocodazole also resulted in profound effects on the molecular interactions between members of the Nup53p-containing complex and Mad1p. In nocodazole arrested cells, Nup53p, Mad1p, and Mad2p are no longer detected in association with Nup157p or Nup170p (Figure 3-3, p.86-87). These changes are accompanied by the phosphorylation of Nup53p (Marelli et al. 1998) and Mad1p (Hardwick and Murray; 1995; Figure 3-3,

p.86-87). Nup53p and Mad1p, however, remain associated and this interaction is required for maintaining Mad1p at the NPC following spindle checkpoint activation (Figure 3-4, p.90). By analogy to higher eukaryotes where extensive changes in protein-protein interactions between nups occur during mitosis, these experiments suggest that distinct molecular rearrangements also occur within the yeast NPC. However, in yeast these specific changes are not functioning in NPC disassembly as they do in higher eukaryotes. We and others have not observed changes in the NPC localization of any nups during mitosis, including those that are part of the Nup53p-containing complex (Marelli et al., 1998; Kerscher et al., 2001). We therefore propose that in yeast specific changes in protein-protein interactions occur during mitosis that alters the functional properties of the NPC, including its association with the checkpoint machinery.

Several observations suggest that the association of the Mad1p/Mad2p complex with the NPC plays an important role in the function of these checkpoint proteins and the structure of the NPC. We have shown that the checkpoint-induced hyperphosphorylation of Mad1p does not occur in the absence of Nup53p suggesting that the physical association of Mad1p with Nup53p promotes the phosphorylation of Mad1p, an event that is believed to be mediated by the kinase Mps1p in response to spindle damage (Hardwick et al., 1996). Surprisingly, this observation suggests that

the phosphorylation of Mad1p is not required for spindle checkpoint function as the *nup53Δ* strain does not exhibit a checkpoint defect, thus raising the question of the role of phosphorylation in the function of Mad1p. Others have also shown that the association of Mad1p with Mad2p is independent of the phosphorylation state of Mad1p (Farr and Hoyt, 1998, Chen et al., 1999). Furthermore, Mad1p phosphorylation has not been observed in higher eukaryotes. (Campbell et al., 2001).

In addition to the role of Nup53p in Mad1p phosphorylation, our results also suggest that the localization of Mad2p to kinetochores induced by checkpoint activation is dependent on the presence of Nup53p (Figure 3-4, p.90). One possibility is that the effects of removing Nup53p occur as a result of changes in the association of Mad1p with the NPC, since the association of Mad2p with the NPC dependents on Mad1p and we have shown that Mad1p is strictly required for the recruitment of Mad2p to kinetochores (Figure 3-5, p. 92). As the *nup53Δ* strain shows no apparent checkpoint defects (Figure 3-7, p.97), these results suggest that Mad2p can still function in checkpoint arrest even though its association with the kinetochores is attenuated.

Since Nup53p and Mad1p do not appear to visually leave the NPC or accumulate at the kinetochores during checkpoint arrest, it seems unlikely that they play a direct role in the binding of Mad2p to the kinetochores. These observations could be

explained if we consider a model in which the NPC acts as a platform for regulating the assembly of complexes between checkpoint proteins. Our data showing significantly higher levels of Mad2p, but not Mad1p, in the cytoplasm are consistent with the idea that a free pool of Mad2p exists in the cytoplasm and that formation of the Mad1p/Mad2p complex may occur at the NPC. It would also seem possible that the formation of other complexes that have been shown to be dependent on Mad1p, including, for example, a Mad2p/Mad3p/Bub3p/Cdc20p complex (Fraschini et al., 2001) occurs at the NPC and that these events contribute to the checkpoint-induced recruitment of Mad2p to kinetochores. Recent, reports also place *S. pombe* Mad2p at the nuclear periphery (Ikui et al., 2002). This potential role for NPC-bound Mad1p represents a topologically distinct model from those proposed in vertebrate cells where the assembly of checkpoint-induced complexes has, in some instances, been suggested to occur at kinetochores (see Shah and Cleveland, 2000; Millband and Hardwick, 2002). NPC components could also play a similar role in higher eukaryotes since these structures disassemble during mitosis and thus the NPC platform could to be recruited to kinetochores. This idea is supported, in theory, by recent data showing that several NPC proteins are detectable at kinetochores during mitosis (Belgareh et al., 2001). We are currently examining the prometaphase

localization of the mammalian counterparts of Nup53p and Nup170p to determine whether they exhibit similar kinetochore binding properties.

It still remains to be determined whether the interactions between the NPC and Mad1p and Mad2p are critical for their checkpoint functions or whether this association plays another role, such as regulating the level of the checkpoint response. The functional redundancy between members of the Nup53p-containing complex makes this difficult to test directly. However, a potential functional link is the benomyl resistant phenotype of the nup null mutants, which is dependent on a functional spindle checkpoint as the deletion of *MAD1* or *MAD2* suppressed this phenotype (Figure 3-6, p.94). The mechanistic basis for this phenotype is not clear, but one possibility is that deletions of its members alters the ability of the Nup53p-containing complex to regulate the level of the checkpoint response. The benomyl resistant phenotype of the nup mutants could reflect an up-regulation of the checkpoint that prolongs mitotic arrest and increases cell survival in the presence of elevated levels of benomyl. Alternatively, the benomyl resistance of these mutants may reflect a separate, as yet undefined, role for these nups in regulating spindle dynamics.

Our data also support the idea that the Mad1p/Mad2p complex plays an active role in NPC structure and function. In the absence of Mad1p, the association of

Nup53p with the NPC becomes thermolabile, being largely released from the NPC at 37°C (Figure 3-8, p.99). A similar phenomenon was also observed in strains lacking Nup170p. These data clearly suggest that Mad1p, like Nup170p, contributes to the structural integrity of the Nup53p-containing complex. These observations may, in part, explain the growth defect of the *nup170Δ mad1Δ* strain since this mutant may partially mimic the lethal phenotype of a *nup170Δ nup53Δ* mutant (Marelli et al., 1998). Of note, Mad1p has structural features in common with several nups including a region rich in asparagines residues and a predicted secondary structure containing coiled-coil repeats. It will be of interest to determine what other roles Mad1p and Mad2p play in NPC function.

In conclusion, we have shown that nucleoporins impart a temporal and spatial component to the assembly and function of checkpoint proteins. Checkpoint proteins are conserved throughout the eukaryotic phyla, including humans. Mutations in the genes encoding these proteins can result in chromosome loss (Li and Murray, 1991; Cahill et al., 1998), cancer (Lengauer et al., 1998) and developmental defects (Dobles et al., 2000). Likewise, for the NPC components, a human homolog of *S. cerevisiae NUP170* (hsNUP155), has been implicated in developmental defects (Gigliotti et al., 1998; Zhang et al., 1999). Hence, our data on the functional relationship between checkpoint protein complexes and the NPC may help us understand the molecular

role of these evolutionarily conserved proteins in genome stability in model organisms and humans.

Chapter 4

Rrb1p, a Yeast Nuclear WD-repeat Protein Involved in the Regulation of Ribosome Biosynthesis

4.1. Overview

Ribosome biogenesis is regulated by environmental cues that coordinately modulate the synthesis of ribosomal components and their assembly into functional subunits. We have identified an essential yeast WD-repeat containing protein, termed Rrb1p that has a role in both the assembly of 60S ribosomal subunits and in the transcriptional regulation of ribosomal protein (RP) genes (Iouk et al., 2001). Rrb1p is located in the nucleus and is concentrated in the nucleolus. Its presence is required to maintain normal cellular levels of 60S subunits, 80S ribosomes, and polyribosomes. The function of Rrb1p in ribosome biogenesis appears to be linked to its association with the ribosomal protein rpL3. Immunoprecipitation of Rrb1p from nuclear extracts revealed that it physically interacts with rpL3. Moreover, the overproduction of Rrb1p led to increases in cellular levels of free rpL3 that accumulated in the nucleus together with Rrb1p. The concentration of these proteins within the nucleus was dependent on ongoing protein translation. We have also shown that overexpression of *RRB1* led to a robust increase in the expression of *RPL3,* while all other examined RP genes were unaffected. In contrast, depletion of RRB1 caused an increase in the expression of all RP genes examined except *RPL3*. These results suggest that Rrb1p regulates *RPL3* expression and uncouples it from the coordinated expression of other RP genes.

4.2. Background

Ribosome biogenesis is a complex process that requires the precise regulation of both the synthesis and assembly of its component parts in response to environmental stimuli (reviewed by Nomura, 1999; Warner, 1989 and1999; Woolford and Warner, 1991). In rapidly growing yeast cells, the expression of the ribosomal protein (RP) genes and the ribosomal DNA consumes a major portion of the cell transcriptional activity (Warner, 1999; Woolford and Warner, 1991). Their products contribute to the production of ~2000 ribosomes per minute (Warner, 1999). The rate of ribosome synthesis, however, can be quickly altered by changes in growth conditions. Although numerous steps in this regulatory process have been studied in detail, how these events are intertwined to coordinate ribosome assembly remains unclear.

In the yeast *Saccharomyces cerevisiae*, ribosome assembly is controlled by coordinated transcriptional events that regulate the expression of the RP genes and transcription of ribosomal RNA (for reviews, see Planta, 1997; Warner, 1999). Expression of these components is influenced by a variety of factors including nutrient availability, secretory activity, heat shock, and exposure to to signaling molecules (Warner, 1999). The cell's responses to these cues are mediated by at least two kinase signaling pathways: the *ras*-cAMP-protein kinase A pathway and the 'target of rapamysin' or TOR pathway (Neuman-Silberberg, et al., 1995; Powers and Walter,

1999; Thevelein, 1994). Though distinct, both of these pathways converge to regulate the transcription of RP genes by a mechanism that is dependent on the DNA-binding protein Rap1p (Li et al., 1999; Mizuta et al., 1998; Moehle and Hinnebusch, 1991). Rap1p plays a role in the transcriptional regulation of a large number of genes including the RP genes, exhibiting both activation and silencing activities depending on the locus to which it is bound (reviewed by Planta, 1997, Shore, 1994). For the RP genes, Rap1p acts as an activator of transcription, but it is also required for the suppression of the expression that occurs, for example, as a consequence of defects in the secretory pathway (Mizuta et al., 1998). The varied functions of this protein have led to the idea that Rap1p may play a general role in altering chromatin structure, making it accessible to other transcriptional regulators (Morse, 2000; Planta, 1997).

The coordinated expression of the RP genes leads to the nearly equimolar production of each of the 78 ribosomal proteins (reviewed in Warner, 1999; Woolford and Warner, 1991). Following their synthesis in the cytoplasm, most ribosomal proteins are actively transported into the nucleus. Ribosome assembly is believed to occur primarily in the nucleolus, where an ordered assembly of ribosomal proteins begins on a 35S rRNA precursor (Kruiswijk, 1978; for a review see Venema and Tollervey, 1999) leading to the formation of a 90S preribosomal particle (Trapman et al., 1975). Among the early assembling ribosomal proteins are rpL3 and rpL25. The 90S particle

subsequently undergoes a series of processing steps that separate it into a pre-60S large subunit containing 25S and 5.8S rRNAs and a 43S small subunit precursor containing 20S rRNA (reviewed by Kressler et al., 1999). Both of these subunits are exported from the nucleus and are further modified to form mature ribosomal subunits.

The assembly of ribosomal proteins into ribosomal subunits is required to maintain their stability in the cell. By a mechanism that is not well understood, excess ribosomal proteins that fail to assemble into ribosomes are identified and are targeted for rapid degradation (Maicas et al., 1988). This pathway was revealed, in part, on the basis of experiments examining the fate of individual ribosomal proteins, including, among others, rpL3, rpL25, and rpL16 (rpL11A, Mager et al., 1997), produced by the overexpression their genes (elBaradi et al., 1986; Maicas et al., 1988; Tsay et al., 1988). Their overexpression produces increased levels of mRNA that is efficiently translated; however, the excess proteins have extremely short half-lives of between 30 sec and 3 min (Warner, 1999; Woolford and Warner, 1991). How these excess proteins are identified and where their degradation occurs, in the nucleus or the cytoplasm, are not known. As a consequence of these and other studies, it is generally assumed that cellular levels of free ribosomal proteins are maintained at very low levels (Warner, 1999). Despite this, free ribosomal proteins do have functional roles outside the ribosome. For example, free rpL30 (Dabeva et al., 1993; Eng and Warner, 1991;

Vilardell and Warner, 1994; Vilardell and Warner, 1997) and rpS14 (Fewell and Woolford, 1999) both appear to act as feedback inhibitors of the splicing of their own mRNA.

Here we present data on the identification of an essential WD-repeat protein, termed Rrb1p, that plays a role in the assembly of 60S ribosomal subunits and the regulation of RP gene expression. Rrb1p directly interacts with free rpL3 and it modulates the amount and localization of free rpL3 in the cell. Moreover, changes in the cellular level of Rrb1p alters *RPL3* expression and uncouples it from the coordinated expression of other RP genes.

4.2. The identification of YMR131c

We have identified an uncharacterized ORF (YMR131c) in the *S. cerevisiae* genome whose deduced amino acid sequence displays characteristics that are consistent with a role in nuclear function. YMR131c displays a high degree of sequence identity with uncharacterized ORFs from various species, including *Drosophila melanogaster, Caenorhabditis elegans*, and *Arabidopsis thaliana*. It encodes a protein containing two extended acidic domains within its N-terminal half and five predicted tryptophan-aspartic acid (WD)-repeat motifs located in its C-terminal half. WD-repeats are structural motifs present in a wide range of proteins that establish an interface to which other

proteins bind (reviewed by Smith et al., 1999). The acidic regions present in the N-terminal half of the protein are similar to those previously identified in a number of nucleolar proteins involved in ribosome biogenesis. Their presence has been suggested to reflect the intrinsic ability of a protein to shuttle between the nucleus and the cytoplasm (Xue and Melese, 1994). On the basis of its role in ribosome biogenesis described below, the protein encoded by YMR131c ORF has been termed Rrb1p, for regulator of ribosome biogenesis 1.

4.3. *RRB1* encodes an essential nuclear protein

The phenotype of cells lacking the *RRB1* gene was determined by deletion of the gene and replacement with the *HIS3* selectable marker in a W303 diploid strain. The heterozygous strain was sporulated and tetrads dissected. All viable haploids lacked the *HIS3* marker (data not shown), indicating that the *RRB1* gene is essential for cell viability.

To examine the subcellular localization of Rrb1p, a plasmid-born copy of its gene was tagged by inserting a DNA fragment encoding a hemagglutinin (HA) tag following the C-terminal amino-acid codon. An *rrb1* null strain carrying this plasmid (R1HA) grew at wild-type rates demonstrating that the Rrb1-HA protein was functional (data not shown). The subcellular distribution of this protein was examined by

immunofluorescence microscopy using a monoclonal antibody (12CA5) directed against the HA epitope. As shown in Figure 4-1A,p.118, the Rrb1-HA protein was present throughout the nucleus but was concentrated in the nucleolus adjacent to the intense DAPI staining regions of the nucleus. Its localization to the nucleus was further confirmed by subcellular fractionation. Immunoblotting of fractions derived from the R1HA strain detected a single protein species at ~70 kD in a crude nuclear fraction (Figure 4-1B, p.118). A second lower molecular mass species also cofractionated with an enriched nuclear fraction. The smaller species is thought to be a degradation product of Rrb1-HA since it gradually accumulated following isolation and storage of nuclei.

4.4. Construction of a conditional *RRB1* allele

We have inserted the *RRB1-HA* ORF into the plasmid pYEUra3 (*CEN URA*) behind the *GAL1* promoter and introduced this plasmid into a *rrb1* null strain by plasmid shuffling. The resulting strain (GR1HA; *rrb1Δ, GAL1::RRB1-HA*) grew on galactose-containing plates but its growth was inhibited (upon repression of the *GAL1* promoter) by growth on plates containing glucose (data not shown). A similar strain (GR1GFP; *rrb1Δ, GAL1::RRB1-GFP*) in which the coding region for the *Aequorea victoria* green fluorescent protein (GFP) was inserted in place of the HA tag was also produced and it

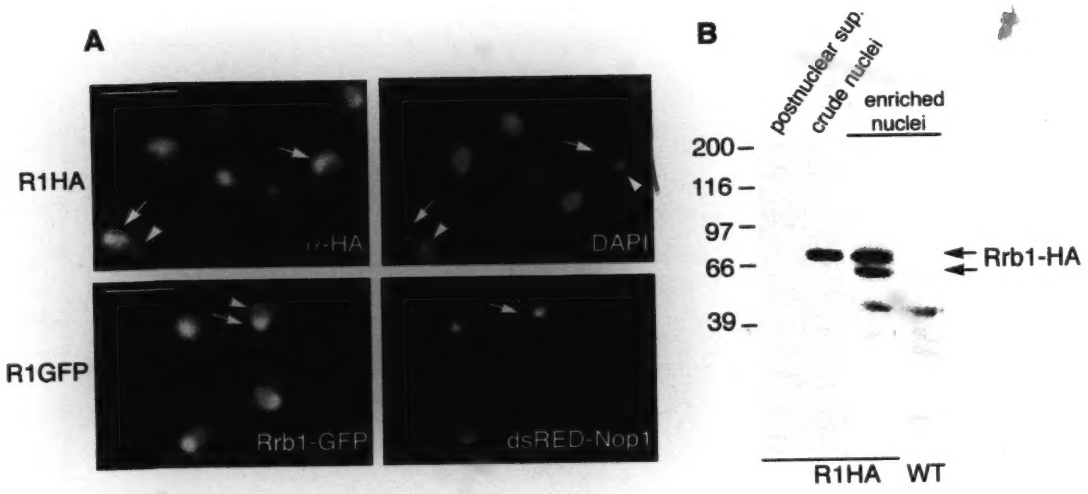

Figure 4-1. Rrb1p is located in the nucleus and concentrated in the nucleolus. A) R1HA cells were fixed, permeabilized, and probed with MAb 12CA5. Binding was detected with rhodamine-conjugated, goat anti-mouse antibodies. Nuclear DNA was visualized by DAPI staining. The corresponding positions of MAb 12CA5 (arrows) and DAPI (arrowheads) binding in several nuclei are shown. Below these are shown images of the strain R1GFP-N expressing an integrated *RRB1-GFP* construct and plasmid-borne DsRED-*NOP1* fusion. Rrb1-GFP and nucleolar DsRED-Nop1 were detected using fluorescein isothiocyanate and rhodamine filters, respectively, and the arrow points to the same region of the nucleus in both images. Bar, 5 μm. B) Rrb1p cofractionates with nuclei. R1HA cells were used to produce a postnuclear supernatant, a crude nuclear pellet, and an enriched nuclear fraction. Rrb1-HA in these fractions was detected by Western analysis using MAb 12CA5. Wild-type (WT) W303 nuclei lacking the Rrb1-HA were also probed with MAb 12CA5. The positions of molecular mass markers are shown in kilodaltons.

showed similar growth characteristics. In these strains, the galactose-induced Rrb1-HA and Rrb1-GFP chimeras were accurately targeted to the nucleus and accumulated in the nucleolus (Figure 4-2A, p.120-121).

The levels of Rrb1-HA synthesized in the GR1HA strain in galactose, glucose, or a combination of both were compared to the amounts of Rrb1p produced by the endogenous *RRB1* promoter (Figure 4-2B, p.120-121). The purpose of these experiments was to define conditions where the *GAL1*-driven expression of *RRB1-HA* approximated that of wild-type cells and thus, identify a starting point for the overexpression or depletion of *RRB1-HA*. As shown in Figure 4-2B,p.120-121, the G57HA strain grown in galactose-containing medium produced higher levels of Rrb1-HA than wild-type strains. However, by combining galactose and glucose at various ratios, we were able reduce *RRB1-HA* expression to levels at, or below, wild-type levels. For the majority of experiments which follow, the GR1HA (and GR1GFP) strain was maintained in medium containing a 70:30 or 60:40 percent ratio of galactose to glucose. These cells still maintained growth rates similar to wild-type cells (Figure 4-2C, p.120-121). Shifting these cells to glucose-containing medium arrested their growth (Figure 4-2C, p.120-121).

Figure 4-2. *GAL1* regulation of *RRB1* expression. A) GR1HA (*GAL1::RRB1-HA*) cells were grown in medium containing a galactose: glucose mixture (60:40) and then shifted to either 2% galactose- or 2% glucose-containing medium for 6 h. Rrb1-HA was detected by immunofluorescence as described for Figure 4-1, p. 118, using MAb 12CA5. Nuclear DNA was visualized by DAPI staining. Bar, 5 μm. B) The levels of Rrb1-HA were examined in GR1HA (*GAL1::RRB1-HA*) and R1HA (*RRB1* controlled by its endogenous promoter) cells grown with various carbon sources. Cells were grown in a 2% carbon source composed of the proportion of galactose (gal) and glucose (glc) indicated. Western blotting was performed on total cell lysates derived from equal amounts of cells, using MAb 12CA5 to detect Rrb1-HA or an antibody directed against the nuclear pore complex protein Nup53p (Marelli et al., 1998). C) Cultures of GR1GFP and R1GFP (*RRB1-GFP* controlled by the *RRB1* promoter) were grown to early logarithmic phase and the mean fluorescent intensity (y axis) of 10^4 cells was determined by fluorescence-activated cell sorter analysis and plotted versus the percentage of galactose in the carbon source mixture. D) GR1GFP, GR1HA, and R1HA cells were grown overnight in media containing a 60:40 mixture of galactose and glucose and then plated onto YP plates containing either galactose or glucose. Plates were incubated for 2 days at 30°C.

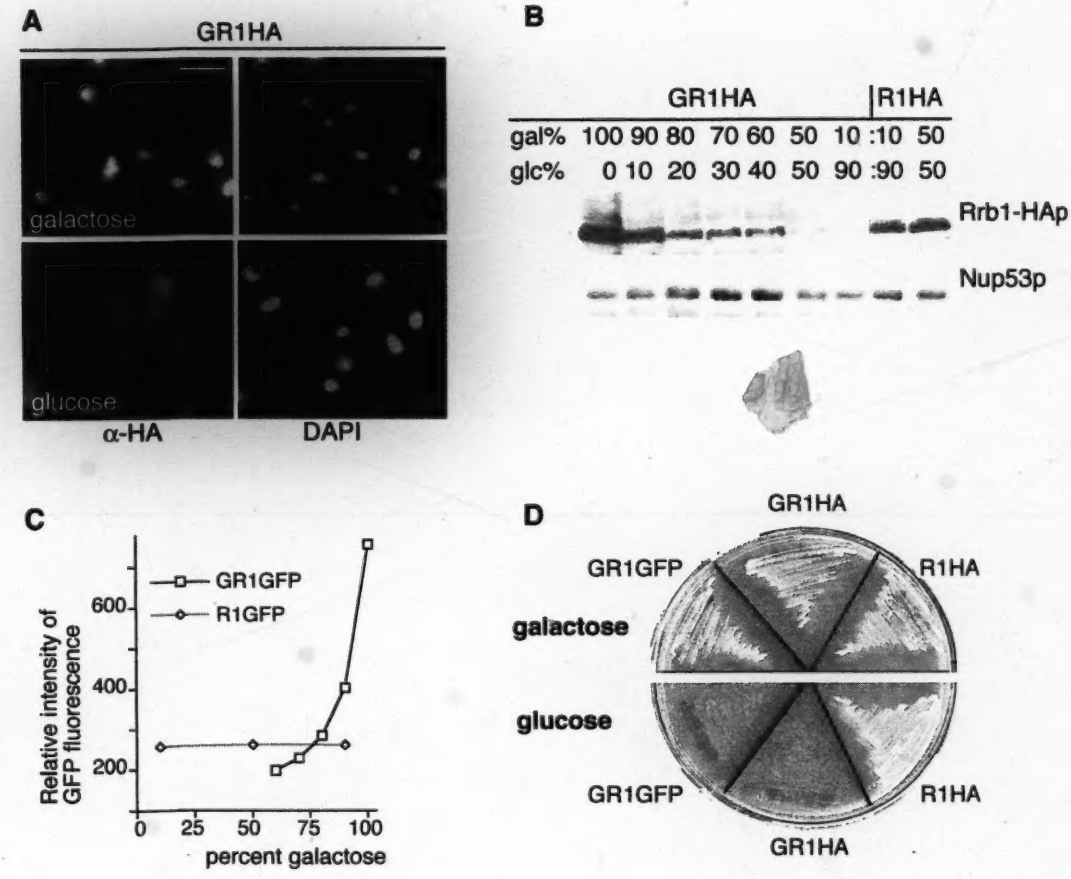
A
GR1HA
galactose
glucose
α-HA
DAPI
B
GR1HA
R1HA
gal% 100 90 80 70 60 50 10 :10 50
glc% 0 10 20 30 40 50 90 :90 50
Rrb1-HAp
Nup53p
C
GR1GFP
R1GFP
Relative intensity of GFP fluorescence
600
400
200
0 25 50 75 100
percent galactose
D
GR1HA
GR1GFP
R1HA
galactose
glucose
GR1GFP
R1HA
GR1HA

4.5. Depletion of Rrb1p results in decreased levels of 60S ribosomal subunits and ribosomes

The concentration of Rrb1p within the nucleolus suggested a potential role for this protein in ribosome biogenesis. To address this possibility, the GR1HA strain was used to examine the effects of altering the cellular amounts of Rrb1p on the levels of cytoplasmic ribosomes. The GR1HA (*GAL1::RRB1*) strain was grown in medium containing a 60:40 galactose:glucose mixture to approximate wild-type levels of Rrb1p and then shifted to medium containing glucose (to reduce levels of Rrb1p) or galactose (to increase levels of Rrb1p). Four hours later their ribosomal profiles were analyzed by sucrose gradient fractionation. As controls, the same carbon source shifts were performed on the R1HA (*RRB1* regulated by it endogenous promoter) strain. As shown in Figure 4-3A, p.123, the levels of 60S subunits, 80S ribosomes, and polysomes directly correlated with the levels of Rrb1p. Each of these species was reduced in GR1HA cells grown in medium containing a 60:40 galactose:glucose mixture where the cellular levels of Rrb1p were moderately reduced relative to the R1HA strain (see Figure 4-3B, p.123). When the GR1HA cells were shifted to glucose-containing medium to repress *RRB1*, a further decrease in the levels of both 60S subunits and 80S ribosomes was observed. In contrast, when the G57HA cells were shifted to galactose, the levels of ribosomes and ribosomal subunits returned to wild-type levels (Figure 4-3A, p.123). By

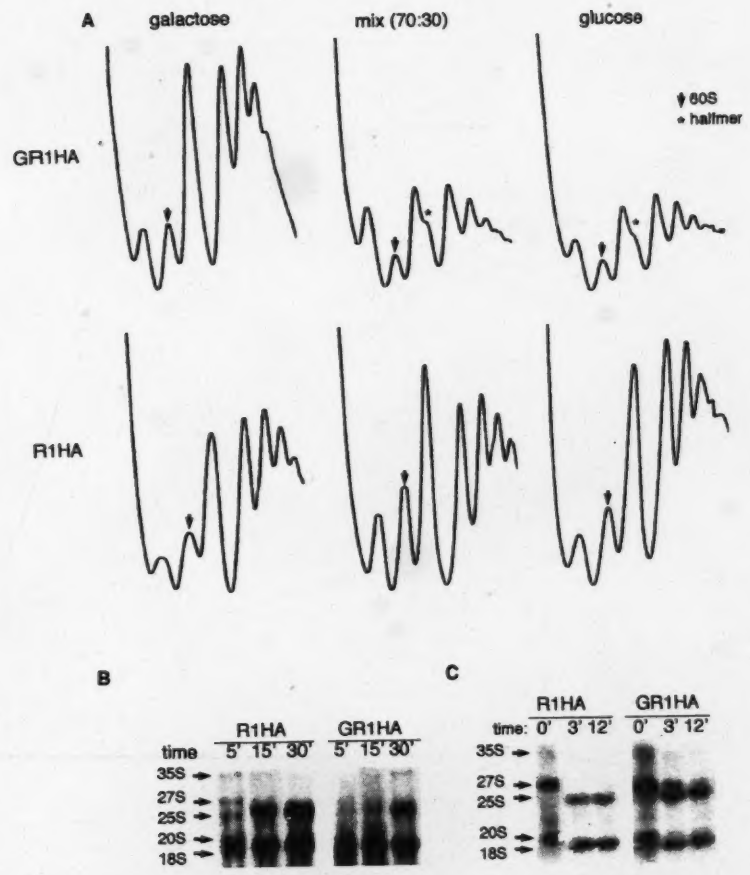

Figure 4-3. The effect of depletion of Rrb1p on ribosome biosynthesis. A) R1HA and GR1HA (*GAL1::RRB1-HA*) cells were grown in medium containing a galactose:glucose (60:40) mixture and then shifted to medium containing either 2% galactose or 2% glucose for 4 h. Ribosomal subunits, ribosomes, and polyribosomes derived from these cultures were then separated on 7-to-47% sucrose gradients and detected by their UV absorbance at 254 nm. The position of the 60S ribosomal subunit is indicated by an arrow. Half-mers are highlighted with an asterisk. B) and C) Pulse-chase analysis of rRNA. R1HA and GR1HA cells were grown in glucose-containing medium for 4 h, pulse-labeled with [5, 6-3H]uridine B) or with [methyl-3H]methionine C) for 3 min, and chased with medium lacking the labeling reagent. Following the indicated chase time, total RNA was isolated, resolved on agarose gels, and detected by autoradiography. The positions of the various rRNA species are indicated according to their sedimentation coefficients.

comparison, no changes were observed in the ribosomal profiles of R1HA cells upon shifting to galactose or glucose-containing medium (Figure 4-3A, p.123).

The *GAL1::RRB1-HA* conditional allele was also used to examine the effects of Rrb1p depletion on the synthesis and accumulation of the rRNA (Figure 4-3B, p.123). rRNA is synthesized as a 35S precursor that is processed to yield mature 25S, 18S, and 5.8S species. The 25S and 5.8S RNAs are components of the 60S subunit whereas the 18S RNA is part of the 40S subunit (Venema and Tollervey, 1999). For these experiments, GR1HA (*GAL1::RRB1-HA)* cells, or the control strains R1HA, were grown in medium containing a 60:40 galactose:glucose and then shifted to glucose-containing medium for 4 h to suppress the expression of Rrb1p. Cells were then pulse-labeled with [5,6-^{3}H] uridine for 3 min to label the rRNA. Following a 5 min chase, various processing intermediates, including the 35S, 27S, and 20S species, were detected in control R1HA cells expressing endogenous levels of RRB1 (Figure 4-3B, p.123). Processing of these intermediates was complete by the 15 min time point and similar amounts of the 25S and 18S species were visible. In comparison, the levels of precursor and mature forms of 25S rRNA, but not the 18S rRNA, were greatly reduced in the Rrb1p depleted cells (Figure 4-3B, p.123). These results suggest that the formation of the 25S rRNA was reduced in these cells. These observations are consistent with the reduction of 60S subunits detected under similar conditions.

4.6. Rrb1p physically interacts with the ribosomal protein L3

To further investigate Rrb1p's function in ribosome biogenesis, we attempted to identify proteins that physically interact with Rrb1p. For these experiments, nuclei were isolated from cells expressing Rrb1-HA and the nuclei were extracted with buffer containing 1% Triton-X100 and 240 mM NaCl. Under these conditions the majority of Rrb1-HA was released into a soluble supernatant fraction. The soluble Rrb1-HA was then immunoprecipitated with mAb 12CA5. As shown in Figure 4-4, p.126, three predominant polypeptides with apparent molecular masses of 70kD, 66kD and 40kD were specifically detected in the bound fraction but not in similar fractions lacking the HA-tag or an HA-tagged version of the nuclear pore complex protein Pom152p (data not shown). This set of polypeptides was also observed when similar experiments were conducted using NaCl concentrations ranging from 150-450 mM. Immunoblots revealed that both the 70kD and 66kd species were derived from Rrb1-HA (Figure 4-4, p.126). The identity of the 40 kD band was determined by peptide microsequencing to be the essential 60S ribosomal subunit protein rpL3 (the product of *RPL3* gene (Fried and Warner, 1981)). This result was further confirmed by Western blotting using an anti-rpL3 antibody (Figure 4-4, p.126).

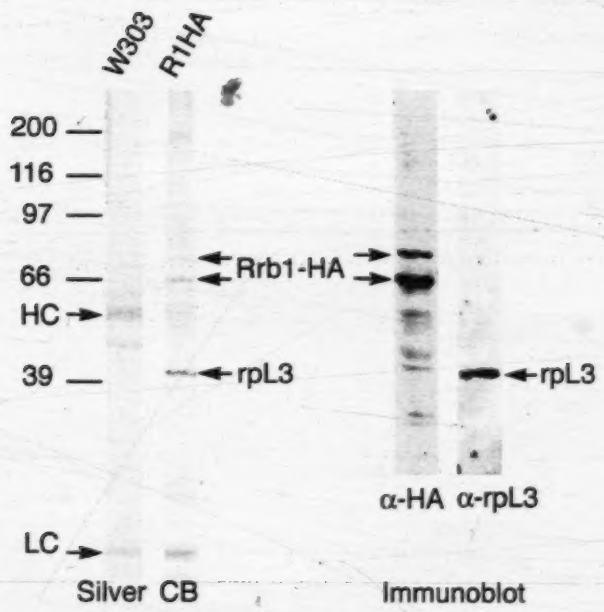

Figure 4-4. The ribosomal protein rpL3 is associated with Rrb1p. Nuclei isolated from R1HA and W303 (lacking an HA tag) strains were extracted with 1% Triton X-100 and 240 mM NaCl. Cleared supernatants were incubated with MAb 12CA5 conjugated to protein G-Sepharose beads to immunoprecipitate Rrb1-HA. The proteins eluted from these beads were then resolved using SDS-PAGE and detected with either silver or Coomassie blue (CB) staining (performed by Shawna Maguire, from the laboratory of Dr. Rick Wozniak, Department of Cell Biology, University of Alberta, Edmonton). Immunoprecipitates derived from the R1HA nuclei were also analyzed by Western blotting using MAb 12CA5 (α-HA) and the MAb TCM1 directed against the ribosomal protein rpL3 (α-rpL3). Of the three major bands visible in the eluate, the 70- and 66-kDa species bound MAb 12CA5, and the 40-kDa species bound the α-rpL3 antibody. The positions of light chain (LC) and heavy chain (HC) species derived from MAb 12CA5 are indicated. The positions of molecular mass markers are shown in kilodaltons.

4.7. Rrb1p modulates cellular levels of L3

Our observation that rpL3 is the only ribosomal protein associated with the immunoprecipitated Rrb1p suggested that it may only interact with free L3, perhaps as a prelude to L3's assembly into preribosomal 90S subunits. Moreover, as the half-life of free ribosomal proteins is short, between 30 sec and 3 minutes (Warner, 1991), we hypothesize that Rrb1p may influence the stability of rpL3. To further explore these possibilities, we examined the effects of altering *RRB1* expression on the cellular levels of the rpL3, its subcellular localization, and the expression of the *RPL3* gene.

We first examined how the changes in *RRB1* expression would affect the cellular levels of the rpL3 in relationship to other ribosomal proteins. GR1HA cells maintained in medium containing a 70:30 galactose:glucose ratio were shifted to either galactose or glucose containing medium for 6 h. Total cell lysates were then examined by Western blotting using various antibodies. As shown in Figure 4-5A, p. 129, the depletion of Rrb1p caused a slight decrease in the levels of rpL3. Alternatively, the induction of *RRB1-HA* (Figure 4-5A, p.129, galactose) led to a distinct increase in the levels of the rpL3 relative to other proteins examined including rpL30 (Figure 4-5, p.129). We also examined whether the levels of rpL3 were higher in GR1HA cells grown in galactose and constitutively overexpressing *RRB1*. As shown in Figure 4-5B, when the levels of rpL3 were compared with rpL30 or the 40S subunit protein rpS2, levels of rpL3 were

higher in the *RRB1* overexpressing cells. These results suggest that the overproduction of Rrb1p specifically increases cellular levels of the rpL3.

As described above (Figure 4-2A, p.129), excess Rrb1p accumulated in the nucleus. If the increased amounts of rpL3 produced in GR1HA cells were associated with Rrb1p, we would predict that excess rpL3 would also accumulate in the nucleus. To test this, immunofluorescence was performed using the anti-rpL3 antibody on the GR1HA strain after shifting to glucose or galactose-containing medium for 6h (Figure 4-6A, p.130). Cells shifted to glucose-containing medium showed a diffuse cytoplasmic staining pattern similar to, albeit weaker than, that observed in wild-type cells. In contrast, cells overexpressing *RRB1* showed both a cytoplasmic staining pattern as well as a strong nuclear signal (Figure 4-6A, p.130). This nuclear accumulation was not observed in R1HA cells grown in galactose. To determine whether the recruitment of rpL3 into the nucleus by Rrb1p was specific for this ribosomal protein, we compared the distribution of rpL3 with two other large subunit proteins, rpL25 and rpL4A, in Rrb1p-overproducing cells. To visualize these proteins, GFP-tagged versions of each (which are capable of assembling into ribosomes [J. D. Aitchison and M. P. Rout, unpublished data]) were examined. As expected, each of these proteins was distributed throughout the cytoplasm in wild-type and R1HA cells

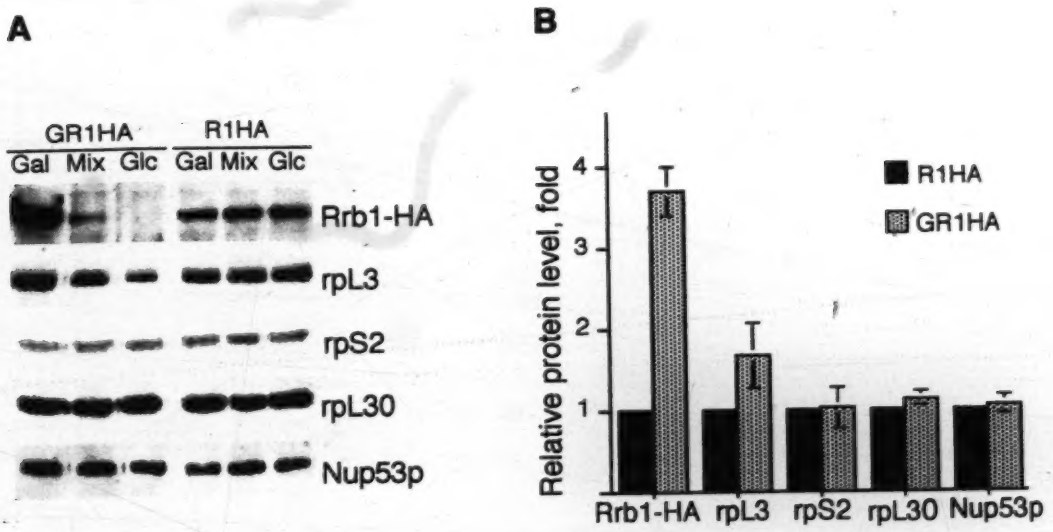

Figure 4-5. Overproduction of Rrb1p leads to an increase in cellular levels of rpL3. A) GR1HA (*GAL1::RRB1-HA*) cells were grown in galactose:glucose (70:30)-containing media (Mix) and then shifted to media containing either galactose (Gal) or glucose (Glc) for 6 h. Total cell lysates were isolated and equal amounts of protein were resolved by SDS-PAGE, transferred to nitrocellulose, and probed with MAb 12CA5 (Rrb1-HA), MAb TCM1 (rpL3), anti-rpL30 (rpL30 and rpS2), and anti-Nup53p (Nup53p). The ribosomal protein rpS2 was detected as a result of its cross-reactivity with anti-rpL30 antibody (Villardell and Warner, 1997). Switching to galactose resulted in increases in the cellular levels of Rrb1p and rpL3 but not rpL30, rpS2, or Nup53p. B) GR1HA (*GAL1::RRB1-HA*) and R1HA (*RRB1-HA* under the control of its endogenous promoter) cells were grown in galactose-containing medium, and equal amounts of total cell lysates were analyzed by Western blotting using antibodies directed against the indicated proteins. The signals detected in the R1HA strain were assigned a value of one. The fold increases in the GR1HA strain of the individual proteins relative to their amounts in the R1HA strain were plotted. Data shown represent the mean ± standard error of the mean (vertical error bars) from three independent experiments.

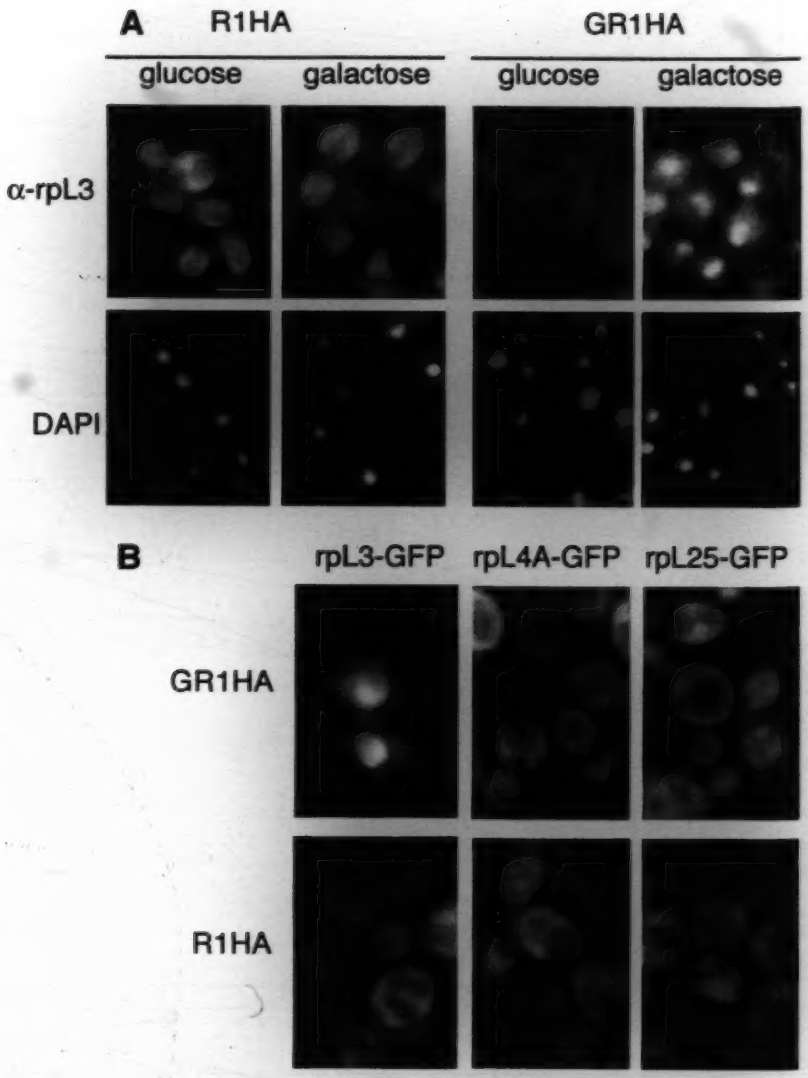

Figure 4-6. rpL3 accumulates in the nuclei of cells overexpressing *RRB1*. A) GR1HA (*GAL1:RRB1-HA*) and R1HA cells were grown in galactose:glucose (70:30)-containing medium and shifted to either galactose or glucose for 6 h. Cells were then fixed, permeabilized, and probed with the MAb TCM1 (α-rpL3). Nuclear DNA was visualized by DAPI staining. B) GR1HA and R1HA cells containing a plasmid-borne copy of the gene fusion *RPL3-GFP, RPL4A-GFP*, or *RPL25-GFP* were grown in medium containing a galactose:glucose (70:30) mixture and then shifted to galactose-containing medium for 6 h. The GFP fusions were visualized directly by fluorescence microscopy. Bar, 5 μm.

grown in medium containing either galactose (Figure 4-6B, p.130) or glucose (data not shown). A similar pattern was also seen in GR1HA cells grown in medium containing a 70:30 galactose:glucose mix (data not shown). However, when Rrb1-HA was overproduced in these cells, rpL3-GFP, but not rpL4A-GFP or rpL25-GFP, accumulated in the nucleus (Fig. 4-6B, GR1HA, p.130), again appearing to concentrate in the nucleolus. In contrast, repression of RRB1-HA expression resulted in the gradual fading of the cytoplasmic signal of each of the three ribosomal protein-GFP chimeras, consistent with the decreased levels of ribosomes observed in Rrb1p-depleted cells (data not shown).

4.8. The nuclear localization of Rrb1p is dependent on protein translation

A number of nucleolar proteins have been shown to shuttle between the nucleus and the cytoplasm (Xue and Melese, 1994). We asked whether Rrb1p might exhibit similar dynamics in an effort to better understand its role in ribosome biogenesis. Classically such studies involve examining the export and reimport of nuclear proteins under conditions that inhibit protein synthesis. During the course of our experiments, we surprisingly observed that protein synthesis inhibitors alone caused a rapid and reversible release of Rrb1p from the nucleus. Treatment of GR1GFP cells with cycloheximide (Figure 4-7A, p.133) or sodium fluoride (data not shown), two well-

characterized protein synthesis inhibitors (Tsay et al., 1998), caused a redistribution of Rrb1-GFP to the cytoplasm. After removal of the drug, Rrb1-GFP reaccumulated in the nucleus and was visible primarily in the nucleolus (Figure 4-7A, p.133). These same dynamics were observed with nuclear rpL3-GFP in G57HA cells overproducing Rrb1-HA. In these cells, the protein synthesis inhibitors also caused a redistribution of the nuclear pool of Rpl3-GFP to the cytoplasm (Figure 4-7A, p.133). Moreover, like Rrb1p, removal of the drugs led to a progressive reaccumulation of rpL3-GFP in the nucleus. These results further suggest that the nuclear rpL3 detected in these cells is associated with Rrb1p.

The requirement of ongoing protein synthesis for the nuclear localization of Rrb1p was further tested using a mutant (prt1-1) containing a thermosensitive allele of the Prt1p, a component of the eIF-3 translation initiation factor (Naranda et al., 1994). At the restrictive temperature, the *prt1-1* mutation prevents the formation of translation preinitiation complex and causes rapid polysome run-off (Hartwell and McLaughlin, 1967; Hinnebusch and Liebman, 1991). For these experiments, a plasmid-linked copy of *RRB1-HA* was introduced into the *prt1-1* strain and the Rrb1-HA protein was detected by immunofluorescence microscopy (Figure 4-7B, p.133). At the permissive temperature (23°C), Rrb1-HA was predominantly nuclear. However, a shift to 37°C for 20 min caused a rapid redistribution of Rrb1-HA into the cytoplasm. By comparison,

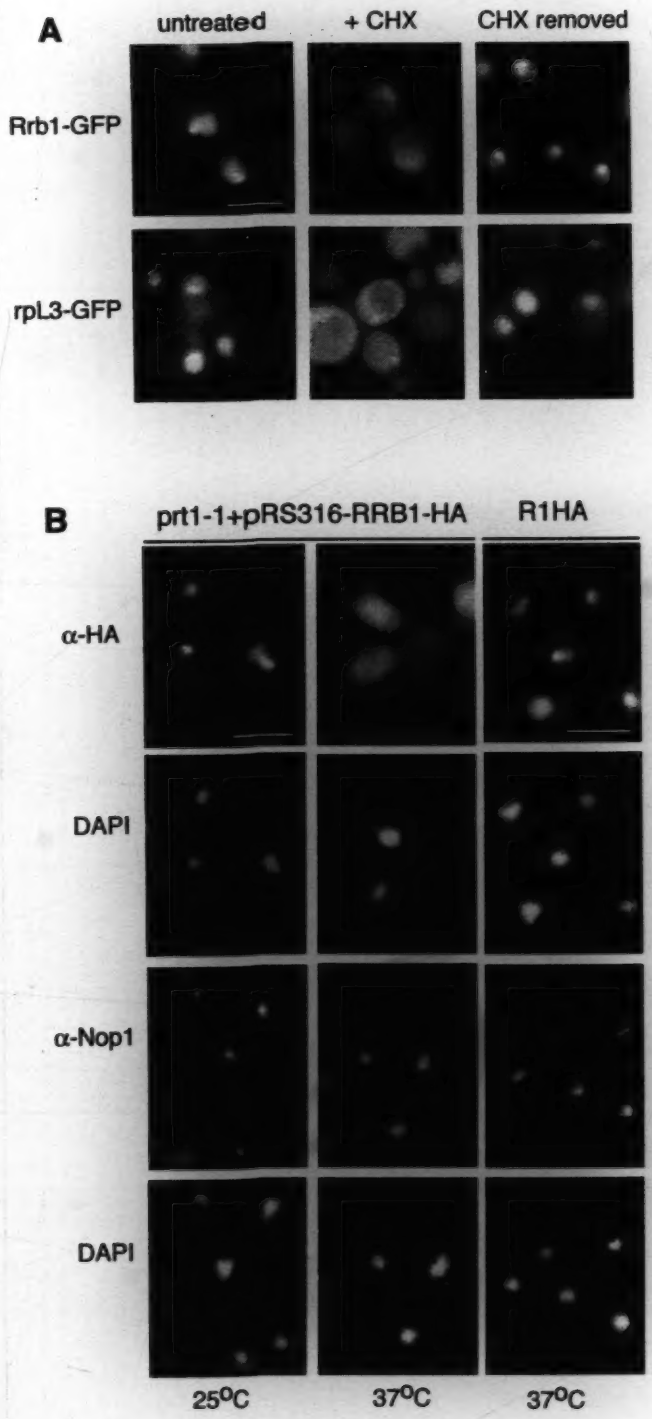

Figure 4-7. Inhibition of protein synthesis causes a reversible relocalization of Rrb1p from the nucleus to the cytoplasm. A) GR1GFP (*GAL1:RRB1-GFP*) cells (Rrb1-GFP) and GR1HA (*GAL1:RRB1-HA*) cells expressing RPL3-GFP (rpL3-GFP) were grown in galactose-containing medium, and the GFP fusions were visualized by fluorescence microscopy (untreated). These cells were then treated with cycloheximide (100 μg/μl) for 1.5 h and reexamined by fluorescence microscopy (+CHX). Following treatment with cycloheximide, cells were washed, resuspended in fresh medium, and allowed to recover for 30 min at 30°C (CHX removed).

B) R1HA cells and the thermosensitive prt1-1 strain containing pRS316-RRB1-HA were grown at 23°C and then shifted to 37°C for 20 min. Cells harvested from both temperatures were fixed, permeabilized, and probed with either MAb 12CA5 (α-HA) or an MAb that specifically binds the nucleolar protein Nop1p (α-Nop1). Nuclear DNA was visualized by DAPI staining. Bar, 5 μm.

temperature shift did not affect the localization of the nucleolar protein Nop1p or the integrity of nucleolus in the prt1-1 strain (Figure 4-7B, p.133). Finally, these effects were specific for the prt1-1 strain, as temperature shift did not change the nuclear localization of Rrb1-HA in R1HA cells (Figure 4-7B, p.133).

4.9. *RRB1* regulates the levels of ribosomal protein mRNAs

The results described above suggested that Rrb1p binds to free rpL3 and that the overproduction of Rrb1p leads to the accumulation of free rpL3 within the nucleus. We have also observed that elevated levels of rpL3 induced by overexpressing *RRB1* are accompanied by a dramatic increase in *RPL3* mRNA in these cells (Figure 4-8, p.135-136). We examined, by Northern blot analysis, the levels of *RPL3* mRNA upon induction and repression of *RRB1* expression. As shown in Figure 4-8, the induction of *RRB1-HA* overexpression, stimulated in the GR1HA stain by switching to galactose-containing medium, led to a striking increase in the amount of *RPL3* mRNA. In contrast, shifting to glucose-containing medium had little effect on the levels of *RPL3* mRNA within the time course examined.

The promoter regions of most RP genes are similar to one another (Planta, 1997) containing binding sites for the regulatory protein Rap1p. *RPL3*, however, is one of a

Figure 4-8. Rrb1p modulates RP mRNA levels. A) GR1HA (*GAL1:RRB1-HA*) and R1HA (WT) cells were grown in galactose:glucose (70:30)-containing medium and then shifted to either galactose-or glucose-containing media. At the indicated time points, total RNA was isolated. Equal amounts of RNA from each of these samples were separated on a 1.2% formaldehyde-agarose gel, transferred to a nylon membrane, and hybridized with the indicated ^{32}P-labeled cDNA probe. Note that the *RRB1* blot was exposed for a time period similar to that for the ribosomal protein mRNA blots and thus it is only visible here in the overexpressing samples. B) Northern blots were performed as for panel A, and signals were quantitated using a phosphorimager. mRNA levels were normalized to *ACT1* mRNA and wild-type levels of RP mRNAs were assigned a value of one. C) Northern analysis was performed on RNA isolated from GR1HA cells expressing *RPL25-GFP* or *RPL3-GFP* driven by an exogenous promoter (see section **2.3,** p. 58). Both mRNAs were detected using a ^{32}P-labeled *RPL25* or *RPL3* cDNA probe. D) The effects of a *GAL10::NOP1* conditional allele on the levels of *RPL25* mRNA were examined in strain Y159. Y159 (*GAL10::NOP1*) and W303 (WT) cells were grown in galactose:glucose (70:30)-containing medium and then shifted to either galactose- or glucose-containing medium for 12 h. Northern analysis was performed on total RNA using a ^{32}P-labeled *RPL25* cDNA probe. The lane order is the same as that shown in panel C.

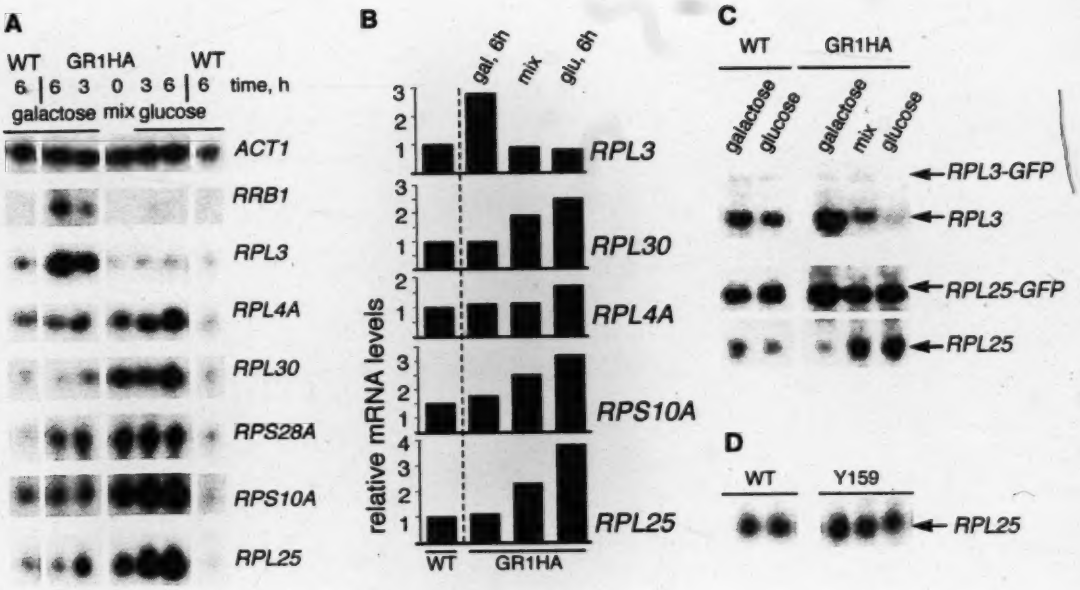
A
WT
GR1HA
WT
6 | 6 3 0 3 6 | 6 time, h
galactose mix glucose
ACT1
RRB1
RPL3
RPL4A
RPL30
RPS28A
RPS10A
RPL25
B
gal, 6h
mix
glu, 6h
relative mRNA levels
RPL3
RPL30
RPL4A
RPS10A
RPL25
WT
GR1HA
C
WT
GR1HA
galactose
glucose
galactose
mix
glucose
RPL3-GFP
RPL3
RPL25-GFP
RPL25
D
WT
Y159
RPL25

few genes whose promoter has a different structure, lacking Rap1p binding sites (Woolford and Warner, 1991). Despite these differences, constitutive levels of expression are similar for all RP genes and it has been generally observed that they are coordinately regulated in response to different stimuli (see section **4.10,** p.138). With this in mind, experiments were performed to examine the effect of altering *RRB1* expression on other RP mRNA levels including those controlled by promoter elements similar to (*RPS28A*, *RPL4A*), or different from (*RPL30*, *RPL25*, *RPS10A*), those controlling *RPL3*. Our selection of examined RP mRNAs also represented components of the 60S and 40S subunits (Planta, 1997). Unexpectedly, the depletion of Rrb1p, which is concurrent with a decline of ribosomal levels (Figure 4-3, p.123), resulted in a dramatic increase in mRNA levels of all RP mRNAs examined except *RPL3* (Figure 4-8, p.135-136). No appreciable change was observed in the actin mRNA control. Similarly, in GR1HA cells grown in medium containing a 70:30 galactose:glucose mix (Figure 4-8, t=0), where levels of Rrb1-HA are below wild-type levels, each of these mRNAs was more abundant than the *RPL3* mRNA. This effect was reversed upon induction of *GAL1::RRB1-HA*. Increases in Rrb1p caused RP mRNA levels (except for *RPL3*) to decrease to approximately wild type levels (Figure 4-8, p.135-136). These changes in RP mRNA levels were likely due to changes in the levels of transcription as they relied on the presence of an endogenous promoter. For example, depletion of *RRB1*

caused an increase the levels of mRNA derived from the endogenous *RPL25* gene, but not from a plasmid-born *RPL25-GFP* gene controlled by the triose phosphate isomerase promoter (Figure 4-8B, p.135-136). Finally, the effects of Rrb1p levels on RP gene expression are specific and not generally associated with defects in ribosome assembly. For example, the suppression of expression of the nucleolar protein gene *NOP1*, which causes in defects in rRNA processing and ribosome assembly, had no effect on the expression of the *RPL25* and *RPS10A* genes (Figure 4-8C, p.135-136).

4.10. Discussion

Rrb1p is a member of a functionally diverse superfamily of WD-repeat-containing proteins (Smith et al., 1999). It is present throughout the nucleus but is concentrated in the nucleolus. The nucleolar concentration of Rrb1p and the fact that patterns of *RRB1* gene expression mirror those of the RP genes during diauxic shift (DeRisi et al., 1997) suggested a possible involvement of Rrb1p in ribosome synthesis. To test this, we studied the effects of varying cellular levels of Rrb1p on the levels of ribosomes and ribosomal subunits. We observed that even moderate levels of Rrb1p depletion led to a decrease in the levels of 60S ribosomal subunits, 80S ribosomes, and polysomes (Figure 4-3, p.123). This was accompanied by a significant inhibition in the production of 25S rRNA. In contrast, Rrb1p depletion had little effect on the levels of 40S subunits and

these subunits were capable of forming 43S preinitiation complexes (half-mers). Moreover, unlike that of 25S rRNA, the formation of 18S rRNA was unaffected by reduced levels of Rrb1p. Similar results have been documented in a variety of mutants that are defective in 60S subunit formation, including those containing mutations in genes encoding constitutive 60S subunit proteins and factors affecting large-subunit assembly and maturation (Mager et al., 1997, Woolford and Warner, 1991). On the basis of these results, we conclude that Rrb1p plays a specific role in the assembly of the 60S subunit.

The function of Rrb1p in ribosome biogenesis is likely linked to its physical association with the ribosomal protein rpL3. We showed by immunoprecipitation of Rrb1p from nuclear extracts that it specifically interacts with rpL3, with no other ribosomal proteins being visibly bound to Rrb1p. These results suggest that Rrb1p interacts with free rpL3 at a point prior to its incorporation into ribosomes. This conclusion is further supported by the observation that excess Rrb1p causes a specific accumulation of rpL3 (but not other ribosomal proteins such as rpL4A or rpL25) within the nucleus (Figure 4-6B, p.130). At what point following its synthesis rpL3 binds to Rrb1p is unclear. The two proteins could associate with one another either after rpL3 enters the nucleus or in the cytoplasm with the resulting complex being imported into the nucleus. The latter scenario is possible since Rrb1p is capable of shuttling between the

nucleus and the cytoplasm (Figure 4-7B, p.133). Interestingly, we observed that Rrb1p's steady-state localization to the nucleus is dependent on ongoing protein translation. Both chemical inhibitors (cycloheximide and sodium fluoride) and mutations (*prt1-1*) that block translation (Hartwell and McLaughlin, 1969; Vazques, 1974) caused Rrb1p to be released into the cytoplasm. Upon reinitiation of translation, Rrb1p again concentrated in the nucleus. Moreover, inhibition of the protein synthesis also led to the coordinated transport of a Rrb1p-rpL3 pool (see below) out of the nucleus (Figure 4-7, p.133). Again, these proteins could be reimported into the nucleus after release of translational arrest, suggesting that a Rrb1p-rpL3 complex is capable of being imported into the nucleus. How the function of Rrb1p is linked to protein translation is yet to be investigated. However, the observation that a nucleolar protein's localization is dependent on translation is, to the best of our knowledge, unprecedented.

Consistent with their physical association, we also showed that the overproduction of Rrb1p leads to a disproportionate increase in steady-state levels of rpL3 relative to other ribosomal proteins (Figure 4-5, p.129). These data were surprising in light of numerous previous reports that the stoichiometric relationships between ribosomal proteins are tightly maintained and that excess unassembled ribosomal proteins are quickly degraded, having half-lives between 30 s and 3 min (Warner, 1999;Woolford and Warner,1991). For example, it was shown that overproduced *RPL3* mRNA

accumulates in the cell (Pearson et al., 1982) and is efficiency translated but that excess rpL3 is rapidly degraded (Maicas et al., 1988). In contrast, in Rrb1p-overproducing cells, both following induction of the *GAL1::RRB1* gene and in constitutively overexpressing cells, a surplus of rpL3 was detected (Figure 4-5B, p.129). The excess pool of rpL3 may be explained in two ways. First, overexpression of *RRB1* stimulates the expression of *RPL3* (see below), thus likely increasing the production of rpL3. Second, the overproduced Rrb1p sequesters rpL3 within the nucleus, concentrating it within the nucleolus (Figure 4-5, p.129). Here it could directly protect rpL3 or segregate it from the proteolytic machinery that would normally degrade it. The latter mechanism is not unprecedented, as recent reports show that the sequestration of proteins within the nucleolus can protect them from degradation (Tao and Levine, 1999; Weber et al., 1999) and regulate their activity (Shou et al., 1999; Straight et al., 1999; Visintin et al., 1999).

Within the nucleolus, the Rrb1p-rpL3 complex could act as a precursor from which rpL3 is recruited into newly forming preribosomes. Since we have not detected Rrb1p in association with precursor or mature 60S subunits (data not shown), the binding of rpL3 to the 90S precursor is likely accompanied by the dissociation of Rrb1p. Such a mechanism would suggest a role for Rrb1p in the deposition of rpL3 on the 90S precursor. Our observation that Rrb1p depletion decreases the rate of 25S rRNA formation (Figure 4-3, p.123) is consistent with a defect in rpL3 incorporation. Similar

phenotypes have been observed when the incorporation of early assembly intermediates, including rpL3, onto pre-rRNA is altered (Nam and Fried, 1986; for a review, see reference Kressler et al., 1999). Interestingly, two other yeast proteins that contain WD-repeats have also been suggested to assist in the incorporation of ribosomal proteins onto ribosomal subunits. The cytoplasmic protein Sqt1p may play a role in depositing Qst1p-rpL10 on the 60S subunit during a late assembly step in the cytoplasm (Eisinger et al., 1997). In another example, Rrp7p, a protein presumed to be nuclear, is required for rRNA processing through a mechanism that is proposed to involve the addition of two proteins, rpS27A and rpS27B, to the 43S precursor (Baudin-Baillieu et al., 1997).

The coordinated increase in the levels of the rpL3 that accompanied Rrb1p overproduction prompted us to examine the effects of the *RRB1* conditional allele on the expression of *RPL3* and various other RP genes. A hallmark of RP gene transcription is that, under normal growth conditions as well as under conditions of stress including carbon source changes (Herruer et al., 1987), heat shock (Herruer et al., 1988), and alterations in protein secretion (Li et al., 1999; Mizuta and Warner 1994; Tsuno et al., 2000), the expression of all RP genes is globally coordinated (DeRisi et al., 1997; Eisen et al., 1998; Planta, 1997). The mechanics of this process, however, are not well understood. The majority of RP genes contain upstream sequences that bind the protein Rap1p. Rap1p has been shown to act as a transcriptional activator of RP gene

expression, and it plays a necessary role in the repression of transcription induced by amino acid starvation and defects in secretion (Mizuta et al., 1998;Moehle and Hinnebusch, 1991). A few RP genes, including *RPL3*, lack the Rap1p-binding site and instead contain binding sites for the transcription factor Abf1p. Still, their expression is coordinated with the other RP genes under each of the various environmental conditions mentioned above (Planta, 1997).

Interestingly, we showed that varying the levels of Rrb1p uncouples the regulation of *RPL3* mRNA levels from the coordinated control of other RP mRNAs, potentially through the control of their transcription. The overexpression of *RRB1* leads to a robust increase in the levels of rpL3 mRNA, while all of the other RP mRNAs examined remained at or near wild-type levels (Figure 4-8B, p.135-136). In contrast, upon depletion of Rrb1p the levels of *RPL3* mRNA appeared unaffected while mRNA levels of all other examined RP genes were increased. This includes RP genes whose promoters contain either Rap1p- or Abf1p-binding sites. Our analysis of the effects of *RRB1* expression on the levels of *RPL3* and *RPL25* mRNAs (Figure 4-8C, p.135-136) showed that the increase induced by overexpression (*RPL3*) or repression (*RPL25*) of *RRB1* was dependent on the presence of RP's endogenous promoter. Thus, the increases in amounts of RP mRNAs that were detected upon depletion of Rrb1p may reflect an increase in transcription rather than a change in the half-life of these mRNAs. However, the latter

possibility has not yet been tested. The effects of Rrb1p on the levels of *RPL3* mRNA may be linked to its physical association with rpL3. One scenario is that the state of Rrb1p, free versus bound to rpL3, would provide a means for Rrb1p to sense ongoing ribosome assembly and adjust *RPL3* expression. For example, increased levels of free Rrb1p caused by a decrease in rpL3 could stimulate the expression of *RPL3*. Rrb1p also appears to play a more global function in ribosome biogenesis by, directly or indirectly, suppressing the expression of other RP genes. How Rrb1p can act as a transcriptional activator in the context of the *RPL3* gene and a repressor for other RP genes remains to be investigated. Of note, the surge in the expression of RP genes observed upon depletion of Rrb1p is similar to that previously reported in mutants expressing truncations of Rap1p, which lack domains implicated in transcriptional silencing or activation (Graham et al., 1999). In both cases, the levels of RP mRNA significantly exceeded normal cellular levels detected in wild-type cells grown under the same conditions. This phenomenon is striking since normal levels of RP gene transcription already account for ~30% of RNA polymerase II-mediated transcription. The simplest explanation is that normal levels of transcription do not represent maximal levels.

While the functional links between the effects of Rrb1p and Rap1p are unclear, it is of interest that Rap1p appears to be functionally linked to a chromatin assembly complex that contains Msi1p (Enomoto et al., 1997), a yeast protein exhibiting a high degree of

sequence similarity to Rrb1p. Both by its association with the chromatin assembly complex and, on a broader scale, as a consequence of its multiple effects on transcription regulation, Rap1p has been suggested to play a general role in chromatin remodeling (Morse et al., 2000). If Rrb1p, like Msi1p, is functionally linked to Rap1p, it could function to modulate Rap1p activity at specific loci such as the RP genes.

Our results clearly indicate that Rrb1p plays a role both in the assembly of 60S ribosomal subunits and in the transcription of RP genes. Rrb1p is therefore positioned to link these two events and coordinate their activities. Moreover, the differential effects of Rrb1p on the expression of *RPL3* as compared to other RP genes suggest that the coordinated regulation of RP gene expression is likely the result of independent, yet intertwined, regulatory pathways that together maintain similar levels of expression for all RP genes.

Chapter 5

Perspectives and Future Studies

5.1. Synopsis

Through the course of this study, we demonstrated that constituents of the nuclear pore complex define the localization and function of spindle checkpoint proteins and their recruitment to kinetochores. In *S. cerevisiae*, little is known about the subcellular distribution of the checkpoint proteins or how their dynamic associations with structures such as the kinetochores and the NPCs influence their function. Here, we begin to address this question by focusing on two checkpoint proteins, Mad1p and Mad2p. We show that both Mad1p and Mad2p are associated with NPCs throughout the cell cycle in budding yeast. Their interactions with the NPC are mediated by the Nup53p-containing complex. Upon activation of the spindle checkpoint, distinct changes are detected in the molecular interactions between components of the Nup53p-containing complex, Mad1p, and Mad2p that lead to the release of Mad2p, but not Mad1p, from the NPC and the subsequent recruitment of Mad2p to kinetochores. Furthermore, we show that Mad1p plays a role in the structural integrity of the Nup53p-containing complex. These findings represent the first report that Mad1p and Mad2p may require specific nucleoporins as a scaffold for checkpoint protein function. This work has also opened several possibilities for future research and has raised numerous important questions, as outlined below.

5.2. Perspectives on the transport of the spindle checkpoint proteins into the nucleus

In different species, from yeast to humans, all checkpoint proteins (Mad1-3p, Bub1-3p and Mps1p) at least partially reside in the nucleus. Depending on the stage of the cell cycle, they are found at the NPC (Mad1p and Mad2p), at the kinetochores (Mad1p, Mad2p, Mad3p(BubR1), Bub1p, Bub3p, Mps1) and at the spindle pole bodies (Bub2p). Reaching these intranuclear destinations requires following steps: import into the nucleus, regulated release into the nucleoplasm, subsequent targeting to intranuclear locations and possible nuclear export. This sequence of events leaves us with the task of identifying the nuclear transport factors appropriate for each step. We began with an examination of the benomyl sensitivity of strains lacking certain karyopherins, reasoning that the lack of those proteins responsible for the transport of the checkpoint proteins may cause the benomyl sensitivity of the cells. We were able to identify at least two potential candidates: Kap123p and Kap121p (T. Iouk and R. Scott, unpublished observations). Kap121p is a Nup53p-interacting Kap that could be involved in the nuclear transport of Mad1p or Mad2p. Kap123p mediates ribosomal protein import into the nucleus. The availability of GFP-tagged versions of the checkpoint proteins and collections of the karyopherin mutant strains will enable us to define checkpoint protein transport pathways.

5.3. On the intranuclear dynamics of the mitotic spindle checkpoint proteins

Throughout the cell cycle, the checkpoint proteins are involved in multiple interchangeable interactions with each other. Mad1p and Mad2p are thought to provide a framework for these interactions (Chen et al., 1999). It is possible that the NPC-associated Mad1p complex functions as a platform for pre-assembly of the mitotic spindle checkpoint complex, including formation of a Mad1p-Bub1p-Bub3p module (Brady and Hardwick, 2000). A few questions should be asked in this regard. Is the NPC localization of Mad1p relevant to the formation of the complex? This question could be addressed by examining Mad-Bub protein interactions in a *nup53Δ* background. These experiments would also reveal whether the phosphorylation state of Mad1p is important for the formation of the complex.

5.4. On the functions of Mad1p and Mad2p

Our findings demonstrate that Mad1p is the NPC constituent. It is required for maintenance of the structural integrity of the Nup53p-containing complex. Like Nup53p, Mad1p undergoes phosphorylation during mitosis. An attractive hypothesis is that Nup53p and Mad1p might be modified by the same kinase, Mps1p. The phosphorylated form of Nup53p was detected in nocodazole-treated cells and in *cdc15* cells, whose growth is arrested at the restrictive temperature, indicating that Nup53p could remain

phosphorylated at least from metaphase to telophase (Marelli et al., 1998; Chapter 3). In parallel, Mad1p is shown to be hyperphosphorylated when the checkpoint is activated and to be dephosphorylated in late mitosis (Hardwick and Murray, 1995). Since Mad1p and Nup53p form a complex prior to their phosphorylation, it is reasonable to propose that: (i) these two proteins are phosphorylated by the same kinase, and (ii) their simultaneous phosphorylation contributes to a disassociation of this complex during mitosis. The latter hypothesis could be tested by the introducing of mutated versions of these proteins that are not susceptible to phosphorylation.

Both Nup53p and Mad1p may have a role in NPC biogenesis. The overexpression of *NUP53* induces the formation of the intranuclear NE-like membranes interrupted by pores (Marelli et al., 2000). Likewise, overexpression of the *MAD1* human homologue HsMAD1 may lead to the formation of annulate lamellae (Campbell et al., 2000). It remains to be determined whether altered levels of expression of *MAD1* will affect the structure and function of the yeast NPC. This could be accomplished upon the construction of a conditional *MAD1* allele.

In contrast to Mad1p, only a portion of Mad2p is associated with the NPC (Chung and Chen, 2002). A significant amount of Mad2p is present in the cytoplasm. We cannot exclude the possibility that Mad2p shuttles between the nucleoplasm, NPCs and the cytoplasm. Our hypothesis could be tested by using heterokaryons and by employing

fluorescence recovery after photobleaching (FRAP) technique. Similar experimental approaches have been successfully used to study the localization of proteins that are dynamically associated with the NPC (Dilworth et al., 2001).

Mad2p may function as a signaling molecule that coordinates activation of the spindle checkpoint with the cytokinesis machinery. Mad2p could also have a role in the nucleoplasmic trafficking of other checkpoint proteins and subcomplexes, since it interacts directly with many of them and since it is a highly mobile protein, which, depending on the stage of the cell cycle, alternates its intranuclear localization (Howell et al., 2000; Campbell et al., 2000). Therefore, particular subsets of Mad2p-interacting proteins should be determined at specific points in the cell cycle. Appropriate drugs and/or mutations will be utilized to arrest cell growth at these points, cells will be fractionated, and Mad2p-containing protein complexes will be isolated from different subcellular fractions.

5.5. On the resistance of nucleoporin gene disruption strains to benzimidazoles

We have shown that *nup170Δ*, *nup59Δ*, *nup53Δ* and *nup157Δ* cells are more benomyl-resistant than their wild-type counterparts. Recently, this list has been extended by addition of a few more nucleoporin gene disruption strains, including *pom34Δ* (R.

Scott and R. Wozniak, unpublished results). As mentioned in section **3.10**, p.100, a possible explanation for an increased resistance to benomyl in the *nup* knockouts is that their deletion may affect the Ran-GTP/Ran-GDP gradient across the nuclear envelope or the intracellular distribution of Ran.

The degree of benomyl resistance could also depend on the availability of tubulin. At the end of anaphase, when microtubules undergo depolymerization, excess tubulin must be removed from the nucleus. Conversely, sufficient amounts of tubulin must be imported into the nucleus prior to mitosis. It remains to be examined whether deletions of *nup* genes of interest affect the intranuclear levels of tubulin at specific stages of the cell cycle. Furthermore, since Nup53p complex functions as the docking site for Kap121p, it should also be determined whether Kap121p is involved in the nuclear import of tubulin.

We have determined that Mad1p-Mad2p-interacting nucleoporins are benzimidazole resistant. An increased resistance to nocodazole has also been observed in *ctf13* and *ndc10-1* mutant strains (Tavormina et al., 1997). In these cells, kinetochore function is disrupted and therefore they are unable to arrest in mitosis in response to the nocodazole treatment (Hardwick et al., 1999; Tavormina et al., 1997). Of note, it has been shown that kinetochore integrity is compromised in the *nup170* mutants (Kerscher et al., 2001). As a means of assessing proper kinetochore function in the strains of

interest, future studies will examine the conditions in which nocodazole causes mitotic arrest, with respect to drug concentration and timing.

Based on the results of this study, including the analysis of genetic interactions between the above listed *MAD* and *NUP* genes, the nucleoporins interacting with the Mad1p-Mad2p complex may play a dual role in the chromosome segregation process. Indeed, the disruption of any single *NUP* gene examined neither had a dramatic effect on the execution of mitosis nor significantly impaired cell viability. This observation might be explained by a pairwise functional redundancy of *NUP157* and *NUP170*, as well as the *NUP53* and *NUP59* genes. Our preliminary data show that a simultaneous deletion or down-regulation of the activity of either pair of the above *NUP* genes has a profound effect on the localization of the Mad1p and Mad2p proteins. These experiments should be continued.

In summary, future studies should further investigate the role for both karyopherins and nucleoporins in the regulation of mitosis. Conversely, potential function of Mad1p in NPC biogenesis and the involvement of Mad2p in nucleo-cytoplasmic communication should be explored.

Chapter 6

References

Adams, A., D. E. Gottschling, C. A. Kaiser, and T. Stearns. 1997. Methods in Yeast Genetics. Cold Spring Harbor Laboratory Press. Cold Spring Harbor. NY.

Adams, B.G. 1972. Induction of galactokinase in *Saccharomyces cerevisiae*: kinetics of induction and glucose effects. J. Bacteriol. **111**:308-315.

Adams, I.R., and J.V. Kilmartin. 2000. Spindle pole body duplication: a model for centrosome duplication. Trends Cell Biol. **10**:329-335.

Aitchison, J.D., G. Blobel, and M. Rout. 1995a. Nup120p: a yeast nucleoporin required for NPC distribution and mRNA transport. J. Cell Biol. **131**:1659-1675.

Aitchison, J.D., M.P.Rout, M.M.Marelli, G.Blobel, and R.W. Wozniak. 1995b. Two novel related yeast nucleoporins Nup170p and Nup157p: Complementation with the vertebrate homologue Nup155p and functional interactions with the yeast nuclear pore-membrane protein Pom152p. J. Cell Biol. **131**:1133-1148.

Aitchison, J.D., and M.P. Rout. 2002. A tense time for the nuclear envelope. Cell. **108**:301-304.

Akey, C.W. 1990. Visualization of transport-related configurations of the nuclear pore transporter. Biophys. J. **58**:341-355.

Akey, C.W., and M. Radermacher. 1993. Architecture of the *Xenopus* nuclear pore complex revealed by three-dimensional cryo-electron microscopy. J. Cell Biol. **122**:1-19.

Allen, N.P., L. Huang, A. Burlinghame, and M. Rexach. 2001. Proteomic analysis of nucleoporin interacting proteins. J. Biol. Chem. **276**: 29268-29274.

Allshire, R.C. 1997. Centromeres, checkpoints and chromatid cohesion. Curr. Opin. Genet. Dev. **2**:264:273.

Amon, A. 1999. The spindle checkpoint. Curr.Opin. Genet.Dev. **9**:69-75.

Amon, A. 2001. Together until separin do us part. Nature Cell Biol. **1**:E12-14.

Anderson, N.G. 1953. On the nuclear envelope. Science. **117**: 517.

Aris, J.P., and G. Blobel. 1988. Identification and characterization of a yeast nucleolar protein that is similar to a rat liver nucleolar protein. J. Cell Biol. **107**:17-31.

Ausubel, F.M., R. Brent, R.E. Kingston, D.D. Moore, J.G. Seidman, J.A. Smith, and K. Struhl. 1992. Short Protocols in Molecular Biology. Greene Publishing Associates, New York.

Baim S.B., D.F. Pietras, D.C. Eustice, and F. Sherman.1985. A mutation allowing an m-RNA secondary structure diminishes translation of *Sacharomyces cerevisiae* iso-1-cytochrome *c*. Mol. Cell. Biol. **11**:1295-1305.

Basrai, M.A., J. Kingsbury, D. Koshland, F. Spencer, and P. Hieter. 1996. Faithful chromosome transmission requires Spt4p, a putative regulator of chromatin structure in *Saccharomyces cerevisiae*. Mol. Cell. Biol. **6**:2838-2847.

Basu, J., B.C. Williams, Z. Li, E.V. Williams, and M.L. Goldberg. 1998. Depletion of a *Drosophila* homolog of yeast Sup35p disrupts spindle assembly, chromosome segregation, and cytokinesis during male meiosis. Cell Motil. Cytoskeleton. **39**:286-302.

Baudin-Baillieu, A., D.Tollervey, C. Cullin, and F. Lacroute. 1997. Functional analysis of Rrp7p, an essential yeast protein involved in pre-RNA processing and ribosome assembly. Mol. Cell Biol. **17**:5023-5032.

Beaudouin, J., D. Gerlich, N. Daigle, R. Eils, J. Ellenberg. 2002. Nuclear envelope breakdown proceeds by microtubule-induced tearing of the lamina. Cell. **108**:83-96.

Belgareh, N., and V. Doye. 1997. Dynamics of nuclear pore distribution in nucleoporin mutant yeast cells. J. Cell Biol. **136**:747-759.

Belgareh, N., G. Rabut, S.W. Bai, M. van Overbeek, J. Beadouin, N. Daigle, O.V. Zatsepina, F. Pasteau, V. Labas, M. Fromont-Racine, J. Ellenberg, and V. Doye. 2001. An evolutionary conserved NPC subcomplex, which redistributes in part to kinetochores in mammalian cells. J. Cell Biol. **154**:1147-1160.

Bi X., and J.R. Broach. 2001. Chromosomal boundaries in *S. cerevisiae*. Curr. Opin. Genet. Dev. **11**:199-204.

Bischoff, F.R., and H. Postingl. 1991. Catalysis of guanine nucleotide exchange on Ran by the mitotic regulator RCC1. Nature. **354**:80-82.

Bischoff, F.R., H. Krebber, T. Kempf, I. Hermes and H. Postingl. 1995a. Human RanGTPase-activating protein RanGAP1 is a homologue of yeast Rna1p involved in mRNA processing and transport. Proc. Natl. Acad. Sci. USA. **92**:1749-1753.

Bodoor, K., S. Shaikh, D. Salina, W.J. Raharjo, R. Bastos, M. Lohka, and B. Burke. 1999b. Sequential recruitment of NPC proteins to the nuclear periphery at the end of mitosis. J. Cell Sci. **112**:2253-2264.

Bodoor, K., S. Shaikh, P. Enarson, S. Chowdhury, D. Salina, W.H. Raharjo, and B. Burke. 1999a. Function and assembly of nuclear pore complex proteins. Biochem. Cell Biol. **77**:321-329.

Bonnerot, C., D. Rocancourt, P. Briand, G. Grimber, and J.F. Nicolas. 1987. A β-galactosidase hybrid protein targeted to the nuclei as a marker for developmental studies. Proc. Natl. Acad. Sci. USA. **19**:6795-6799.

Borer R.A., C.F. Lehner, H.M. Eppenberger, and E.A.Nigg. 1989. Major nucleolar proteins shuttle between nucleus and cytoplasm. Cell. **56**:379-390.

Brachmann C.B., A. Davies, G.J. Cost, E. Capuyo, J. Li, P. Hieter, and J.D. Boeke. 1998. Designer deletion strains derived from *Saccharomyces cerevisiae* S288C: a useful set of strains and plasmids for PCR-mediated gene disruption and other applications. Yeast. **14**:115-132.

Brady, D.M., and K.G. Hardwick. 2000. Complex formation between Mad1p, Bub1p and Bub3p is crucial for spindle checkpoint function. Curr. Biol. **10**:675-678.

Breeden, L.L. 1997. α-factor synchronization in budding yeast. Methods Enzymol. **283**:332-341.

Brunet S., and I. Vernos. 2001. Chromosome motors on the move. EMBO Rep. **21**:669-673.

Bucci, M., and S.R. Wente. 1998. A novel fluorescence-based genetic strategy identifies mutants of *Saccharomyces cerevisiae* defective for nuclear pore complex assembly. Mol. Biol. Cell. **9**:2439-2461.

Bullitt, E., M. Rout, J.V. Kilmartin, and C.W. Akey. 1997. The yeast spindle pole body is assembled around a central crystall of Spc42p. Cell. **89**: 1077-1086.

Byers, B. 1981. In: J.N. Strathern (ed.), Molecular Biology of the Yeast *Sacharomyces*: Life Cycle and Inheritance. p.59. Cold Spring Harbor Laboratory Press, Cold Spring Harbor, NY.

Byers, B. 1993. *NDC1*: a nuclear periphery component required for yeast spindle pole body duplication. J. Cell Biol. **122**:743-751.

Cahill, D.P., C. Lengauer, J. Yu, G.J. Riggins, J.K. Willson, S.D. Markowitz, K.W. Kinzler, and B. Vogelstein. 1998. Mutations of mitotic checkpoint genes in human cancers. Nature. **392**:300-303.

Campbell, M.S., G.K. Chan, and T.J. Yen. 2001. Mitotic checkpoint proteins HsMAD1 and HsMAD2 are associated with nuclear pore complexes in interphase. J. Cell Sci. **114**:953-963.

Chen, R.H., J.C. Waters, E. D. Salmon, and A.W. Murray. 1996. Association of spindle assembly checkpoint component XMAD2 with unattached kinetochores. Science. **274**:242-246.

Chen, R.H., A. Shevchenko, M. Mann, and A.W. Murray. 1998. Spindle checkpoint protein Xmad1 recruits Xmad2 to unattached kinetochores. J. Cell Biol. **143**:283-295.

Chen, R.H., D.M. Brady, D. Smith, A.W. Murray, and K.G. Hardwick. 1999. The spindle checkpoint of budding yeast depends on a tight complex between the Mad1 and Mad2 proteins. Mol. Biol. Cell. **10**:2607-2618.

Chial, H.G., M.P. Rout, T.H. Giddings, and M. Winey. 1998. *Saccharomyces cerevisiae* Ndc1p is a shared component of nuclear pore complexes and spindle pole bodies. J. Cell Biol. **143**:1789-1800.

Chook, Y.M., and G. Blobel. 2001. Karyopherins and nuclear import. Curr. Opin. Struct. Biol. **11**:703-715.

Chung, E., and R.H. Chen. 2002. Spindle checkpoint requires Mad1-bound and Mad1-free Mad2. Mol. Biol. Cell. **13**:1501-1511.

Cimini, D., B. Howell, P. Maddox, A. Khodjakov, F. Degrasi, E.D. Salmon. 2001. Merotelic kinetochore orientation is a major mechanism of aneupolidy in mitotic mammalian tissue cells. J. Cell Biol. **153**:517-527.

Ciosk, R., W. Zachariae, C. Michaelis, A. Shevchenko, M. Mann, and K. Nasmyth. 1998. An ESP1/PDS1 complex regulates loss of sister chromatid cohesion at the metaphase to anaphase transition in yeast. Cell. **93**:1067-1076.

Clark, M. W. Nucleolar-specific positive strains for optical and electron microscopy. 1991. Meth. Enzymol. **194**:717-728.

Clegg, R.M. 1996. Fluorescence resonance energy transfer. In: X.F. Wang and B. Herman (ed.), Fluorescence Imaging Spectroscopy and Microscopy. Wiley, NY.

Collas, I., and J.C. Courvalin. 2000. Sorting nuclear membrane proteins at mitosis. Trends Cell Biol. **10**:5-8.

Conti, E., and J. Kuriyan. 2000. Crystallographic analysis of the specific yet versatile recognition of distinct nuclear localization signals by karyopherin α. Structure Fold. Des. **8**:329-338.

Conti, E., and E. Izaurralde. 2001. Nucleocytoplasmic transport enters the atomic age. Curr. Opin. Cell Biol. **13**:310-319.

Cordes, V.C., S. Reidenbach, , H.R. Rackwitz, and W.W. Franke. 1997. Identification of protein p270/Tpr as a constitutive component of the nuclear pore complex-attached intranuclear filaments. J. Cell Biol. **136**: 531-544.

Dabeva, M.D., and J.R.Warner. 1993. Ribosomal protein L32 of *Saccharomyces cerevisiae* regulates both splicing and translation of its own transcript. J. Biol. Chem. **268**: 19669-19674.

Daigle, N., J. Beaudouin, L. Hartnell, G. Imreh, E. Hallberg, J. Lippincott-Schwartz, and J. Ellenberg. 2001. Nuclear pore complexes form immobile networks and have a very low turnover in live mammalian cells. J. Cell Biol. **154**:71-84.

Damelin, M., and P.A. Silver. 2000. Mapping interactions between nuclear transport factors in living cells reveals pathways through the nuclear pore complex. Mol. Cell.**5**:133-140.

De Beus, E., J.S. Brockenbrough, B. Hong, and J. P. Aris. 1994. Yeast NOP2 encodes an essential nucleolar protein with homology to a human proliferation marker. J. Cell Biol. **127**:799-813.

Delorme, E.1989. Transformation of *Sacharomyces cerevisiae* by electroporation. Appl. Environ. Microbiol. **55**:2242-2246.

Desay, A., and T.J. Mitchison. 1997. Microtubule polymerization dynamics. Annu. Rev. Cell Dev. Biol. **13**:83-117.

Dilworth, D.J., A. Suprapto, J.C. Padovan, B.T. Chait, R.W. Wozniak, M.P.Rout, and J.D. Aitchison. 2001. Nup2p dynamically associates with the distal regions of the yeast nuclear pore complex. J. Cell Biol. **153**:1465-1478.

Dingwall, C., and R.A. Laskey. 1991. Nuclear targeting sequences – a consensus? Trends Biochem. Sci. **16**:478-481.

Dobles, M., V. Liberal, M.L. Scott, R. Benezra, and P.K. Sorger. 2000. Chromosome missegregation and apoptosis in mice lacking the mitotic checkpoint protein Mad2. Cell. **101**:635-645.

Doxsey, S. 2001. Re-evaluating centrosome function. Nature Rev. Mol. Cell Biol. **2**:688-698.

Eisinger, D.P., F.A. Dick, and B.L. Trumpower. 1997. Qsr1p, a 60S ribosomal subunit protein, is required for joining of 40S and 60S subunits. Mol. Cell. Biol. **17**:5146-5155.

Eissenberg, J. C. 2001. Decisive factors: a transcription activator can overcome heterochromatin silencing. Bioessays. **23**: 767-771.

El Baradi, T.T., C.A. can der Sande, W.H. Mager, H.A. Raue, and R.J. Planta. 1986. The cellular level of yeast ribosomal protein L25 is controlled principally by rapid degradation of excess protein. Curr. Genet. **10**:733-739.

Eng, F.J., and J.R. Warner. 1991. Structural basis for the regulation of splicing of yeast messenger RNA. Cell. **65**:797-804.

Enomoto, S., P.D. McCune-Zierath, M. Gerami-Nejad, M.A. Sanders, and J. Berman. 1997. RLF2, a subunit of yeast chromatin assembly factor-1, is required for telomeric chromatin function in vivo. Genes Dev. **11**:358-370.

Fabre, E. and E. Hurt. 1997. Yeast genetics to dissect the nuclear pore complex and nucleocytoplasmic trafficking. Annu. Rev. Genet. **31**:277-313.

Fahrenkrog, B., E.C. Hurt, U. Aebi, and N. Pante. 1998. Molecular architecture of the yeast nuclear pore complex: localization of Nsp1p subcomplexes. J. Cell Biol. **143**:577–588.

Fang, G., H. Yu, and M.W. Kirschner. 1998. Direct binding of CDC20 protein family members activates the anaphase-promoting complex in mitosis and G1. Mol. Cell. **2**:163-171.

Farr, K.A., and M.A. Hoyt. 1998. Bub1p kinase activates the *Saccharomyces cerevisiae* spindle assembly checkpoint. Mol. Cell Biol. **18**: 2738-2747.

Favreau, C., H.J. Worman, R.W. Wozniak, T. Frappier, and J.C. Courvalin. 1996. Cell cycle-dependent phosphorylation of nucleoporins and nuclear pore membrane protein Gp210. Biochemistry. **35**:8035-8044.

Feuerbach, F., V. Galy, E. Trelles-Sticken, M. Fromont-Racine, A. Jacquier, E Gilson, J. C. Olivo-Marin, H. Scherthan, and U. Nehrbass. 2002. Nuclear architecture and spatial positioning help establish transcriptional states of telomeres in yeast. Nature Cell Biol. **3**:214-221.

Fewell, S.W., and J.L. Woolford, Jr. 1999. Ribosomal protein S14 *of Saccharomyces cerevisiae* regulates its expression by binding to *RPS14B* pre-mRNA and to 18S rRNA. Mol. Cell Biol. **19**:826-834.

Ficarro, S.B., M.L. McCleland, P.T. Stukenberg, D.J. Burke, M.M. Ross, J. Shabanowitz, D.F. Hunt, and F.M. White FM. 2002. Phosphoproteome analysis by mass spectrometry and its application to *Saccharomyces cerevisiae*. Nature Biotechnol. **3**:301-305.

Fontoura B.M., G. Blobel, and M.J. Matunis. 1999. A conserved biogenesis pathway for nucleoporins: proteolytic processing of a 186-kilodalton precursor generates Nup98 and the novel nucleoporin, Nup96. J. Cell Biol. **144**:1097-1112.

Fornerod, M., M. Ohno, M. Yoshida, and I.W. Mattaj. 1997. CRM1 is an export receptor for leucine-rich nuclear export signals. Cell. 90:1051-1060.

Fraschini, R., A. Beretta, G. Lucchini, and S. Piatti. 2001. Role of the kinetochore protein Ndc10 in mitotic checkpoint activation in *Saccharomyces cerevisiae*. Mol. Genet. Genomics. **266**:115-125.

Fried, H.M., and J.R. Warner. 1981. Cloning of yeast gene for trichodermin resistance and ribosomal protein L3. Proc. Natl. Acad. Sci. USA. **78**: 238-242.

Gall, J.G. 1967. Octagonal nuclear pores. J. Cell Biol. **31**:391-399.

Galy, V., J.C. Olivo-Martin, H. Scherthan, V. Doye, N. Rascalou, and U. Nehbrass. 2000. Nuclear pore complexes in the organization of silent telomeric chromatin. Nature. **403**:108-112.

Gardner, R.D., and D.J. Burke. 2000. The spindle checkpoint: two transitions, two pathways.Trends Cell Biol. **10**:154-158.

Gerace, L. 1995. Nuclear export signal and the fast track to the cytoplasm. Cell. **82**:341-344.

Gigliotti S., G. Callaini, S., M.G. Riparbelli, R. Pernas-Alonso, G. Hoffmann, F. Graziani, and C. Malva. 1998. *Nup154*, a new *Drosophila* gene essential for male and female gametogenesis is related to the *NUP155* vertebrate nucleoporin gene. J. Cell Biol. **142**:1195-1207.

Goldberg, M.W., and T.D. Allen. 1992. High resolution scanning electron microscopy of the nuclear envelope: demonstration of a new, regular, fibrous lattice attached to the baskets of the nucleoplasmic face of the nuclear pores. J. Cell Biol. **119**:1429-1440.

Goldberg, M.W., and T.D. Allen. 1993. The nuclear pore complex: three-dimensional surface structure revealed by field emission, in-lens scanning electron microscopy, with underlying structure uncovered by proteolysis. J. Cell Sci. **106**:261-274.

Goldberg, M.W., C. Wiese, T.D. Allen, and K.L. Wilson. 1997. Dimples, pores, starrings and thin rings on growing nuclear envelopes: evidence for structural intermediates in nuclear pore complex assembly. J. Cell Sci. **110**:409-420.

Gomez-Ospina, N., G. Morgan, T.H. Giddings, Jr., B. Kosova, E. Hurt, and M. Winey. 2000. Yeast nuclear pore complex assembly defects determined by nuclear envelope reconstruction. J. Struct. Biol. **132**:1-5.

Gorbsky, G.J., R. H. Chen, and A.W. Murray. 1998. Microinjection of antibody to Mad2 protein into mammalian cells in mitosis induces premature anaphase. J. Cell Biol. **142**:1193-1205.

Görlich, D., S. Prehn, R.A. Laskey, and E. Hartmann. 1994. Isolation of a protein that is essential for the first step of nuclear import. Cell. **79**:767-778.

Görlich, D., and U. Kutay. 1999. Transport between the cell nucleus and the cytoplasm. Annu. Rev. Cell Dev. Biol. **15**:607-660.

Goshima, G., M. Yanagida. 2000. Establishing biorientation occurs with precocious separation of the sister kinetochores, but not the arms, in the early spindle in budding yeast. Cell. **100**:619-633.

Graham, I.R., R.A. Haw, K.G. Spink, K.A. Halden, and A. Chambers. 1999. In vivo anlysis of functional regions within yeast Rap1p. Mol. Cell. Biol. **11**:7481-7490.

Grass, O.J., R. E. Carazo-Salas, C.A. Schatz, G. Guarguaglini, J. Kast, M. Wilm, N. Le Bot, I. Vernos, E. Karsenti, and I. W. Mattaj. 2001. Ran induces spindle assembly by reversing the inhibitory effect of importin α on TPX2 activity. Cell. **104**:83-93.

Gruter, P., C. Tabernero, C. von Kobbe, C. Schmitt, C. Saavedra, A. Bachi, M. Wilm, B.K. Felber, and E. Izaurralde. 1998. TAP, the human homolog of Mex67p, mediates CTE-dependent RNA export from the nucleus. Mol. Cell. **5**:649-659.

Hanic-Joyce, P.J., R.A.Singer RA, and G.C.Johnston 1987.Molecular characterization of the yeast *PRT*1 gene in which mutations affect translation initiation and regulation of cell proliferation. J. Biol. Chem. **262**:2845-2851.

Hardwick, K.G., and A. W. Murray. 1995. Mad1p, a phosphoprotein component of the spindle assembly checkpoint in budding yeast. J. Cell Biol. **131**:709-720.

Hardwick, K.G., E. Weiss, F.C. Luca, M. Winey, and A.W. Murray. 1996. Activation of the budding yeast spindle asembly checkpoint without mitotic spindle disruption. Science. **273**:953-956.

Hardwick, K.G., R. C. Johnson, D. L. Smith, and A. W. Murray. 2000. Mad2 encodes a novel component of the spindle checkpoint, which interacts with Bub3p, Cdc20p, and Mad2p. J. Cell Biol. **148**:871-882.

Hartwell, L. H., and C.S. McLaughlin. 1969. A mutant of yeast apparently defective in the initiation of protein synthesis. Proc. Natl. Acad. Sci. USA. **62**:468-474.

Heath, C.V., C.S. Copeland, D.C. Amberg, V. Del Priore, M. Snyder, and C.N. Cole. 1995. Nuclear pore complex clustering and nuclear accumulation of poly(A)+ RNA associated with mutation of the *Saccharomyces cerevisiae RAT2/NUP120* gene. J. Cell. Biol. **131**:1677-1697.

Herruer M.H., W. H. Mager, L.P.Woudt, R.T.Nieuwint, G.M.Wassenaar, P. Groeneveld, and R.J. Planta 1987. Transcriptional control of yeast ribosomal protein synthesis during carbon-source upshift. Nucleic Acids Res. **15:**10133-10144.

Hildebrandt, E.R., and M.A. Hoyt. 2000. Mitotic motors in *Saccharomyces cerevisiae*. Biochim. Biophys. Acta. **1496**: 99-116.

Hinnebusch A.G., and S.W. Liebman. 1991. Protein synthesis and translational control in. *Saccharomyces cerevisiae.* In: J.R. Broach, J.R. Pringle, and E.W. Jones (ed.), The Molecular Biology and Cellular Biology of the Yeast *Saccharomyces*. Genome Dynamics, Protein Synthesis, and Energetics. p. 627-679. Cold Spring Harbor Laboratory Press, Cold Spring Harbor, NY.

Hodges P.E., A.H. McKee, B.P. Davis, W.E. Payne and J.I. Garrels. 1999. The Yeast Proteome Database (YPD): a model for the organization and presentation of genomic-wide functional data. Nucleic Acids Res. **27**:69-73.

Hood, J.K., J.M. Casolari, and P.A. Silver. 2000. Nup2p is located on the nuclear side of the nuclear pore complex and coordinates Srp1p/importin-alpha export. J. Cell. Sci. **113**:1471-1480.

Howell, B.J., D.B. Hoffman, G. Fang, A. W. Murray, and E.D. Salmon. 2000. Visualization of Mad2 dynamics at kinetochores, along spindle fibers, and at the spindle poles in living cells. J. Cell Biol. **150**:1233-1250.

Hoyt, M.A. 2000. Exit from mitosis: spindle pole power. Cell. **102**:267-270.

Hoyt, M.A. 2001. A new view of the spindle checkpoint. J. Cell Biol. **154**:909-911.

Hoyt, M.A., L. Totis, and B.T. Roberts. 1991. *S. cerevisiae* genes required for cell cycle arrest in response to loss of microtubule function. Cell. **66**:507-517.

Hwang, H.L., L.F. Lau, D.L. Smith, C.A. Mistrot, K.G. Hardwick, E.S. Hwang, A. Amon, and A.W. Murray. 1998. Budding yeast Cdc20: a target of the spindle checkpoint. Science. **279**:1041-1044.

Hyland, K.M., J. Kingsbury, D. Koshland, and P. Hieter. 1999. Ctf19p: A novel kinetochore protein in *Saccharomyces cerevisiae* and a potential link between the kinetochore and mitotic spindle. J. Cell Biol. **145**:15-28.

Ikui, A.E., K. Furuya, M. Yanagida, and T. Matsumoto. 2002. Control of localization of a spindle checkpoint protein, Mad2, in fission yeast. J. Cell Sci. **115**:1603-1610.

Iouk, T.L., J.D. Aitchison, S. Maguire, and R.W. Wozniak. 2001. Rrb1p, a yeast nuclear WD-repeat protein involved in the regulation of ribosome synthesis. Mol. Cell. Biol. **21**: 1260-1271.

Iouk, T.L., O. Kerscher, M. Basrai, and R.W. Wozniak. 2002. Functional Associations Between the Yeast NPC and the Spindle Checkpoint Machinery. *Submitted to* J. Cell Biol.

Jablonski, S.A., G.K. Chan, C.A. Cooke, W.C. Earnshaw, and T.J. Yen. 1998. The hBUB1 and hBUBR1 kinases sequentially assemble onto kinetochores during prophase with hBUBR1 concentrating at the kinetochore plates in mitosis. Chromosoma. **107**:386-396.

Jensen, S., M. Segal, D.J. Clarke, and S.T. Reed. 2001. A novel role of the budding yeast separin Esp1 in anaphase spindle elongation: evidence that proper spindle association of Esp1 is regulated by Pds1. J. Cell Biol. **152**:27-40.

Jin, Q., J. Fuchs, and J. Loidl. 2000. Centromere clustering is a major determinant of yeast interphase nuclear organization. J. Cell. Sci. **113**:1903-1912.

Johnson, M., and M. Carlson. 1992. Regulation of carbon and phosphate utilization. In: E.W. Jones, J.R. Pringle, and J.R. Broach (ed.), Molecular and Cellular Biology of the Yeast *Saccharomyces*: Gene Expression. p.193-282. Cold Spring Harbor Laboratory Press, Cold Spring Harbor, NY.

Jones, E.W., G.C. Webb, and M.A. Hiller. 1997. Biogenesis and function of the yeast vacuole. In: J. R. Pringle, J. R. Broach, and E. W. Jones (ed.), The Molecular and Cellular Biology of

the Yeast *Saccharomyces*. p. 363-470 Cold Spring Harbor Laboratory Press, Cold Spring Harbor, NY.

Kaffman, A., and E.K. O'Shea. 1999. Regulation of nuclear localization: A key to a door. Annu. Rev. Cell Dev. Biol. **15**:291-339.

Kahana, J.A., and D.W. Cleveland. 2001. Some importin news about spindle assembly. Science. **291**:1718-1719.

Kehlenbach, R.H., A. Dickmanns, A. Kehlenbach, T. Guan, and L. Gerace. 1999. A role for RanBP1 in the release of CRM1 from the nuclear pore complex in a terminal step of nuclear export. J. Cell Biol. **145**:645-657.

Kenna, M.A., J.G. Petranka, J.L. Reilly, and L.I.Davis. 1996. Yeast Nle3p/Nup170p is required for normal stoichiometry of FG nucleoporins within the nuclear pore complex. Mol. Cell. Biol. **16**:2025-2036.

Kerscher, O., P. Hieter, M. Winey, and M.A. Basrai. 2001. Novel role for a *Saccharomyces cerevisiae* nucleoporin, Nup170p, in chromosome segregation. Genetics. **157**:1543-1553.

Kiger, A.A., S. Giggliotti, and M.T. Fuller. 1999. Developmental genetics of the essential Drosophila Nucleoporin *nup154*: allelic differences due to an outward-directed promoter in the *P*-element 3'end. Genetics. **153**:799-812.

Kihlmark, M., G. Imreh, and E. Hallberg. 2001. Sequential degradation of proteins from the nuclear envelope during apoptosis. J. Cell Sci. **114**:3643-3653.

Kilmartin, J.V., and A.E.M. Adams. 1984. Structural rearrangements of tubulin and actin during the cell cycle of the yeast *Saccharomyces cerevisiae*. J. Cell. Biol. **98**:922-933.

Kiseleva E., M.W. Goldberg, T.D. Allen, and C.W. Akey. 1998. Active nuclear pore complexes in Chironomus: visualization of transporter configurations related to mRNP export. J. Cell Sci. **111**:223-236.

Kiseleva, E., M.W. Goldberg, J. Cronshaw, and T.D. Allen. 2000. The nuclear pore complex: structure, function, and dynamics. Crit. Rev. Eukaryot. Gene Expr. **10**:101-112.

Kiseleva, E., S. Rutherford, L.M. Cotter, T.D. Allen TD, and M.W. Goldberg. 2001. Steps of nuclear pore complex disassembly and reassembly during mitosis in early *Drosophila* embryos. J. Cell Sci. **114**:3607-3618.

Kitagawa, K., and P.Hieter. 2001. Evolutionary conservation between budding yeast and human kinetochores. Nature Rev. Mol. Cell Biol. **2**:678-687.

Kitagawa, K., and P.Hieter. 2001. Evolutionary conservation between budding yeast and human kinetochores. Nature Rev. Mol. Cell Biol. **2**:678-687.

Köhrer K., and K. Domdey 1991. Preparation of high molecular weight RNA. Methods Enzymol. **194**:398-401.

Komeili, A., and E.K. O'Shea. 2001. New perspectives on nuclear transport. Annu. Rev. Genet. **35**:341-364.

Kosova, B., N. Pante, C. Rolenhagen, and E. Hurt. 1999. Nup192 is a conserved nucleoporin with a preferential location at the inner side of the nuclear membrane. J. Biol. Chem. **274**:22646-22651.

Kosova, B., N. Pante, C. Rollenhagen, A. Podteleinikov, M. Mann, U. Aebi and E. Hurt. 2000. Mlp2p, a component of nuclear pore attached intranuclear filaments, associates with Nic96p. J. Biol. Chem. **275**:343-350.

Kressler, D., P.Linder, and J. de la Cruz. 1999. Protein *trans*-acting factors involved in ribosome biogenesis in *Saccharomyces cerevisiae*. Mol. Cell. Biol. **19**:7897-7912.

Kruiswijk, T., R. J. Planta, and J.M. Krop. 1978. The course of the assembly of ribosomal subunits in yeast. Biochim. Biophys. Acta. **517**:378-389.

Künzler, M., and E. Hurt. 2001. Targeting of Ran: variation on a common theme? J. Cell Sci. **114**:3233-3241.

Laroche, T., S.G. Martin, M. Tsay-Pflugfelder, and S.M. Casser. 2001. The dynamics of yeast telomeres and silencing proteins through the cell cycle. J. Struct. Biol. **129**:159-174.

Lauze, E., B. Stoelcker, F.C. Luca, E. Weiss, A.R. Schultz, and M. Winey. 1995. Yeast spindle pole body duplication gene *MPS1* encodes an essential dual specificity protein kinase. EMBO J. **14**:1655-1663.

Leger-Silvestre, I., S. Trumtel, J. Noaillac-Depeyre, and N. Gas. 1999. Functional compartmentalization of the nucleus in the budding yeast *Saccharomyces cerevisiae*. Chromosoma. **108**:103-113.

Lengauer, C., K.W. Kinzler, and B. Vogelstein. 1998. Genetic instabilities in human cancers. Nature. **396**:643-649.

Lew, D.J. 1997. Cell cycle control in *Saccharomyces cerevisiae*. In: J.R Pringle. (ed.) The Molecular and Cellular Biology of the Yeast *Saccharomyces*. p.607-695.Cold Spring Harbor Laboratory Press. Cold Spring Harbor, NY.

Li, R. 2000. Shutting the door behind when you leave. Curr. Biol. **10**:R781-R784.

Li, Y., and R. Benezra. 1996. Identification of a human mitotic checkpoint gene: hsMAD2. Science. **274**:246-8.

Li, X., and M. Cai. 1997. Inactivation of the cyclin-dependent kinase Cdc28 abrogates cell cycle arrest induced by DNA damage and disassembly of mitotic spindles in *Saccharomyces cerevisiae*. Mol. Cell. Biol. **17**:2723-2734.

Li, Y., C. Gorbea, D. Mahaffey, M. Rechsteiner, and R. Benezra. 1997. MAD2 associates with the cyclosome/anaphase-promoting complex and inhibits its activity. Proc. Natl. Acad. Sci. USA. **94**:12431-12436.

Li, R., and A. W. Murray. 1991. Feedback control of mitosis in budding yeast. Cell. **66**:519-531.

Li, B, C.R. Nierras, and J.R. Warner. 1999. Transcriptional elements involved in the repression of ribosomal protein synthesis. Mol. Cell. Biol.**19**:5393-5404.

Lusk, C.P., T. Makhnevych, M. Marelli, J. D. Aitchison, and R.W. Wozniak. 2002. A role for karyopherins in the assembly of the nuclear pore complex. *Submitted to* J. Cell Biol.

Macara, I.G. 2001. Transport into and out of the nucleus. Microbiol. Mol. Biol. Rev. **65**:570-594.

Mager, W.H., R.J. Planta, J.G. Ballesta, J.C. Lee, K. Mizuta, K. Suzuki, J.R. Warner, and J. Woolford. 1997. A new nomenclature for the cytoplasmic ribosomal proteins of *Saccharomyces cerevisiae*. Nucleic Acids Res. **25**:4872-4875.

Maicas E., F.G. Pluthero, and J.D. Friesen. 1988. The accumulation of three yeast ribosomal proteins under conditions of excess mRNA is determined primarily by fast protein decay. Mol. Cell. Biol. **1**:169-175

Maillet, L., C. Boscheron, M. Gotta, S. Marcand, E. Gilson, and S.M. Gasser.1996. Evidence for silencing compartments within the yeast nucleus: a role for telomere proximity and Sir protein concentration in silencer-mediated repression. Genes Dev. **10**:1796-1811.

Macaulay, C., E. Meier, and D.J. Forbes. 1995. Differential mitotic phosphorylation of proteins of the nuclear pore complex. J Biol Chem. **270**:254-262.

Macaulay, C., and D.J. Forbes. 1996. Assembly of the nuclear pore-biochemically distinct steps revealed with NEM, GTP-γ-S, and BAPTA. J. Cell Biol. **132**:5-20.

Marelli, M.M., J.D. Aitchison, and R.W. Wozniak. 1998. Specific binding of the karyopherin Kap121p to a subunit of the nuclear pore complex containing Nup53p, Nup59p, and Nup170p. J. Cell Biol. **143**:1813-1830.

Marelli, M.M., C.P. Lusk, H. Chan, J.D. Aitchison, and R.W. Wozniak. 2001. A link between the synthesis of nucleoporins and the biogenesis of the nuclear envelope. J. Cell. Biol. **153**:709-724.

Mattaj, I.W., and L. Englmeier. 1998. Nucleocytoplasmic transport: the soluble phase. Annu. Rev. Biochem. **67**:265-306

McEwen, B.F., G.K.T. Chan, B. Zubrowski, M. Savoian, M.T. Sauer, and T.J. Yen. 2001. CENP-E is essential for reliable bioriented spindle attachment, but chromosome alignment can be achieved via redundant mechanisms in mammalian cells. Mol. Biol. Cell. **12**:2776-2789.

Millband, D.N., and K.G. Hardwick. 2002. Fission yeast Mad3p is required for Mad2p to inhibit the anaphase-promoting complex and localizes to kinetochores in a Bub1p-, Bub3p-, and Mph1p-dependent manner. Mol. Cell. Biol. **22**:2728-2742.

Mizuta, K., and J.R. Warner. 1994. Continuing functioning of the secretory pathway is essential for ribosome synthesis. Mol. Cell Biol. **14**:2493-2502.

Mizuta K., R. Tsujii, J.R. Warner, and M. Nishiyama. 1998. The C-terminal silencing domain of Rap1p is essential for the repression of ribosomal protein genes in response to a defect in the secretory pathway. Nucleic Acids Res. **26**:1063-1069.

Moehle C.M., and A.G. Hinnebusch. 1991. Association of RAP1 binding sites with stringent control of ribosomal protein gene transcription in *Saccharomyces cerevisiae*. Mol. Cell. Biol. **11**:2723-2735.

Moore, M.S. 1998. Ran and nuclear transport. J. Biol. Chem. **273**:22857-22860.

Moore, J.D. 2001. The Ran-GTPase and cell-cycle control. Bioessays. **23**:77-85.

Morse, R.H. 2000. RAP, RAP, open up! New rinkles for RAP1 in yeast. Trends Genet. **16**:51-53.

Nachury, M.V., T.J. Maresca, W.C. Salmon, C.M. Waterman-Storer, R. Heald, K. Weis. 2001. Importin β is a mitotic target of the small GTPase Ran in spindle assembly. Cell. **104**: 95-106.

Nachury, M.V., and K. Weis. 1999. The direction of transport through the nuclear pore can be inverted. Proc. Natl. Acad. Sci. U S A. **96**:9622-9627.

Nakielny, S., and G. Dreyfuss. 1999. Transport of proteins and RNAs in and out of the nucleus. Cell. **99**: 677-690.

Naranda T., S.E. MacMillan, and J W.B. Hersey. 1994. Purified yeast translational initiation factor eIF-3 is an RNA-binding protein complex that contains the PRT1 protein. J. Biol. Chem. **269**:33286-33292.

Nasmyth, K., J.M. Peters, and F. Uhlmann. 2000. Splitting the chromosome: cutting the ties that bind sister chromatids. Science. **288**:1379-1385.

Neuman-Silberberg, F.S., S. Bhattacharaya, and J.R. Broach. 1995. Nutrient availability and the RAS/cyclic AMP pathway both induce expression of ribosomal protein genes in *Saccharomyces cerevisiae* but by different mechanisms. Mol. Cell. Biol. **15**:3187-3196.

Nicklas, R.B. 1997. How cells get the right chromosomes. Science. **275**:632-637.

Nierras CR, and J.R. Warner. 1999. Protein kinase C enables the regulatory circuit that connects membrane synthesis to ribosome synthesis in *Saccharomyces cerevisiae*. J. Biol. Chem. **274**:13235-13241.

Noma K., C.D. Allis, and S.I. Grewal. 2001. Transitions in distinct histone H3 methylation patterns at the heterochromatin boundaries. Science. **293**:1150-1155.

Nomura, M. 1999. Regulation of ribosome biosynthesis in *Escherichia co*li and *Saccharomyces cerevisiae*: diversity and common principles. J. Bacteriol. **181**: 6857-6864.

O'Toole, E., M. Winey, and J.R. McIntosh. 1999. High-voltage electron tomography of spindle pole bodies and early mitotic spindles in the yeast *Saccharomyces cerevisiae*. Mol. Biol. Cell. **10**:2017-2031.

Ohno, M., M. Fornerod, and I.W. Mattaj. 1998. Nucleocytoplasmic transport: the last 200 nanometers. Cell. **92**:327-336.

Page, A.M., and P. Hieter. 1999. The anaphase –promoting complex: new subunits and regulators. Annu. Rev. Biochem. **68**:583-609.

Paine, P.L., L.C. Moore, and S.B. Horowitz. 1975. Nuclear envelope permeability. Nature. **254**:109-114.

Pan, X., P. Roberts, Y. Chen, E. Kvam, N. Shulga, K. Huang, S. Lemmon, and D.S. Goldfarb. 2000. Nucleus-vacuole junctions in *Saccharomyces cerevisiae* are formed through the direct interaction of Vac8p with Nvj1p. Mol. Biol. Cell. **11**:2445-2457.

Panté, N., and U. Aebi. 1996. Sequential binding of import ligands to distinct nucleopore regions during their nuclear import. Science. **273**:1729-1732.

Pearson, N.J., H.M. Fried, and J.R. Warner. 1982. Yeast use translational control to compensate for extra copies of ribosomal protein genes. Cell. **30**:347-355.

Pemberton, L.F., M.P. Rout, and G. Blobel. 1995. Disruption of the nucleoporin gene *NUP133* results in clustering of nuclear pore complexes. Proc. Natl. Acad. Sci. USA. **92**:1187-1194.

Peterson, J., and H. Ris. 1974. Electron-microscopic study of the spindle and chromosome movement in the yeast *Saccharomyces cerevisiae*. J. Cell Sci. **22**:219-242.

Planta R.J. 1997. Regulation of ribosome synthesis in yeast. Yeast. **13**:1505-1518.

Planta R.J., and W.H.Mager. 1998. The list of cytoplasmic ribosomal proteins of Saccharomyces cerevisiae. Yeast. **14**: 471-477.

Planta. R.J., and H.A. Raue. 1988. Control of ribosome biogenesis in yeast. Trends Genet. **4**:64-68.

Powers, T., and P. Walter. 1999. Regulation of ribosome synthesis in yeast. Yeast. **13**:1505-1518.

Pringle, J.R., A.E. Adams, D.G. Drubin, and B.K. Haarer. 1991. Immunofluorescence methods for yeast. Methods Enzymol. **194**:565-602.

Qian Y.W., and E.Y. Lee. 1995. Dual retinoblastoma-binding proteins with properties related to a negative regulator of ras in yeast. J. Biol. Chem. **270**:25507-25513.

Quimby, B.B., C.A. Wilson, and A.H. Corbett. 2000. The interaction between Ran and NTF2 is required for cell cycle progression. Mol. Biol. Cell. **11**:2617-2629.

Rabut, G., and J. Ellenberg. 2001. Nucleocytoplasmic transport: diffusion channel or phase transition? Curr. Biol. **14**:R551-554.

Radu, A., G. Blobel, M.S. Moore. 1995. Identification of a protein complex that is required for nuclear protein import and mediates docking of import substrate to distinct nucleoporins. Proc. Natl. Acad. Sci. U S A. **92**:1769-1773.

Reichelt, R., A. Holzenburg, E.L. Buhle, Jr., M. Jarnik, A. Engel, and U. Aebi. 1990. Correlation between structure and mass distribution of the nuclear pore complex and of distinct pore complex components. J. Cell Biol. **110**:883-894.

Rexach, M., and G. Blobel. 1995. Protein import into nuclei: association and dissociation reactions involving transport substrate, transport factors, and nucleoporins. Cell. **83**:683-692.

Ribbeck, K., and D. Gorlich. 2001. Kinetic analysis of translocation through nuclear pore complexes. EMBO J. **20**:1320-1330.

Ribbeck, K., and D. Gorlich. 2002. The permeability barrier of nuclear pore complexes appears to operate via hydrophobic exclusion. EMBO J. **21**:2664-2671.

Ribbeck, K., G. Lipowsky, H.M. Kent, M. Stewart, and D. Gorlich. 1998. NTF2 mediates nuclear import of Ran. EMBO J. **22**:6587-6598.

Rieder, C.L., R.W. Cole, A. Khodjakov, and G. Sluder. 1995. The checkpoint delaying anaphase in response to chromosome monoorientation is mediated by an inhibitory signal produced by unattached kinetochores. J. Cell Biol. **130**:941-948.

Robinow, C.F., and J.A. Marak. 1966. A fiber apparatus in the nucleus of the yeast cell. J. Cell Biol. **29**:129-150.

Roeder, G.S., and J.M. Bailis. 2000. The pachytene checkpoint. Trends Genet. **16**:395-403.

Roos, U.P. 1973. Light and electron microscopy of rat kangaroo cells in mitosis. II. Kinetochore structure and function. Chromosoma. **41**:195-220.

Rout, M.P. and J.D. Aitchison. 2001. The nuclear pore complex as a transport machine. J. Biol. Chem. **276**:16593-16596.

Rout, M.P., and G. Blobel. 1993. Isolation of the yeast nuclear pore complex. J. Cell Biol. **123**:771-783.

Rout, M.P., and J.V. Kilmartin. 1990. Components of the yeast spindle and spindle pole body. J. Cell Biol. **111**:1913-1927.

Rout, M.P., J.D. Aitchison, A. Suprapto, K. Hjertaas, Y. Zhao, and B.T. Chait. 2000. A comprehensive analysis of the yeast nuclear pore complex. J. Cell Biol. **148**:635-651.

Rutherford, S.A., M.W. Goldberg, and T.D. Allen. 1997. Three-dimensional visualization of the route of protein import: the role of nuclear pore complex substructures. Exp. Cell Res. **232**:146-160.

Ryan, K.J., and S.R. Wente. 2000. The nuclear pore complex: a protein machine bridging the nucleus and cytoplasm. Curr. Opin. Cell Biol. **12**:361-371.

Saffery, R., D.V. Irvine, B. Griffiths, P. Kalitsis, and K.H. Choo. 2000. Components of the human spindle checkpoint control mechanism localize specifically to the active centromere on dicentric chromosomes. Hum. Genet. **107**:376-384.

Salina, D., K. Bodoor, D.M. Eckley, T.A. Schroer, J.B. Rattner, and B. Burke. 2002. Cytoplasmic dynein as a facilitator of nuclear envelope breakdown. Cell. **108**:97-107.

Schwoebel, E.D., B. Talcott, I. Cushman, and M.S. Moore. 1998. Ran-dependent signal-mediated nuclear import does not require GTP hydrolysis by Ran. J. Biol. Chem. **273**:35170-35175.

Segref, A., K. Sharma, V. Doye, A Hellwig, J. Huber, R. Luhrmann, and E. Hurt. 1997. Mex67p, a novel factor for nuclear mRNA export, binds to both poly(A)+ RNA and nuclear pores. EMBO J. **16**:3256-3271.

Sesaki, H., and R.E. Jensen. 1999. Division versus fusion: Dnm1p and Fzo1p antagonistically regulate mitochondrial shape. J. Cell Biol. **147**:699-706.

Severs, N.J. 1976. Nuclear envelope inclusions demonstrated by freeze-fracture. Cytobios. **62**:125-132.

Sikorski, R.S. and P. Hieter. 1989. A system of shuttle vectors and yeast host strains designed for efficient manipulation of DNA in *Saccharomyces cerevisiae*. Genetics. **122**:19-27.

Shah, J.V., and D.W. Cleveland. 2000. Waiting for anaphase: Mad2 and the spindle assembly checkpoint. Cell. **103**:997-1000.

Sharp-Baker, H., and R.H. Chen. 2001. Spindle checkpoint protein Bub1 is required for kinetochore localization of Mad1, Mad2, Bub3, and CENP-E, independently of its kinase activity. J. Cell Biol. **153**:1239-1249.

Sherman, F., G.R.Fink, and J.B.Hicks. 1986. Methods in yeast genetics. Cold Spring Harbor Laboratory Press, Cold Spring Harbor, NY. 186pp.

Shore, D. 1994. RAP1: a protean regulator in yeast. Trends Genet. **10**:408-412.

Shou, W., J.H. Seol, A. Shevchenko, C. Baskerville, D. Moazed, Z.W. Chen, J. Jang, A. Shevchenko, H. Charbonneau, and R.H. Deshaies. 1999. Exit from mitosis is triggered by Tem1-dependent release of the protein phosphatase Cdc14 from nuclear RENT complex. Cell. **97**:233-244.

Shulga, N., N. Mosammaparast, R. Wozniak, and D.S. Goldfarb. 2000. Yeast nucleoporins involved in passive nuclear envelope permeability. J. Cell Biol. **149**:1027-1038.

Shulga N., P. Roberts, Z. Gu, L. Spitz, M.M. Tabb, M. Nomura, and D.S. Goldfarb. 1996. In vivo nuclear transport kinetics in *Saccharomyces cerevisiae*: a role for heat shock protein 70 during targeting and translocation. J. Cell Biol. **135**:329-339.

Sikorski, R.S., and P. Hieter. 1989. A system of shuttle vectors and yeast host strains designed for efficient manipulation of DNA in *Saccharomyces cerevisiae*. Genetics. **122**:19-27.

Sironi, L., M. Melixetian, M. Faretta, E. Prosperini, K. Helin, A. Mussukhio. 2001. Mad2 binding to Mad1 and Cdc20, rather than oligomerization, is required for the spindle checkpoint. EMBO J. **20**:6371-6382.

Skibbens, R.V., and P. Hieter. 1998. Kinetochores and the checkpoint mechanism that monitors for defects in the chromosome segregation machinery. Annu. Rev. Genet. **32**:307-337.

Smith T.F., C. Gaitatzes, K. Saxena, and E. J. Neer. 1999. The WD repeat: a common architecture for diverse functions. Trends Biochem. Sci. **24**: 181-185.

Stade, K., C.S. Ford, C. Guthrie, and K. Weis. 1997. Exportin 1 (Crm1p) is an essential nuclear export factor. **90**:1041-1050.

Stafstrom, J.P., and L.A. Staehelin. 1984. Dynamics of the nuclear envelope and of nuclear pore complexes during mitosis in the *Drosophila* embryo. Eur. J. Cell Biol. **34**:179-189.

Straight, A.F., W. Shou, G.J. Dowd, C.W. Turck, R.J. Deshaies, A.D. Johnson, and D. Moazed. 1999. Net1, a Sir2-associated nucleolar protein required for rDNA silencing and nucleolar integrity. Cell. **97**:245-256.

Straight, A.F., and A.W. Murray. 1997. The spindle assembly point in budding yeast. Methods Enzymol. **283**:425-440.

Strambio-de-Castillia, C., G. Blobel, and M.P. Rout. 1995. Isolation and characterization of nuclear envelopes from the yeast *Sacharomyces*. J. Cell Biol. **131**:19-31.

Strambio-de-Castillia, C., G. Blobel, and M.P. Rout. 1999. Proteins connecting the nuclear pore complex with the nuclear interior. J. Cell Biol. **144**:839-855.

Strom, A.C., and K. Weis. 2001. Importin-beta-like nuclear transport receptors. Genome Biol. **2**:3008.

Stryer, L. 1978. Fluorescence energy transfer as a spectroscopic ruler. Annu. Rev. Biochem. **47**:819–846.

Sudakin, V., G.K.T. Chan, and T.J. Yen. 2001. Checkpoint inhibition of the APC/C in HeLa cells is mediated by a complex of BUBR1, BUB3, CDC20, MAD2. J. Cell Biol. **154**:925-936.

Sun Ch., and J.L. Woolford, Jr. 1994. The yeast *NOP4* gene product is an essential nucleolar protein required for pre-rRNA processing and accumulation of 60S ribosomal subunits. EMBO J. **13**:3127-3135.

Tanaka, T., J. Fuchs, J. Loidl, and K. Nasmyth. 2000. Cohesin ensures bipolar attachment of microtubules to sister centromeres and resists their precocious separation. Nature Cell Biol. **2**:492-499.

Tang, Z., R. Bharadwaj, B. Li, and H. Yu. 2001. Mad2-independent inhibition of APC by the mitotic checkpoint protein BubR1. Dev. Cell. **1**:227-237.

Tao, W., and A.J. Levine. 1999. P19(ARF) stabilizes p53 by blocking nucleo-cytoplasmic shuttling of Mdm2. Proc. Natl. Acad. Sci. USA. **96**:6937-6941.

Tavormina, P.A., Y. Wang, and D. Burke. 1997. Differential requirements for DNA replication in the activation of mitotic checkpoints in *Saccharomyces cerevisiae*. Mol. Cell. Biol. **17**:3315-3322.

Taylor, SS. 1999. Cromosome segregation: Dual control ensures fidelity. Curr. Biol. **9**:R562-R564.

Taylor, S.S., E. Ha, and F. McKeon. 1998. The human homologue of bub3 is required for kinetochore localization of bub1 and a Mad3/Bub1-related protein kinase. J. Cell Biol. **142**:1-11.

Tcheperegine, S., M. Marelli, and R.W. Wozniak. 1999. Topology and functional domains of the yeast pore membrane protein Pom152p. J. Biol. Chem. **274**:5252-5258.

Tham, W.H., and V.A. Zakian. 2000. Telomeric tethers. Nature. **403**:34-35.

Tham, W.H., J.S. Wyithe, P.K. Ferrigno, P.A. Silver, and V.A. Zakian. 2001. Localization of yeast telomeres to the nuclear periphery is separable from transcriptional repression and telomere stability functions. Mol. Cell. **8**:189-199.

Thevelein, J.M. 1994. Signal trunsduction in yeast. Yeast. **13**:1753-1790.

Thomas G., and M.N. Hall. 1997. TOR signalling and control of cell growth. Curr. Opin. Cell Biol. **9**:782-787.

Tollervey, D., H. Lehtonen, M. Carmo-Fonceska, and E.C. Hurt. 1991. The small RNP protein NOP1 (fibrillarin) is required for pre-RNA processing in yeast. EMBO J. **10**:573-583.

Trapman, J., J. Retel, and R.J. Planta. 1975. Ribosomal precursor particles from yeast. Exp. Cell Res. **90**: 95-104.

Trumtel, S., I. Leger-Silvestre, P.-E. Gleizes, F. Teulieres, and N. Gas. 2000. Assembly and functional organization of the nucleolus: ultrastructural analysis of *Saccharomyces cerevisiae* mutants. Mol. Biol. Cell. **11**:2175-2189.

Uetz, P., L. Giot, G. Cagney, T.A. Mansfield, R.S. Judson, J.R. Knight, D. Lockshon, V. Narayan, M. Srinivasan, P. Pochart, A. Qureshi-Emili, Y. Li, B. Godwin, D. Conover, T. Kalbfleisch, G. Vijayadamodar, M. Yang, M. Johnston, S. Fields, and J.M. Rothberg. 2000. A comprehensive analysis of protein-protein interactions in *Saccharomyces cerevisiae*. Nature. **403**:601-603.

Unwin, P.N., and R.A. Milligan. 1982. A large particle associated with the perimeter of the nuclear pore complex. J. Cell Biol. **93**:63-75.

Vasu, S.K., and D.J. Forbes. 2001. Nuclear pores and nuclear assembly. Curr. Opin Cell Biol. **3**:363-375.

Vazques, D. 1974. Inhibitors of protein synthesis. FEBS Lett.**40:** S63- S78.

Venema, J., and D. Tollervey. 1999. Ribosome synthesis in *Saccharomyces cerevisiae*. Annu. Rev. Genet. **33**:261-311.

Villardel, J., and J.R. Warner. 1994. Regulation of splicing at an intermediate step of in the formation of spiceosome. Genes Dev. 8:211-220.

Villardel, J., and J. R. Warner. 1997. Ribosomal protein L32 of *Saccharomyces cerevisiae* influences both the splicing of its own transcript and the processing of rRNA. Mol. Cell Biol. **17**:1959-1965.

Visintin, R., and A. Amon. 2000. The nucleolus: the magician's hat for cell cycle tricks. Curr. Opin. Cell Biol. **12**:372-377.

Voos, W., B.D. Gambil, S. Laloraya, D. Ang, E.A. Craig, and N. Pfanner. 1994. Mitochondrial GrpE is present in a complex with Hsp70 and preproteins in transit across membranes. Mol.Cell. Biol. **14**:6627-6634.

Wach, A., A. Brachat, R. Pohlmann, and P. Philippsen. 1994. New heterologous modules for classical or PCR-based gene disruptions in *Saccharomyces cerevisiae*. Yeast. **13**:1793-1808.

Wang, S., J.R. Babu, J.M. Harden, S.A. Jablonski, M.H. Gazi, W. L. Lingle, P.C. de Groen, T. J. Yen, and J.M.A. van Deursen. 2001. The mitotic checkpoint protein hBUB3 and the mRNA export factor hRAE1 interact with GLE2p-binding sequence (GLEBS)-containing proteins. J. Biol. Chem. **276**:26559-26567.

Wang, Y. and D. Burke. 1995. Checkpoint genes required to delay cell division in response to nocodazole respond to impaired kinetochore function in the yeast *Saccharomyces cervisiae*. Mol. Cell. Biol. **15**:6838-6844.

Warner, J.R. 1989. Synthesis of ribosomes in *Saccharomyces cerevisiae*. Microbiol. Rev. **53**: 256-271.

Warner, J.R. 1990. The nucleolus and ribosome formation . Curr. Opin. Cell Biol. **2**: 521-527.

Warner, J.R. 1999. The economics of ribosome biosynthesis in yeast. Trends Biochem. Sci. **42**:437-440.

Wassman, K., and R. Benezra. 2001. Mitotic checkpoints: from yeast to cancer. Curr. Opin. Genet. Dev. **11**:83-90.

Weber, J.D., L.J. Taylor, M.F. Roussel, C.J. Sherr, and D. Bar-Sagi. 1999. Nucleolar Arf sequesters Mdm2 and activates p53. Nature Cell Biol. **1**:20-26.

Wente, S.R. 2000. Gatekeepers of the nucleus. Science. **288**:1374-1377.

Wente, S.R., and G. Blobel. 1994. *NUP145* encodes a novel yeast glycine-leucine-phenylalanine-glycine (GLFG) nucleoporin required for nuclear envelope structure. J. Cell Biol. **125**:955-969.

Wigge, P.A., O.N. Jensen, S.Holmes, S. Soues, M. Mann, and J.V. Kilmartin. 1998. Analysis of the *Saccharomyces* spindle pole by matrix-assisted laser desorption/ionization (MALDI) mass spectrometry. J. Cell Biol. **141**:967-977.

Winey, M., L. Goetsch, P. Baum, and B. Byers. 1991. *MPS1* and *MPS2*: novel yeast genes defining distinct steps of spindle pole body duplication. J. Cell Biol. **114**:745-754.

Winey, M., C.J. Mamay, E.T. O'Toole, D.N. Mastronarde, T.H. Giddings, Jr., K.L. McDonald, and J.R. McIntosh. 1995. Three-dimensional structural analysis of the *Sacharomyces cerevisiae* mitotic spindle. J. Cell Biol. **129**:1601-1615.

Winey, M., D. Yarar, Th. Giddings, Jr., and D.N. Mastronade. 1997. Nuclear pore complex number and distribution throughout the *Saccharomyces cerevisiae* cell cycle by three-dimensional reconstruction from electron micrographs of nuclear envelopes. Mol. Biol. Cell. **8**:2119-2132.

Winey, M. and E. O'Toole. 2001. The spindle cycle in budding yeast. Nature Cell Biol. **3**:E23-E27.

Wittmann, T., A. Hyman, and A. Desay. 2001. The spindle: a dynamic assembly of microtubules and motors. Nature Cell Biol. **3**:E28-E34.

Wood, K.W., R. Sakowicz, L.S. Goldstein, and D.W. Cleveland. 1997. CENP-E is a plus-end directed kinetochore motor required for metaphase chromosome alignment. Cell. **91**:357-366.

Woolford, J.L.,Jr., and J.R. Warner. 1991. The ribosome and its synthesis. In: J.R. Broach, J.R. Pringle, and E.W. Jones (ed.),The Molecular Biology and Cellular Biology of the Yeast *Saccharomyces*. Genome Dynamics, Protein Synthesis, and Energetics. p. 587-626. Cold Spring Harbor Laboratory Press, Cold Spring Harbor, NY.

Wozniak, R.W., G. Blobel, and M.P. Rout. 1994. POM152 is an integral protein of the pore membrane domain of the yeast nuclear envelope. J. Cell Biol. **125**:31-42.

Wozniak, R.W., M.P. Rout, and J.D. Aitchison. 1998. Karyopherins and kissing cousins. Trends Cell Biol. **5**:184-188.

Xue, Zh., and T. Melese. 1994. Nucleolar proteins that bind NLSs: a role in nuclear import or ribosome biogenesis? Trends Cell Biol. **4**:414-417.

Yaffe, M.P., and G. Schatz. 1984 Two nuclear mutations that block mitochondrial protein import in yeast. Proc. Natl. Acad. Sci. USA. **81**:4819-4823.

Yang, Q., M.P. Rout, and C.W. Akey. 1998. Three-dimensional architecture of the isolated yeast nuclear pore complex: functional and evolutionary implications. Mol. Cell. **1**:223-234.

Yuste-Rojas, M., and F.R. Cross. Mutations in CDC14 result in high sensitivity to cyclin gene dosage in *Saccharomyces cerevisiae*. Mol. Gen. Genet. **263**:60-72.

Zacharie, W., and K. Nasmyth. 1999. Whose end is destruction: cell division and the anaphase-promoting complex. Genes Dev. **13**: 2039-2058.

Zardoya, R., A. Diez, P.J. Mason, L. Luzzatto, A. Garrido-Pertierra, and J.M. Bautista. 1994. High resolution of proteins by double-inverted gradient polyacrylamide gel electrophoresis (DG-PAGE). Biotechniques. **16**:270-272.

Zhang, C., and P.R. Clarke. 2001. Roles of Ran-GTP and Ran-GDP in precursor vesicle recruitment and fusion during nuclear envelope assembly in a human cell-free system. Curr. Biol. **11**:208-221.

Zhang, X., H. Yang, J. Yu, C. Chen, G Zhang, J. Bao, Y. Du, M. Kibukawa, Z. Li, J. Wang, S. Hu, W. Dong, J. Wang, N. Gregersen, E. Niebuhr, and L. Bolund. 2002. Genomic organization, transcript variants and comparative analysis of the human nucleoporin 155 (NUP155) gene. Gene. **288**:9-18.